INCREASED LIGHT SENSITIVITY IN MICE EXPRESSING A MUTANT HUMAN RHODOPSIN TRANSGENE

By

ALAN WHITE

A DISSERTATION PRESENTED TO THE GRADUATE SCHOOL
OF THE UNIVERSITY OF FLORIDA IN PARTIAL FULFILLMENT
OF THE REQUIREMENTS FOR THE DEGREE OF
DOCTOR OF PHILOSOPHY

UNIVERSITY OF FLORIDA

2005

For my family, and for Tom Baldwin.

ACKNOWLEDGMENTS

I would like to thank Dr. Alfred Lewin for his continuous friendship, support, and advice during my graduate education. I would also like to thank my committee members, Drs. William Hauswirth, Clay Smith, and Terence Flotte, for their helpful input and critical analysis as my studies progressed.

Dr. Adrian Timmers was of particular help in developing methods for and performing animal injections and ERG analysis, and I also appreciate his cheerful encouragement. Dr. Lynn Shaw patiently oversaw much of my training in the basics of molecular biology and recombinant DNA technology and for that I am grateful. I thank Dr. Quihong Li for performing the funduscopy described in this dissertation. Drs. JiJing Pang, Seok Hong Min, and Marina Gorbatyuk also performed subretinal injections. Dr. Henry Baker was a great help during my development as a scientific speaker, and as a student of science in general.

I would like to extend special thanks to Mr. James Thomas Jr. for sharing his friendship and his knowledge of PCR and DNA analytical techniques, and for keeping the lab running smoothly, and Ms. Chrissy Street for managing my training grant and being my friendly liason to the Hauswirth lab. Mr. Tom Doyle was another valuable resource for animal techniques and general good input. I also extend my warmest thanks to all of my labmates and friends from other labs and departments, whose help, advice, and goodwill have been invaluable over the past few years.

This dissertation work could never have been completed without the heroic assistance of Ms. Joyce Conners. I would like to extend my warmest thanks to her for her assistance as my department graduate student secretary. Through her diligence I kept more deadlines than I missed, and was guided through the mass of bureaucratic necessities that beleaguer every graduate student. Her friendship will always be valued.

Finally I would like to thank my grandparents, Bette Womack and Esther and Dick White, my parents, Dennis and Joan White, and my sister, Elizabeth White Spratlin, for their constant love and support throughout my life.

TABLE OF CONTENTS

page

LIST OF TABLES

LIST OF FIGURES

Abstract of Dissertation Presented to the Graduate School
of the University of Florida in Partial Fulfillment of the
Requirements for the Degree of Doctor of Philosophy

INCREASED LIGHT SENSITIVITY IN MICE EXPRESSING A MUTANT HUMAN RHODOPSIN TRANSGENE

By

Alan White

December 2005

Chair: Alfred Lewin
Major Department: Medical Sciences--Genetics

Retinitis Pigmentosa (RP) is a heterogeneous class of retinal disorders characterized by an initial loss of peripheral and night vision, followed by loss of central and daylight vision, affecting around 1.5 million people worldwide. Many RP patients develop the disease because of mutations in a retinal protein called rhodopsin. Normal rhodopsin is a vital component of the phototransduction cascade that allows the retina to detect light, while mutant versions of this protein cause the cells of the retina to become sick and die, leading to blindness.

Mouse models of the disease that are genetically engineered to express mutant rhodopsin proteins are vital for studying the progression of RP and developing treatments for the disease. My work describes one of these models, which expresses a human rhodopsin transgene with a tyrosine to methionine mutation at the 17th amino acid of the protein (hT17M). We bred our line to express the T17M human transgene on a

background that was hemizygous null for mouse rhodopsin (mrho+/-), which closely modeled RP mutations in human patients in expressing one copy of mutant rhodopsin and one copy of wild-type rhodopsin. We performed electroretinographic analysis (ERG) to show that this line loses its visual responses over time. Histology confirmed that ERG attenuation was accompanied by a loss of rod photoreceptors in the retina.

Unsuccessful attempts to treat the hT17M; mrho+/- mice with subretinal injections of rAAV-expressed ribozymes led to the discovery of an hT17M-specific light sensitivity that caused severe loss of a- and b-wave ERG responses. Histological analysis showed a concomitant loss of photoreceptors, and TUNEL labeling of fragmented DNA in rod photoreceptor cells demonstrated that the damage was occurring via an apoptotic pathway. Attempts to reproduce this light damage phenotype in another mouse model of retinal disease that expressed a human rhodopsin transgene with a proline to histidine mutation at the 23rd amino acid were unsuccessful, leading us to conclude that this light sensitivity was not common to all rhodopsin mutations. Finally, filters were developed that removed the wavelengths of light responsible for the retinal damage, allowing for non-damaging subretinal injections of the hT17M mice.

CHAPTER 1
INTRODUCTION

Retinitis Pigmentosa

History and Pathology

Retinitis pigmentosa (RP) is the common name for a group of retinal disorders characterized by progressive photoreceptor degeneration that culminates in loss of vision (Flannery et al., 1989; Hims et al., 2003; Farrar et al., 2002). The disease affects from 50,000 to 100,000 people in the United States and around 1.5 million people worldwide. Initial symptoms include night blindness and loss of peripheral vision, usually occurring during the late teens or early twenties. As the photoreceptors continue to degrade the visual impairment progresses towards the center of the retina, eventually affecting the cone photoreceptors that are responsible for central vision in bright light conditions, and resulting in the manifestation of "tunnel vision", in which the visual fields of the patient constrict to less than 20^{o}.

The loss of vision is accompanied by visual pigment depositions in the retina for which the disease is named (Figure 1-1) (Stricker et al., 2005; Farber et al., 1987). In most cases this is accompanied by a waxy pallor to the optic nerve, attenuated retinal vasculature, and thinning of the retinal pigmented epithelium. In many cases, abnormal ERG responses predict the development of retinitis pigmentosa in affected individuals well before other symptoms present. For most patients the visual fields will continue to constrict until they are completely blind (Humphries et al., 1992).

Causes of Retinitis Pigmentosa

Retinitis pigmentosa shows a high degree of genetic heterogeneity. Causative mutations can be subdivided into several genetic categories: autosomal dominant (ADRP), autosomal recessive (ARRP), X–linked (XLRP), or syndromic (Hims et al., 2003; Farrar et al., 2002). The percent contribution of each type of disease varies among different populations, but it is generally agreed that ADRP accounts for around 25% of all cases, ARRP for 20%, X-linked and syndromic for around 8%, with the rest of the cases believed to be the result of spontaneous mutations arising in the affected individual (Diager et al., 2005). The majority of causative genes identified to date lead to the autosomal dominant form of RP.

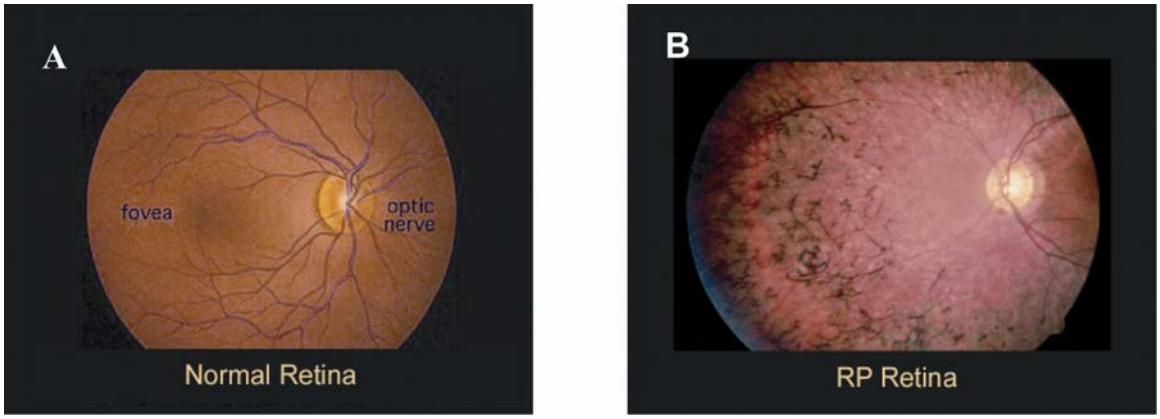

Figure 1-1. Funduscopic presentation of Retinitis Pigmentosa. This series shows a normal retina (A) and a retina exhibiting evidence of Retinitis Pigmentosa (B) (Rosenfeld and Dryja, 1995).

Retinitis pigmentosa can be caused by mutations in a wide variety of genes. The first of these candidate genes to be discovered was rhodopsin, which is expressed in rod photoreceptor cells and is an integral part of the phototransduction cascade. Subsequently a mutation in the peripherin RDS gene, which is a structural protein involved in maintaining rod photoreceptor outer segment disc morphology, was also

shown to be linked to the disease. More recently, mutations in phototransduction proteins including the α and β subunits of rod cGMP phosphodiesterase, the α subunit of the rod cGMP-gated channel, and arrestin have been shown to lead to RP. RPE65, which is expressed in the retinal pigmented epithelium and is involved in visual pigment regeneration, as well as ROM 1, which has a structural role related to peripherin RDS, have also been identified as RP candidate genes. In all, 44 different loci have been identified as being associated with RP, of which 35 have been cloned (Humphries et al., 1992; Diager et al., 2005; Kennan et al., 2005). It is of interest that some of the genes associated with RP encode proteins needed in all cells for functions such as RNA splicing or purine metabolism. Why mutations in these genes lead to retinal degeneration and not other phenotypes is unknown (Bowne et al., 2002; Kennan et al., 2002; Martinez-Gimeno et al., 2003; Maita et al., 2005).

Rhodopsin

Opsin is a seven-transmembrane G-coupled receptor protein found in the disc membranes of the outer segments of rod and cone photoreceptor cells (Figure 1-2). The protein is oriented in the rod outer segment (ROS) membrane such that its amino terminus is located on the inside of the disc in the intralumenal space, while the carboxyl terminus is found on the outside of the disc in the cytoplasmic space. The amino terminus of the protein contains two glycosolation sites, at Asn2 and Asn 15, and there is extensive association between the intralumenal portions of opsin and these carbohydrate moieties (Stenkamp et al., 2005; Hargrave and Mcdowell, 1992). Opsin is incredibly abundant, accounting for around 90% of the total protein in the rod outer segments (Daiger et al., 1995).

Rhodopsin and the Visual Cycle

In its active form, the protein binds the visual pigment 11-*cis* retinal to form rhodopsin. The term "rhodopsin" will be used to refer to this protein-chromophore complex for the remainder of this dissertation. The 11-*cis* retinal is covalently bound to rhodopsin via a protonated Schiff-base at Lys296 (Bownds, 1967). The opsin protein itself does not absorb visible

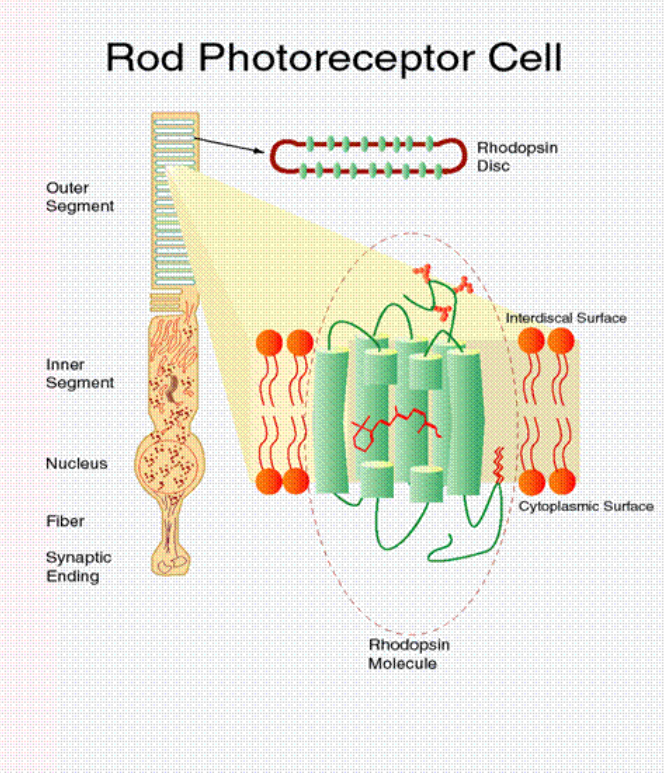

Figure 1-2 A rod photoreceptor cell, with expanded views showing outer segment disc morphology and the orientation or rhodopsin within the outer disc membrane. The chromophore 11-cis retinal is shown in a cutaway view to be bound to the interior of the rhodopsin protein. Figure adapted from Hargrave and McDowell, 1992.

light, but when it is bound to 11-*cis* retinal to form rhodopsin, the resultant molecule has a broad absorption band with a peak at around 500nm. Photons impacting upon rhodopsin provide energy that is able to temporarily convert the *cis*-double bond between C-11 and C-12 of 11-*cis* retinal into a single bond, allowing the molecule to rotate

through 180° to an all-*trans* configuration (Figure 1-4). This isomerization leads to conformational changes in rhodopsin that allow it to interact with downstream molecules in the phototransduction cascade.

After light activation, rhodopsin shifts between two conformations, termed metarhodopsin I and metarhodopsin II. Metarhodopsin II is able to transiently bind to the next protein in the cascade, transducin, which is a heterotrimeric G-protein consisting of

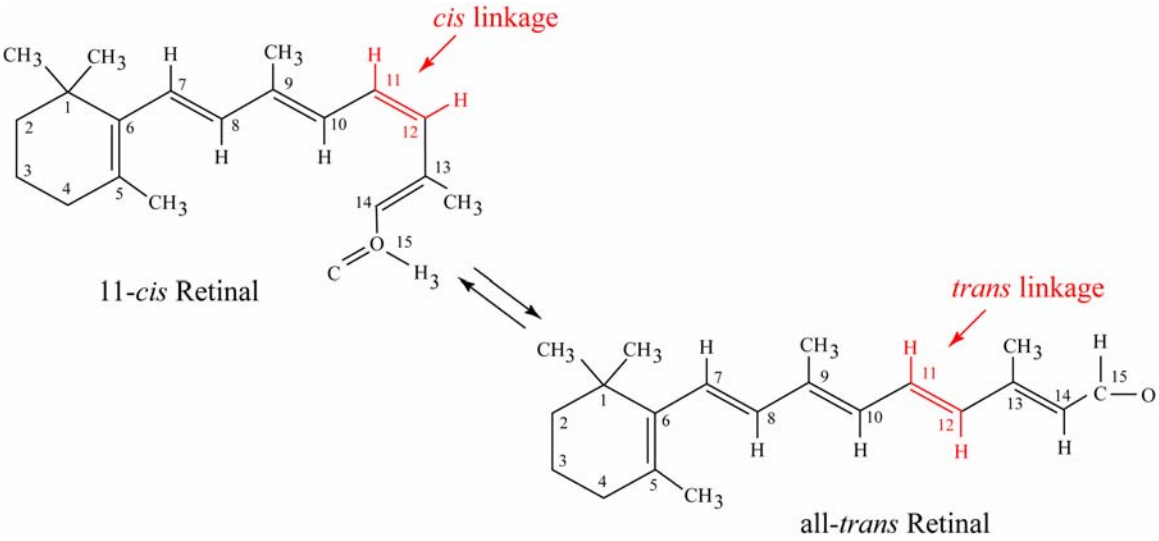

Figure 1-3. Isomerization of 11-*cis* to all-*trans* retinal. The C-11 to C-12 linkage about which the rotation occurs is highlighted in red.

three subunits, α, β, and γ. Each molecule of light-activated rhodopsin is able to interact with hundreds of transducin molecules, resulting in the first of a series of signal amplifications. The α subunit of transducin in its inactive state is bound to GDP. Interaction with metarhodopsin II causes the α subunit to exchange its GDP for a GTP molecule, causing it to dissociate from the other subunits and allowing it to bind to cGMP phosphodiesterase, the next player in the cascade. cGMP phosphodiesterase is composed of catalytic α and β subunits that are bound to and inhibited by two γ subunits.

Interaction between activated transducin and one of the γ subunits releases the α and β subunits to hydrolyze cGMP to 5'GMP.

The resultant drop in the intracellular cGMP concentration results in the closing of a few hundred to a few thousand cGMP-gated Ca^{2+} channels, resulting in a decrease in the intracellular concentration of Ca^{2+}, which causes a hyperpolarization of the ROS plasma membrane. This signal is propagated along the plasma membrane to the synaptic terminus of the rod photoreceptor (Figure 1-2), resulting in a reduction in the release of glutamate. This decreases the activity of nearby bipolar cell glutamate receptors, which in turn decreases the activation of a G-coupled receptor protein and

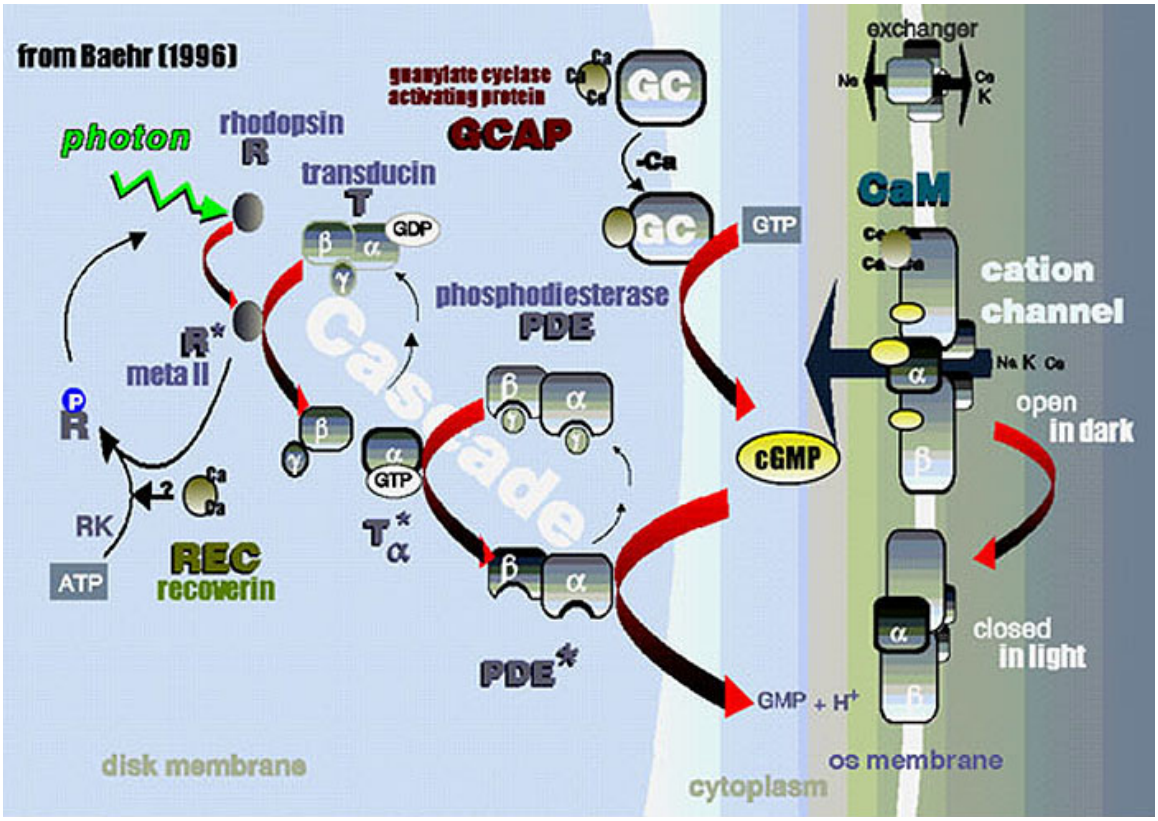

Figure 1-4. The phototransduction cascade. Figure courtesy of Dr. Helga Kolb (Kolb et al., 2005).

leads to an increase in the cGMP concentration in the bipolar cell. The increase in cGMP results in the opening of large numbers of cationic channels, resulting in bipolar cell depolarization and the generation of an action potential (Figure 1-4) (Hargrave and Mcdowell, 1992; Daiger et al., 1995; Maple and Wu, 1996).

Inactivation of this cascade is initiated by rhodopsin kinase, which binds to and phosphorylates metarhodopisn II. Phosphorylated metarhodopsin II is then able to interact with arrestin, which prevents interactions with transducin until metarhodopsin releases the all-trans retinal. Release of all *trans* retinal is thought to inhibit the re-opening of the cGMP-gated ion channels. Eleven-*cis*-retinal is eventually recycled through the retinoid cycle that has steps in both photoreceptors and the retinal pigmented epithelium (McCabe et al., 2004). In the meantime, cGMP is regenerated from GMP by the protein guanylate cyclase, and the cGMP is able to bind to and eventually reopen the cGMP-gated ion channels. This causes an influx of Ca^{2+} that restores the resting potential of the ROS, stimulating the release of glutamate at the synaptic terminus and terminating the light-induced signal.

Rhodopsin and Retinitis Pigmentosa

The first ADRP gene was identified and localized to the long arm of chromosome 3 in 1989 by researchers investigating the pedigree of a large Irish family with over fifty individuals reporting symptoms consistent with retinitis pigmentosa (Bradley et al., 1989; McWilliam et al., 1989). As RP was known to affect rod photoreceptors, and the gene encoding the ROS protein rhodopsin had recently also been localized to the long arm of chromosome 3, the race was on to identify a point mutation in rhodopsin that was associated with ADRP. In 1990, the first ADRP-causing rhodopsin mutation was

reported, consisting of a DNA mutation (CCC to CAC) that caused histidine to be substituted for proline (P23H) at the 23rd amino acid of the protein (Dryja et al., 1990).

Rhodopsin has subsequently become the most extensively characterized gene associated with retinitis pigmentosa. Mutations in the rhodopsin gene account for around 10% of all reported cases of RP (Rivolta et al., 2002). Since discovery of the P23H mutation, around 150 different mutations of rhodopsin have been shown to cause the disease. A vast majority of these mutations lead to autosomal dominant RP, and most of these mutations are thought to cause retinal degeneration by either a toxic gain of function or a dominant negative fashion (Wilson and Wensel, 2003). Many of these mutations are illustrated in Figure 1-5.

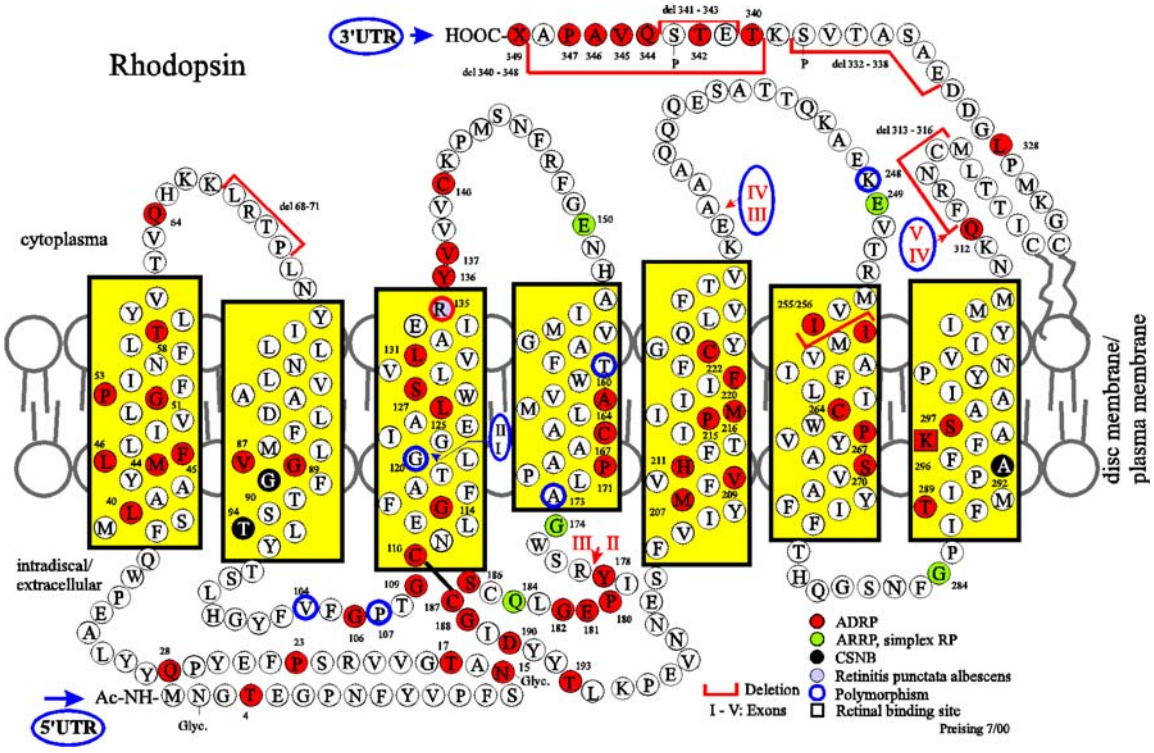

Figure 1-5. Illustration of rhodopsin as it is inserted into the outer segment disc membrane. The image depicts some secondary structure and also illustrates key amino acids in which mutations lead to retinitis pigmentosa (Diager et al., 2005).

Mutations affecting the Lys295 residue prevent rhodopsin from binding to 11-*cis* retinal, and cause the protein to be constitutively activated, leading to retinitis pigmentosa, possibly because this protein is able to continuously bind to and sequester arrestin (Berson, 1996). It is also known that mutations at the Tyr4 and Tyr17 residues abolish the glycosylation sites at the N-terminus of rhodopsin, leading to its aberrant trafficking in cell culture models, and in the case of the T17M mutation, inefficient regeneration of the protein with 11-cis retinal (Kaushal et al., 1994). Addtionally, the cystine residues at positions 110 and 187, which form a conformationally vital disulfide bond, and the glutamate residue at codon 114, which provides the counter ion for the Schiff's base retinal linkage at codon 296, are structurally important residues that, when mutated, can lead to RP (Karnik et al., 1988; Karnik and Khorana, 1990; Daiger et al., 1995). However, the mechanisms by which the majority of rhodopsin mutations lead to RP are not well understood.

Several groups have attempted to categorize rhodopsin mutations by expressing rhodopsin genes containing them in cultured cells and then analyzing the resultant proteins with respect to a variety of factors. One such analysis utilized rhodopsin cDNAs engineered to contain thirty four mutations known to cause ADRP in patients and expressed in H293S cells. These experiments lead to two categories of rhodopsin mutations, Class I and Class II. Class I mutations were less numerous, accounting for only six of the 34 mutations studied. Class I mutants were similar to wild-type rhodopsin expressed in the same system in terms of yield, subcellular localization (the plasma membrane), and regeneration with 11-*cis* retinal, and tended to cluster in both the first transmembrane and carboxyl terminal domains of the protein. Class II mutations were

more numerous, and were found clustered in the transmembrane and loop domains of rhodopsin. Class II mutants accumulated to significantly lower than wild-type levels, regenerated poorly with 11-cis retinal, were predominately mislocalized to the endoplasmic reticulum, and were shown to form intracellular aggregates (Sung et al., 1991; Sung et al., 1993).

A concurrent study involved introducing 35 mutations into a synthetic bovine rhodopsin gene and expressing them in COS cells (Kaushal and Khorana, 1994). The proteins expressed in this study were classified into three classes. Class I, like those of the studies of Sung and coworkers, consisted of proteins that showed expression levels, subcellular localization (to the plasma membrane) and chromophore regeneration that were similar to wild-type rhodopsin. Class II consisted of proteins that showed folding defects, were mislocalized to the endoplasmic reticulum, and were not able to reconstitute with 11-cis retinal. Class III mutations also showed folding and localization defects, but were able to partially regenerate with 11-*cis* retinal. Taken together, these two studies provide evidence for at least two types of rhodopsin defect that can lead to ADRP. Recently, Mendes and coworkers have proposed classifying rhodopsin mutations into five groups based on additional characteristics such as whether they affect endocytosis or whether they remain constituively activated (Mendes et al., 2005).

There are several theories concerning the mechanism of retinal degenerations caused by rhodopsin mutations. Sung and coworkers note that their class II rhodopsin mutations show retention/mislocalization to the endoplasmic reticulum that is similar to that seen in other disease-causing mutant proteins such as Class II low density lipoprotein receptors and cystic fibrosis transmembrane conductance regulator proteins. Indeed,

there is evidence for a variety of neurodegenerative diseases that share an accumulation of aggregated, ubiquitinated mutant proteins, suggesting that these proteins are targeted for destruction, possibly due to toxicity resulting from their expression (Wilson and Wensel, 2003; Rajan et al., 2001; Bence et al., 2001; Illing et al., 2002). It is also thought that overloading the cellular machinery responsible for the removal of misfolded and toxic proteins, termed the unfolded-protein or ER-stress response, can lead to programmed cell death (Mendes et al., 2005; Rutkowski and Kaufman, 2004).

In the case of mutations affecting the tyrosine residues at codons 4 and 17, the pathogenic mechanism may in part be explained by the abolishment of glycosylation at nearby residues, which has been shown to cause defective ROS membrane morphogenesis in *Xenopus laevis* retinas (Fliesler et al., 1985). Defects in outer segment morphogenesis are thought to lead to photoreceptor cell death, and can result from mutations in rhodopsin that prevent it from being properly transported to the OS disc membranes. It is known that the ROS sheds ~10% of its outer segment discs each day (Young and Bok, 1969). These discs are phagocytosed by the retinal pigmented epithelium, and more must be synthesized at the base of the ROS each day to replace them (Young and Bok, 1969; Papermaster et al., 1986; Steinberg et al., 1980). Studies of carboxy terminal rhodopsin mutations have shown that this region of the protein is important for dynein binding and cellular transport. Mutations in this region have been shown to lead to a mislocalization of rhodopsin in the rod photoreceptors, causing abnormal ROS disc morphogenesis, which would help to explain the pathogenesis of Class I rhodopsin mutations (Tai et al., 1999; Sung et al., 1994). Additionally, overwhelming synthesis of aberrantly folded rhodopsin may interfere with the subcellular

trafficking of non-mutant rhodopsin, again resulting in a hindering or prevention of disc morphogenesis and causing a progressive shortening of the ROS that eventually leads to cell death (Mendes et al., 2005; Besharse and Wetzel, 1995).

While the exact mechanisms by which the various rhodopsin mutations lead to RP are still uncertain, it is clear that the ultimate fate of the affected photoreceptors is programmed cell death, or apoptosis. Apoptosis is a thoroughly documented phenomenon by which cells initiate a specific program of self-destruction in response to intrinsic or extrinsic factors (Wenzel et al., 2005). These can include mechanical damage, toxic chemical exposure, bacterial or viral infection, and various forms of irradiation. Apoptosis is also responsible for the programmed deaths of cells for developmental reasons, deaths of auto-reactive cells of the immune system, and deaths of cells that have lost growth inhibition and could become cancerous. Two major apoptotic pathways have been described, an extrinsic pathway involving CD95 and CD95 ligand and an intrinsic pathway involving mitochondrial damage. Activation of the aspartyl proteases, termed caspases, is common to both mechanisms, as is the ultimate release of mitochondrial cytochrome c, which leads to full apoptotic activation. While the extrinsic pathway plays an important role in shutting down the immune response, the intrinsic pathway is thought to be more important in pathologic apoptosis such as that occurring in RP (Vermeulen et al., 2005; Mohamad et al., 2005).

Additionally, caspase-independent pathways have also been described that involve effector molecules including cathepsins, calpains, granzyme A and B, and serine proteases such as AP24. Two major players in the caspase independent pathway are apoptosis inducing factor (AIF) and PARP-1. AIF is an oxioreductase found in the

mitochondria, and decreased levels of AIF have been correlated with an increased sensitivity to oxidative stress. Activation of the caspase-independent apoptotic pathway leads to mitochondrial secretion of AIF, which is ultimately involved chromatin condensation and recruits the endonuclease EndoG to effect chromatin degradation. PARP-1 is involved in DNA repair, and overstimulation as a result of DNA damage is thought to lead to cell death through metabolic depletion. Interestingly, PARP-1 is actually a target for caspase cleavage in caspase-dependent apoptosis – this is thought to be a cell strategy to reduce metabolic depletion and increase the energy available to effect orderly apoptosis through the caspase-dependent pathway (Wenzel et al., 2005).

Hallmarks of apoptosis include reduced cell size and the appearance of bubble-like "blebs" on the surface of the plasma membrane. The nuclear chromatin breaks down, leading to a diagnostic "DNA laddering" morphology, and the mitochondria begin to lose integrity, releasing cytochrome c into the cytoplasm. Eventually the entire cell breaks down into small, membranous vesicles, which are finally engulfed by macrophages and dendritic cells that recognize the apoptotic cells (Vaux, 1993; Reme et al., 1998).

The link between apoptosis and RP-related photoreceptor cell death has been well established (Reme et al., 1998). In 1994, Portera-Cailliau and coworkers investigated the mechanism of cell death in the three mouse models of retinitis pigmentosa: the rd mouse, which contains a defect in the rod cGMP phosphodiesterase gene, the rds mouse, which contains a defect in the structural gene peripherin, and in mice containing a Q334 termination mutation in the rhodopsin gene (Portera-Cailliau et al., 1994). In each mouse, DNA fragmentation, a hallmark of apoptosis was seen in the photoreceptors. In concurrent studies, researchers showed similar evidence for apoptotic cell death in RCS

rats, which carry defects in the ability of the RPE to phagocytose ROS discs (Tso et al., 1994). In 1996, another study showed apoptotic cell death as the ultimate fate of rod photoreceptors in mice engineered to contain a P23H rhodopsin mutation, and a correlation was noted between increasing amounts of apoptosis and decreased ERG findings in the same animals (Naash et al., 1996).

A hallmark of retinal degeneration resulting from RP is that after a certain number of rod photoreceptors have died, normal rods and cones that do not express mutant opsins begin to die as well. In 1993, chimeras between normal mice and mice carrying a P347S mutant rhodopsin transgene were created in order to address this issue. *In situ* hybridization assays confirmed that the chimeric retinas were made up of mixtures of adjacent mutant and non-mutant rod photoreceptor cells, while histological examination revealed that cell death was occurring simultaneously in both mutant and non-mutant sections of the retina (Huang et al., 1993). This, taken together with the observations of cone cell death resulting from a rod defect, has led to the belief that photoreceptor cells secrete "survival factors" necessary to the survival of their neighbors, and thus the deaths of mutant rod photoreceptors can have deleterious effects upon neighboring cones and non-mutant rods (Rosenfeld and Dryja, 1995; Bredesen et al., 2005). This theory is supported by experiments in which various cell survival factors (e.g. BDNF, CNTF, and NGF) were injected intravitreally into both naturally occurring and artificial models of retinal degeneration. These cellular factors slowed the degenerations in several of the mouse lines (LaVail et al., 1998).

Animal Models of Retinitis Pigmentosa

The development of animal models has been vital to the study of retinitis pigmentosa. Initial lines consisted of naturally occurring mutants that showed early onset

photoreceptor degeneration, the first of which was the rd mouse, identified in 1966, which is currently known to involve a spontaneous mutation in the beta subunit of rod cGMP phosphodiesterase (Keeler, 1966). Many other naturally occurring mouse mutants have since been isolated including, among others, mouse models of Purkinje cell degeneration, the rds mouse, which as mentioned before contains defects in its peripherin gene, and models of Leber Congenital Amaurosis and cone photoreceptor function loss (Chang et al., 2002; Pang et al., 2005). In addition to the naturally occurring mutations, targeted gene disruption techniques have enabled researchers to create and study mouse lines which lack other integral phototransduction proteins, such as arrestin and the Rpe-65 protein.

With mutations in the rhodopsin gene accounting for over 10% of all incidences of RP, it is not surprising that a large number of mouse models involving target rhodopsin deletions and mutations have been designed. In 1992, a mouse model was created to express a either a wild-type human rhodopsin transgene or a human rhodopsin transgene carrying the P23H mutation. Three lines expressing the mutant transgene were created, each of which expressed the mutant rhodopsin at a different level, and although all three lines exhibited retinal degeneration, it was observed that the rate of retinal degeneration was directly proportional to the expression level of the mutant transgene. This model was also important in that it demonstrated that ADRP could arise from a single point mutation in a single gene (Olsson et al., 1992).

Two lines expressing the normal human rhodopsin transgene were also created in the studies by Olsson and coworkers, one of which expressed rhodopsin at levels comparable to non-transgenic mice, and one that expressed five times as much rhodopsin.

Intriguingly, the line that exhibited overexpression of the wild-type human transgene also showed a retinal degeneration, even though there was no mutation involved, which suggests that overexpression of rhodopsin can lead to similar trafficking and aggregation problems as expression of mutant rhodopsins at normal levels. Subsequent studies on this mouse showed accumulation of mutant rhodopsin at abnormal sites in the rod photoreceptor cells (Roof et al., 1994).

Another mouse model involved germline insertion of a mouse rhodopsin transgene that was mutated to contain two silent RFLPs and three amino acid substitutions, one of which was the P23H mutation, and the other two being nearby non ADRP-associated amino acid substitutions that were included to provide an epitope tag. This mouse model, termed the "VPP" model because of the three amino acid substitutions that were introduced, showed normal expression levels of a mixture of wild-type and mutant rhodopsin, and exhibited a slow photoreceptor degeneration that mimicked that seen in human patients. Study of this mouse line revealed that dark-reared mutant animals had significantly reduced rates of photoreceptor degeneration, with a threefold decrease in the appearance of apoptotic photoreceptor cells when compared to mutant siblings raised in twelve hour cyclic light. This suggests that light activation of mutant rhodopsin is a key causative agent in rhodopsin-mediated RP (Naash et al., 1993; Naash et al., 1996; Goto et al., 1995; Goto et al., 1996). The exacerbation of RP symptoms by intense light exposure is a well-documented phenomenon that is crucial to this work and will be discussed in more detail in future chapters. Further work with the VPP mouse line involving immunohistochemical tracking of the mutant rhodopsin molecules revealed that the mutant opsin was correctly synthesized and localized, that there was normal outer

segment disc shedding, but that there were defective and disorganized basal discs at the connecting cilium, the site of outer segment disc morphogenesis, providing further evidence of a trafficking/disc morphogenesis defect associated with some rhodopsin mutations (Wu et al., 1998; Liu et al., 1997).

An interesting and very useful model of ADRP was created in 1997 via a targeted disruption of the entire rhodopsin gene. This model contained a Pol2: neomycin insertion in exon II of the endogenous mouse rhodopsin gene. Subsequent mouse lines were bred to contain either one disrupted rhodopsin gene (hemizygous null, or mRho+/- mice), or two disrupted rhodopsin genes (homozygous null, or mRho-/- mice). Hemizygous null mice showed some subcellular disorganization of the ROS, as well as shortening of the outer segments in older mice when compared to wild-type mice, but little ERG reduction or other signs of disease. Homozygous null mice, however, which completely lacked expression of mouse rhodopsin, never formed rod outer segments, showed no ERG response at eight weeks of age, and showed loss of cone photoreceptors by three months of age (Humphries et al., 1997). These mice, along with a separate rhodopsin knockout model that was subsequently developed (Lem et al., 1999), were important for several reasons. Chief among these was their usefulness at providing a genetic background that allowed researchers to breed hemizygous null (mrho+/-) rhodopsin lines upon which they could express rhodopsin transgenes at an allelic ratio identical to that seen in human patients with ADRP (i.e., one mutant copy and one wild-type copy).

Further mouse lines expressing rhodopsin mutations were created in the 1990s, including one containing a Q344Ter mutation which caused synthesis of a rhodopsin protein with an abnormally short carboxyl terminus. This mutant line exhibited

rhodopsin accumulation in the plasma membranes of rod photoreceptor cells, demonstrating, as mentioned before, that the carboxy terminal of rhodopsin is necessary for efficient and proper trafficking of rhodopsin (Sung et al., 1994). In 1998, Li et al. reported creation of mouse models of ADRP expressing human rhodopsin transgenes with either a T17M mutation (a class I mutation that abolishes the glycosylation site at Arg15), or a P347S mutation (a class II mutation). Both lines exhibited progressive loss of ERG response and decreasing thickness of the ONL. Interestingly, treatment with Vitamin A supplementation led to partial rescue of the T17M-medaited RP, but not of the P347S animals, providing further evidence that the separate classes of rhodopsin mutations lead to retinitis pigmentosa via different biochemical or morphological pathways (Li et al., 1998).

Gene Therapy for Retinitis Pigmentosa

It has long been the goal of medical scientists to effect therapies that act in targeted cells at the level of the gene. In cases where disease symptoms are created by missing or non-functional gene products, gene replacement strategies could be used to introduce healthy gene products into tissues of interest. In cases where there is a toxic gain of function caused by a mutant protein, therapeutic techniques designed to specifically abolish expression of the mutant gene encoding that protein would be warranted. Both types of gene therapy have been successfully demonstrated in animal models of retinitis pigmentosa (Hauswirth and Lewin, 2000; Hauswirth et al., 2004).

The first efforts at gene replacement involved creating transgenic mice expressing the corrective gene and crossing these with mice showing a retinal defect. In the case of the naturally occurring rd mice, which undergo retinal degeneration due to a defect in the beta subunit of the rod cGMP phosphodiesterase gene (βPDE), the introduction of a

functional human gene replacement through this method restored normal photoreceptor morphology and function (Lem et al., 1992). In another study, these transgenic techniques were used to express a human rhodopsin transgene on the homozygous null rhodopsin (mRho-/-) mouse model of retinal degeneration. Expression of the functional human rhodopsin in this case resulted in rescue of photoreceptor ultrastructure and ERG response, and demonstrated the ability of the group's targeting construct to express the transgene at therapeutic levels (McNally et al., 1999).

Following up on the work of Lem and colleagues with the rd mouse, two groups have reported rescue of the photoreceptors through viral-mediated delivery of functional βPDE genes. In 1996, researchers used replication-deficient adenoviral vectors to deliver a murine cDNA expressing the wild-type βPDE gene into the subretinal space of rd mice (Bennett et al., 1996). This therapy resulted in expression of functional βPDE that resulted in a six week delay in photoreceptor degeneration. A similar strategy that utilized intravitreal injection an adeno-associated viral vector delivering a wild-type βPDE gene resulted in increased survival of photoreceptors and an increased ERG response in rd mice receiving the therapy (Jomary et al., 1997). Gene replacement has also been effective in treating the retinal degeneration seen in the naturally occurring rds mouse, which as mentioned before suffers from defects in the ROS structural protein, peripherin. Subretinal injection an adeno-associated viral vector engineered to express a wild-type peripherin gene resulted in restoration of ROS ultrastructure and function in these mice though the result was temporary (Ali et al., 2000). Long term rescue was also seen with gene replacement designed to deliver a functional RPE65 gene to the retinas of

the rd12 naturally occurring mouse model of the recessive retinal disease, Leber Congenital Amaurosis (Pang et al., 2005).

Gene therapy designed to alleviate dominant retinal disease by suppressing expression of mutant genes has also shown efficacy in mouse models. One such study involved a rat model of retinal disease that was engineered to express a P23H mutant rhodopsin transgene. Subretinal delivery of adeno-associated viral vectors engineered to deliver catalytic RNAs, or ribozymes, designed to selectively degrade the mutant transgene, while sparing the endogenous wild-type rat rhodopsin, was shown to result in substantial, long-term rescue of photoreceptor structure and fuction (Lewin et al., 1998) . This rescue, which was shown to be effective to eight months age in these animals, as well as in treating animals that had already entered late stages of the disease (LaVail et al., 2000), shows promise for the treatment of other forms of autosomal dominant disease.

Ribozymes

Riboymes are RNA molecules with the ability to catalyze the cleavage and joining of RNA. They were initially discovered by Altman and Cech, who described the catalytic activity of the RNA component of RNaseP and the group I introns, respectively (Cech, 1988a; Cech, 1988b; Guerrier-Takada et al., 1983; Guerrier-Takada and Altman, 1984). Initial Group I intron catalysis was seen to occur in *cis*, but it was soon discovered that one could liberate the catalytic structure of the RNA from its substrate to generate a ribozyme with the ability to cleave target molecules in *trans*.

Shortly after the work of Altman and Cech, smaller catalytic structures were discovered in the sequences of certain plant pathogens which undergo site-specific, self-catalyzed RNA cleavage as a part of their replicative process (Buzayan et al., 1988;

Haseloff and Gerlach, 1988). These are the hammerhead and hairpin ribozymes, which are receiving much of the present attention for applications in gene therapy (Cech, 1988b; Sigurdsson and Eckstein, 1995; Phylactou et al., 1998; Citti and Rainaldi, 2005). Hammerhead ribozymes consist of three base paired stems surrounding a central catalytic core of fifteen conserved nucleotides, eleven of which are necessary for catalytic activity. The crystal structure of the hammerhead ribozyme reveals noncanonical base pairing within the catalytic core and a magnesium binding site that is distal to the site of catalysis (Scott et al., 1995). The helices are designated I, II, and III; the first and last helices (I and III) form via base-pairing with the target molecule while the middle helix (II) is responsible for stabilizing the catalytic core structure (Figure 1-4) (Sigurdsson and Eckstein, 1995; Pierce and Ruffner, 1998). Hairpin ribozymes have two 5' stretches of sequence which base pair with their RNA targets, forming helices I and II, followed by two downstream helices (III and IV), which interact with one another and the substrate to comprise the catalytic core (Figure 1-5) (Joseph et al., 1993; Berzal-Herranz et al., 1993). The hairpin ribozyme has been crystallized either as a protein complex or as a pure RNA, revealing internal base pairing within and essential interactions between the loop regions of the secondary structure (Rupert and Ferre-D'Amare, 2001; Grum-Tokars et al., 2003). No magnesium is seen at the catalytic site.

Mechanistic Description

Ribozymes achieve their cleavage by binding to their RNA target via complementary base pairing with sequences flanking the cleavage site, folding into a specific catalytic conformation, catalyzing the hydrolysis of the 5'3' phosphodiester bond at the cleavage site, and dissociating from the resultant cleavage products (Figure 1-6). The reaction generates two RNA fragments with either 5' hydroxyl or 2'3' cyclic

phosphate moieties. Divalent cations, such as magnesium, are thought to aid in the folding of the ribozyme into the proper catalytic structure.

These cleavage reactions are sequence specific. The sequences flanking the catalytic core of the ribozyme must be able to form helices with sequences flanking the target cleavage site, and hydrolysis will only occur at a site containing certain combinations of nucleotides. Hammerhead ribozymes will cleave 3' of a triplet sequence of NUX, where N is any nucleotide, U is a uridine, and X is any nucleotide but a

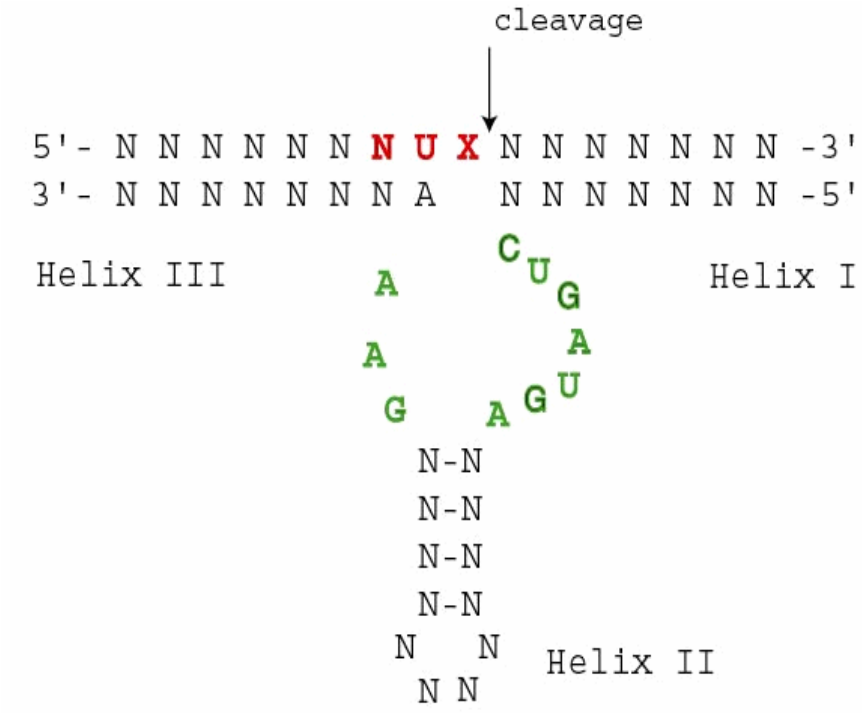

Figure 1-6. Generic structure of a hammerhead ribozyme. The requisite NUX cleavage triplet is shown in red, with the position of cleavage indicated by an arrow. Green nucleotides indicate conserved ribozyme sequences necessary for catalysis.

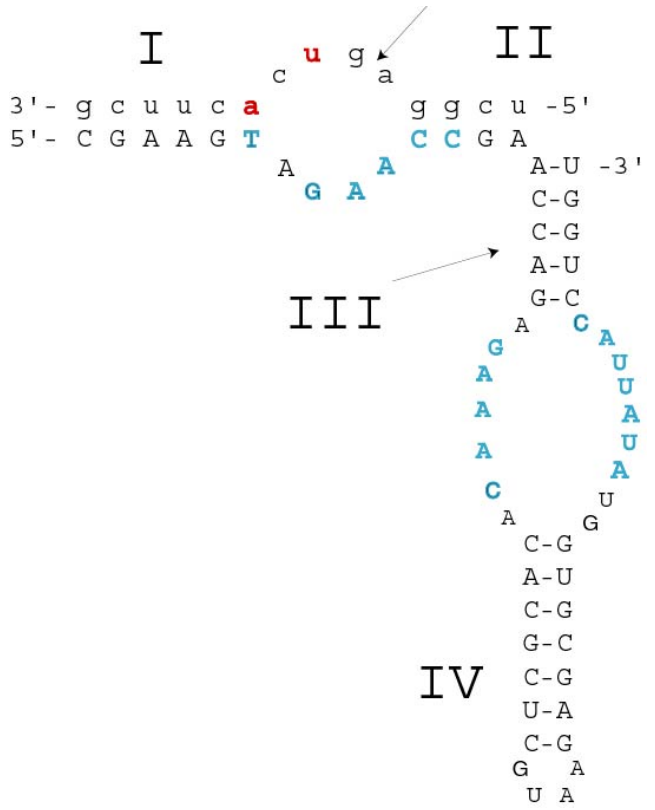

Figure 1-7. Structure of a specific hairpin ribozyme. Cleavage is indicated by an arrow. Blue nucleotides indicate conserved ribozyme sequences necessary for catalysis

guanosine. The hairpin ribozymes show greater sequence constraint, and can be engineered to cleave 5' of the G in the sequence 5'-NBNGUC, where N is any nucleotide and B is G, C, or U. This theoretically allows a wide range of cleavage possibilities for therapeutic applications of ribozymes.

In addition, recent experiments using large combinatorial libraries of ribozyme candidate molecules have shown that it is possible to achieve cleavage of almost any RNA target (Nieuwlandt, 2000; Piganeau et al., 2001). Most importantly, targets that deviate from a ribozyme's optimal cleavage sequence, especially in the area of the catalytic site, undergo reduced cleavage or none at all; even a single nucleotide difference in critical areas is enough to completely abolish cleavage activity (Werner and

Uhlenbeck, 1995). This allows researchers to design ribozymes that are able to cleave mutant RNA transcripts while leaving wild-type messages able to integrate into the target cell genome, which makes them attractive as therapeutic effectors for the treatment of autosomal dominant disease.

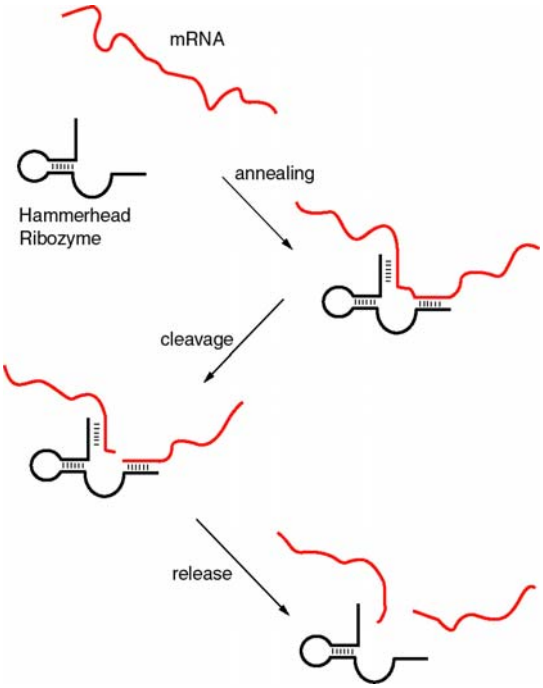

Figure 1-8. Ribozyme cleavage in *trans*. A hammerhead ribozyme (black) is shown annealing to its target mRNA (red) through complementary base-pairing, cleaving it, and releasing the 5' and 3' cleavage products. Ribozymes are truly catalytic, able to catalyze the cleavage of many successive target molecules. Figure courtesy of Dr. Lynn C. Shaw.

AAV

Recombinant adeno-associated viral vectors offer a number of features ideal for gene therapy, including the ability to infect a wide variety of both non-dividing and dividing cell types (Loiler et al., 2003; Flotte, 2005; Fisher et al., 1997), the lack of pathogenicity absence of immune or inflammatory response in transduced cells (Bennett, 2003; Hernandez et al., 1999; Conrad et al., 1996), and the ability to achieve long-term

expression of therapeutic genes (Guy et al., 1999). Adeno-associated viruses (AAV) are human parvoviruses composed of a 4.7 kb single-stranded linear DNA genome packaged in a capsid composed of three structural proteins. The genome is a model of efficiency, consisting of overlapping open reading frames (orfs) that utilize alternative splicing and variation in translation initiation sites to express several proteins from a relatively small genome. The genes encoded by the orfs (and their gene products) are termed Rep (for replication-associated proteins) and Cap (for capsid-associated proteins). The Rep genes produce four protein products, termed Rep78, Rep68, Rep52, and Rep40, with the numbers indicating the respective sizes in kilodaltons of each protein. The Cap genes produce three capsid-forming gene products of 87, 73, and 62 kilodaltons in size, termed VP1, VP2 and VP3, respectively, which are present in the viral capsid at a ratio of 1:1:10 (VP1:VP2:VP3). These genes are present in the genome between two inverted terminal repeats (TRs) consisting of 145 bases, which contain the viral origin of replication and are necessary for viral packaging and integration. The entire genome is packaged within a nonenveloped, icosahedral capsid that is around 20nm in diameter.

AAV belong to the class of viruses known as dependoviruses, because they require co-infection of a helper virus to produce productive infection of their own. In the latent phase of the virus it is found preferentially integrated into a particular site on human chromosome 19 (Kotin et al., 1990). In this phase, the products of the Rep gene have actually been found to be inhibitory to AAV replication. The latent phase of infection will persist until the infected cell is rendered permissive, which can result from certain cytotoxic exposures (including heat shock, irradiation, cycloheximide treatment), or until the cell receives a secondary helper virus infection, usually with adenovirus, herpesvirus,

cytomegalovirus, or poxvirus. This co-infection is accompanied by the expression of helper gene products from the new virus that help AAV achieve productive, lytic infection. In the case of secondary adenoviral infection, expression of the early set of genes (E1a, E1b, E2a, and E4) have been shown to provide helper functions such as transcriptional transactivation and assistance in AAV mRNA accumulation and transport.

The ability of AAV to achieve stable, long term integration into target genomes, coupled with a lack of association with insertional oncogenesis, led to the initial interest in its use as a gene therapy vector. It has since become understood that integration of the virus involves interactions between the chromosomal target site, the AAV TR structures, and the Rep gene products (McLaughlin et al., 1988; Kotin et al., 1990; Surosky et al., 1997; Weitzman et al., 1994). Since the recombinant AAV used for gene therapy lack the Rep gene, integration seen with these vectors is random when it is seen at all. This finding is of concern, as it raises the possibility of insertional activation of a proto-oncogene, but these concerns are somewhat alleviated by a lack of reproducible tumorigenesis in animals treated with rAAV therapy vectors (Donsante et al., 2001) and by the fact that the rAAV genomes are generally thought to persist within the target cells in an episomal fashion (Schnepp et al., 2005).

Production of AAV Vectors

To make recombinant AAV vectors, therapeutic sequences are inserted into a packaging plasmid containing a cloning site and regulatory sequences flanked by the AAV TR sequences that are necessary and sufficient for packaging as recombinant AAV (McLaughlin et al., 1988). This construct is then co-transfected into HK 293 cells along with a helper plasmid that encodes both the Rep and Cap AAV genes and the adenovirus helper gene products. By this method it is possible to generate replication deficient,

recombinant AAV containing up to 4.5 kb of therapeutic DNA sequence bounded by the AAV TRs (Hermonat et al., 1997; Zhou and Muzyczka, 1998). Providing helper gene products on a plasmid rather than by adenoviral co-infection eliminates the possibility of adenoviral contamination in the final viral preparation. These recombinant AAV (rAAV) vectors are able to infect target cells and, with the inclusion of strong *cis*-acting promoter sequences, generate good levels of expression of the therapeutic gene products of interest for extended periods of time. Continued advances in the production and purification of rAAV, including the use of high-volume cell factories and efficient, high-throughput column purification methods, have led to consistently high yields of highly purified viral vectors (Kapturczak et al., 2001; Potter et al., 2002; Blouin et al., 2004). Drawbacks associated with first-generation therapeutic rAAV vectors included a delay in the expression of therapeutic genes for as much as two weeks to a month, and limited transduction of certain cell types. Both issues have been greatly overcome to large extent through the use of pseudotyped rAAV vectors.

Different serotypes of adeno-associated virus can show great diversity in the amino acid composition of their capsid proteins (Grimm and Kay, 2003). Although the original viral delivery vectors were developed from serotype 2, many more serotypes have been found to exist(Gao et al., 2002; Gao et al., 2005). The capsid divergence exhibited by these serotypes cause them to have profound differences in the efficiency and speed with which they are able to transduce various cell types (Grimm and Kay, 2003; Auricchio et al., 2001; Hildinger et al., 2001; Rabinowitz et al., 2002). By using the AAV type 2 packaging vector in combination with helper plasmids providing capsid proteins from the various other serotypes it is possible to create rAAV pseudotype vectors containing the

gene of interest and its ancillary sequences flanked by AAV2 TRs and packaged into capsids derived from one of the other serotypes (Grimm, 2002; Burger et al., 2004; Choi et al., 2005; Gao et al., 2005). Vectors created in this manner are termed pseudotype 2/*, where the first number indicates that the packaging vector was derived from AAV serotype 2 while the asterisk represents the serotype number of the capsid proteins (thus, serotype 2 sequences packaged into a capsid derived from AAV serotype 4 would be referred to as pseudotype 2/4). Table 1-1 summarizes the cell tropisms of the various coat protein serotypes.

Table 1-1. Tissue tropism and site of isolation of the various AAV serotypes. Bold type indicates high levels of expression, while bold italic type denotes highest expression of all AAV serotypes. Adapted from Hildinger and Aurricchio, 2004.

Serotype	Isolated In	Tissue/Cell Tropsim
AAV1	Cell line	Muscle, eye, liver, lung
AAV2	Cell line	Muscle, brain, liver, eye
AAV3	Cell line	Not determined
AAV4	Cell line	Brain
AAV5	Human lesion	Brain, muscle, liver, lung, eye
AAV6	Cell line	Muscle, eye, liver, lung
AAV7	Monkey	Muscle, liver
AAV8	Monkey	Liver

The usefulness of pseudotyped delivery vectors becomes apparent when examining the different transduction efficiencies of AAV 2/1, AAV 2/2 and AAV 2/5 when used to deliver a green fluorescent marker protein (GFP) to the retina. GFP expression is seen in both the retinal pigmented epithelium and in photoreceptor cells of retinas receiving subretinal injection of either AAV 2/2 or AAV 2/5. However, the use of AAV 2/5

resulted in a 400-fold increase in the number of transgene-expressing cells, as compared to transduction by AAV 2/2, and the number of viral genome copies per eye was thirty times higher. Additionally, AAV2/5 showed a faster onset of transgene expression, and was shown to achieve higher levels of transgene expression. AAV2/1, in contrast, transduces cells of the retinal pigmented epithelium almost exclusively, being fifteen times more efficient than AAV2 and achieving higher levels of transgene expression (Yang et al., 2002). Clearly the selection of the proper rAAV pseudotype is of great importance in designing rAAV-mediated gene therapies (Dinculescu et al., 2005; Auricchio and Rolling, 2005). Recent advances in this area have focused on directly altering individual capsid epitopes to further enhance and refine the selective tropism of these vector systems (Opie et al., 2003; Warrington, Jr. et al., 2004; Gigout et al., 2005; Muzyczka and Warrington, Jr., 2005).

AAV and Retinal Gene Therapy

Adeno-associated vectors are ideally suited to deliver therapeutic DNA sequences to retinal cells. These recombinant viruses are able to achieve long term expression in retinal photoreceptor cells, retinal ganglion cells, and cells of the retinal pigmented epithelium (Dinculescu et al., 2005; Guy et al., 1999; Flannery et al., 1997). Transduction of retinal cells by rAAV is achieved with little or no toxic or immunogenic side-effects (Bennett, 2003). Finally, the use of the various adeno-associated viral pseudotypes with their selective tropism allows researchers to selectively target specific retinal cell types for transduction.

Additionally, there are many characteristics of the retina itself that make it attractive for rAAV-mediated gene therapy. Injections into the subretinal space can be routinely performed with great speed and precision, and when properly performed lead to

little or damage of the injected tissues (Timmers et al., 2001). Also, the eye itself is held to a certain extent to be an immune privileged site, a characteristic which enhances the lack of an immune response to rAAV and the therapeutic proteins or sequences that it delivers (Streilein et al., 1992; Sonoda and Streilein, 1992). Finally, the presence of two eyes in animal models ensures that there is always a built-in control available to the researcher in every experimental animal, as one eye can simply remain uninjected and then be compared to the contralateral, treated eye.

As mentioned before, rAAV gene delivery vectors have been used to treat wide variety of retinal disease, including the rd, rds, rd12 mouse models of retinal degeneration, and mouse and rat models of P23H mutant rhodopsin-mediated ADRP. These vectors have also been successful components of therapies designed to treat the lysosomal storage defects in the retinal pigmented epithelium seen in the MPVII (Bosch et al., 2000; Hennig et al., 2004) and MP IIIB (Fu et al., 2002) mice, MerTK deficiency in the Royal College of Surgeons (RCS) rat (Smith et al., 2003), retinal degeneration in the naturally occurring RPE65-/- Briard dog analogue of the rd12 mouse (Acland et al., 2005; Acland et al., 2001), and retinal degeneration in a mouse model of X-linked juvenile retinoschisis (Min et al., 2005). rAAV-delivered neurotrophic factors such as GDNF (Wu et al., 2004), CNTF (Adamus et al., 2003; Liang et al., 2001), and FGF (Lau et al., 2000; Lau and Flannery, 2003) have also been used to alleviate retinal degeneration in various animal models of retinal disease. Finally, these vectors have been used to deliver anti-angiogenic molecules such as PEDF and angiostatin for the treatment of ocular neovascularization in animal models of diabetic retinopathy, retinopathy of prmaturity, and the wet form of age-related macular degeneration (Raisler et al., 2002;

Auricchio et al., 2002). Although rAAV has been shown to be effective at delivering therapy to a wide variety of organs and tissues, it is clearly the vector of choice for transduction of retinal cells.

Project

The following chapters describe experiments designed to characterize and treat a mouse model of retinitis pigmentosa that expresses a human rhodopsin transgene with a tyrosine to methionine mutation at the 17th amino acid of the protein. I will discuss breedings designed to express this transgene on a hemizygous null mouse rhodopsin background to more closely imitate the genotype found in human RP patients. The progression of retinitis pigmentosa in this mouse line will be docmumented, as will the development of a ribozyme-mediated gene therapy strategy to treat the mice. Finally I will discuss the results of a pilot study involving subretinal injection of rAAV expressing these therapeutic ribozymes that led to some interesting observations concerning the light sensitivity of the hT17M transgenic line, and strategies to circumvent this issue.

CHAPTER 2
CHARACTERIZATION OF A NOVEL MOUSE MODEL OF RETINITIS PIGMENTOSA

Introduction

Human patients with the T17M rhodopsin mutation exhibit classic symptoms of autosomal dominant retinitis pigmentosa. Affected individuals report loss of peripheral and vision and night blindness, accompanied by decreased ERG response and eventually culminating in loss of central vision. Postmortem examination of eyes from affected patients reveals heavy deposits of bone spicule-like pigmentation in the inferior retina that are accompanied by severe loss of photoreceptors (Li et al., 1994). Interestingly, photoreceptors of the superior retina are relatively well-preserved, a feature that is uncommon in RP patients. These mutants are intriguing in that they reduce or abolish glycosylation at position 15 of the gene (Kaushal et al., 1994). As inhibition of glycosylation by tunicamycin causes defects in ROS morphology in frogs (Fliesler et al., 1985), this raises the possibility that T17M rhodopsin may not be correctly incorporated into the outer segment discs.

In 1998, Li et al. described the creation of a mouse model of T17M rhodopsin-mediated ADRP. These transgenic mice were created using a 17 kilobase human geneome fragment that included the rhodopsin gene flanked by 4.8 kilobases of upstream and 6.2 kilobases of downstream sequence. The gene contained a single nucleotide substitiution to change codon 17 from threonine to methionine. ERG analysis of these mutant animals demonstrated that they underwent complete photoreceptor degeneration

by eight months of age. Subsequent studies with this animal model demonstrated a therapeutic effect of vitamin A supplementation, which reduced the rate of decline in a- and b-wave ERG amplitudes. This partial rescue was accompanied by an increase in photoreceptor survival in the outer nuclear layer. Parallel experiments involving a mouse line containing a P347S rhodopsin mutation did not show vitamin A rescue, providing evidence for different paths of retinal degeneration between the two mutants (Li et al., 1998).

We obtained this line from Dr. Li with the goal of developing a ribozyme therapy for T17M-mediated ADRP. It was impossible to create mice containing two copies of the human transgene (the cross led to embryonic lethality), with the result that mice containing a 1:1 genotypic ratio of mutant to wild-type rhodopsin could not be created on a wild-type rhodopsin background. In order to establish a mouse model that underwent a more rapid degeneration, as well as one in which the genotype of the model more closely mimicked the naturally occurring disease phenotype (i.e. one mutant allele and one wild-type allele), we decided to breed our hT17M animals onto a mouse rhodopsin knockout (mrho-/-) background (Lem et al., 1999). The resultant animals, which would contain one copy of mutant hT17M human rhodopsin transgene and no copies of wild-type mouse rhodopsin, could then be crossed to wild-type (mrho+/+) mice to produce animals that are heterozygous null at the mouse rhodopsin locus (mrho+/-), of which half would also contain the hT17M mutant rhodopsin transgene.

In this chapter I describe the creation and analysis of an mrho+/-; hT17M mouse model of retinal disease. I will discuss the breeding and PCR genotyping of these

animals, and will document the visual degeneration in this line as assayed by ERG, funduscopy, and histological examination.

Materials and Methods

DNA Oligonucleotides

DNA oligonucleotides were ordered from Invitrogen (Palo Alto, CA), at a 50 nmole scale of synthesis. Oligonucleotides were desalted, but otherwise unpurified by the manufacturer. The sequences were as follows:

hExon 2 sense primer: 5'-GAGTGCACCCTCCTTAGGCA-3'

hExon 2 antisense primer: 5'-TCCTGACTGGAGGACCCTAC-3'

mRHO Exon 1 sense primer: 5'-CCAAGCAGCCTTGGTCTCTGTCTA-3'

mRHO Exon 1 antisense primer: 5'-TGTGCGCAGCTTCTTGTGGCT-3'

Neo sense primer: 5'-AGGATCTCCTGTCATCTCACCTTGCTCCTG-3'

Neo antisense primer: 5'-AAGAACTCGTCAAGAAGGCGATAGAAGGCG-3'

Isolation of Genomic DNA

Genomic DNA was isolated from 0.5 cm tail snips from candidate mice using the Quiagen DNeasy Kit (Quaigen Inc, Valencia, CA), as per the manufacturer's instructions. In brief, the tails were digested overnight at 50^{o}C in digestion buffer supplemented with Proteinase K. The resultant suspension was diluted, bound to the DNeasy column, washed twice, and eluted twice with 100 microliters of elution buffer, for a final volume of 200 microliters of genomic DNA suspension. Three microliters of this genomic DNA were used for PCR analysis, the rest was stored at either -20^{o} or 4^{o}C.

PCR Analysis of Genomic DNA

Endogenous mouse rhodopsin genotypes were determined using mRHO Exon 1 and Neo primers. Genomic DNA from mice that are wild-type at the mouse rhodopsin locus (mrho+/+) produce products with the mRHO Exon 1 primers, which amplify a 270 bp fragment, while the Neo primers will produce no product, as there is no Neo knock-out cassette to amplify.

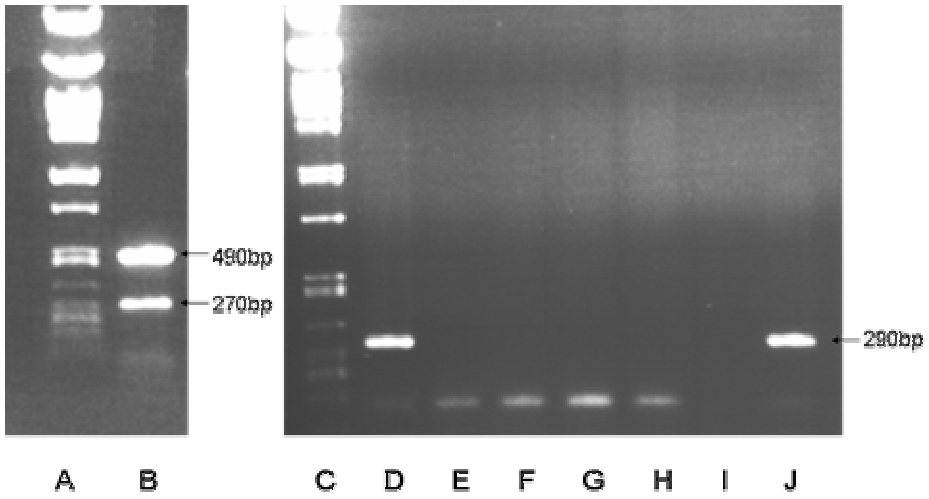

Figure 2-1. Agarose gel electrophoresis of PCR reactions performed to determine the mouse rhodopsin genotype (left gel) or confirm the presence or absence of the hT17M transgene (right gel). Lane B shows amplification of the 490 bp Neo and 270 bp mRho PCR products from a mRho+/- mouse. Lanes D and J show amplification of the 290 bp human rhodopsin PCR product. Lanes E - I are negative for human rhodopsin. Lanes A and C are size standards.

Conversely, DNA from mice that are homozygous for a knockout at the mouse rhodopsin locus (mrho-/-) will produce a 490 bp fragment with the Neo primers, while producing no product when amplified with the mRHO Exon 1 primers. DNA from mice that are heterozygous null at the mouse rhodopsin locus (mrho+/-) are able to produce both fragments. Presence of the human T17M rhodopsin transgene was determined by PCR amplification of genomic DNA with the hExon 2 primers, which amplify a 290 bp fragment in the presence of the transgene (Figure 2-1).

PCR reactions were set up in 50 µl volumes as follows: 3µl (~1µg) genomic DNA, 5µl 10X PCR Buffer (Sigma, St. Louis, MO), 0.5 µl 100mM dNTP mix (Sigma), 0.25µl 100mM sense primer, 0.25µl 100mM antisense primer, 0.5µl (1 Unit) Taq Polymerase (Promega, San Luis, CA), and 40.5 ml dH20. PCR was then carried out as follows: 1) 95^{o}C for 10 minutes; 2) 95 ^{o}C for 45 seconds; 3) 54 ^{o}C for 45 seconds; 4) 72 ^{o}C for 60 seconds; 5) repeat steps 2-4 for 28 cycles; 6) 72 ^{o}C for 10 minutes. PCR amplifications were performed on a Gene Amp PCR System 2700 thermocycler (Applied Biosystems, Foster City, CA). The presence or absence of the PCR product of interest was verified by agarose gel electrophoresis.

Electroretinography

Mice were dark adapted overnight. All subsequent ERG procedures were performed under dim red light (wavelength >600nm), which does not activate rhodopsin. Mice were anesthetized with IP injections of xylazine (13mg/kg) and ketamine (87mg/kg) (Phoenix Pharmaceuticals, St. Joseph, MO). The mouse corneas were anesthetized with a drop of 0.5% proparacaine HCl (Akorn, Buffalo Grove, IL), and dilated with a drop of 2.5% phenylephrine HCl (Akorn). Measurement electrodes tipped with gold wire loops were placed upon both corneas with a drop of 2.5% hypromellose (Akorn) to maintain electrode contact and corneal hydration. A reference electrode was placed subcutaneously in the center of the lower scalp of the mouse, and a ground electrode was placed subcutaneously in the hind leg. The mouse rested on a homemade sliding platform that kept the animal at a constant temperature of 37^{o} C. The animal was positioned so that its entire head rested inside of the Ganzfeld (full-field) illumination dome of a UTAS-E 2000 Visual Electrodiagnostic System (LKC Technologies, Inc.,

Gaithersburg, MD), as shown in Figure 2-2. Full-field scotopic ERGs were measured by 10 msec flashes at an intensity of 0.9 and and 1.9 log cd m-2 at 1 minute intervals.

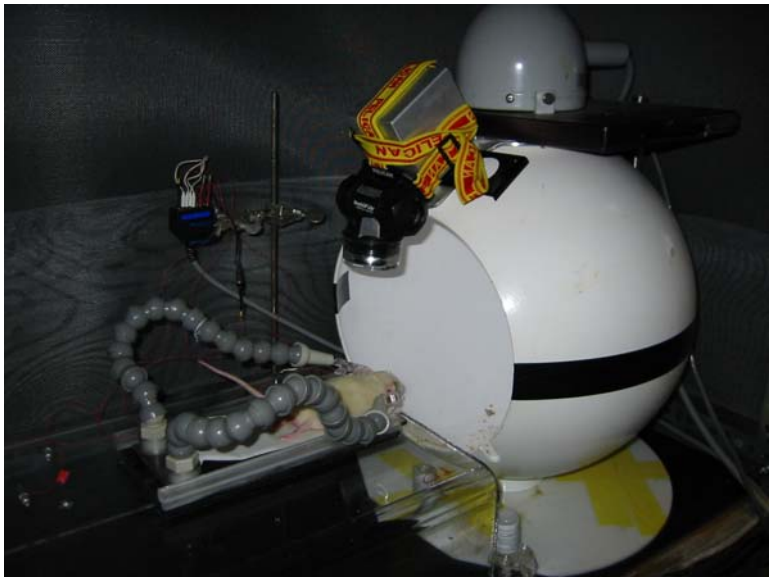

Figure 2-2. Electroretinographic apparatus. The anesthetized animal rests on a warming tray that can slide in and out of a Ganzfeld illumination dome. Electrodes are held in place with homemade articulable plastic arms.

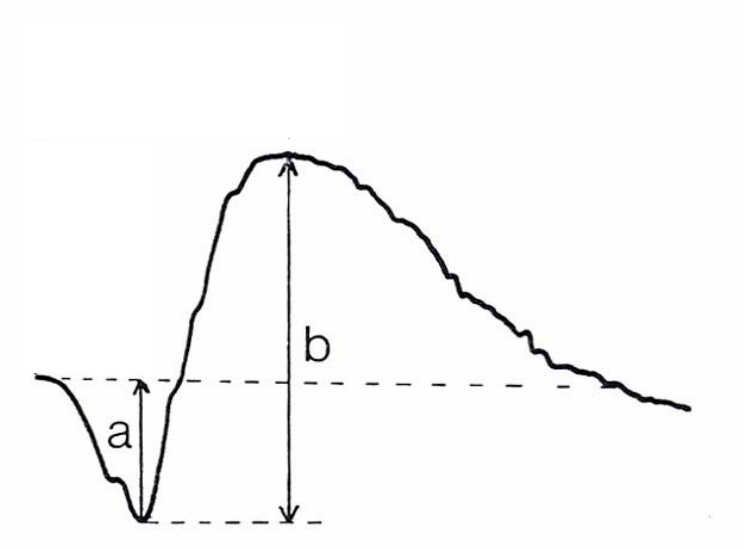

Figure 2-3. An example of an ERG tracing. The X axis of this trace represents the elapsed time of the signal, while the Y axis shows the intensity of the response. The amplitudes used to calculate a and b-waves are shown .

Responses were amplified at a gain of 4,000, filtered between 0.3 to 500Hz and digitized at a rate of 2,000 Hz on two channels. Five responses were averaged at each intensity. The wave traces analyzed using UTAS-E 2000 software package (LKC Technologies, Inc.). A-waves were measured from the baseline to the peak in the cornea-negative direction; b-waves were measured from the cornea-negative peak to the major cornea-positive peak (Figure 2-3).

Funduscopy

Mice were anesthetized, and their corneas anesthetized and dilated as described above. Fundus photography was performed by Dr. Quihong Li with a Kowa Genesis hand held fundus camera (Kowa Company, Ltd., Tokyo, Japan) focused through a Volk Super 66 Stereo Fundus Lens (Keeler, Berkshire, England). Two pictures of each eye were generally taken to ensure a properly focused image.

Histology

Mice were euthanized by an overdose of Isoflurane (Abbot, North Chicago, IL) followed by cervical dislocation. Eyes were quickly removed and fixed overnight in 4% paraformaldehyde and transferred to a solution of phosbate buffered saline (PBS) (137mM NaCl, 10mM PO_4, 2.7Mm KCl, pH 7.4). Histological sectioning and subsequent H&E staining was performed by UF Histology core technicians. This program of sectioning resulted in twelve serial sections through the entire eye. Sections that contained the optic nerve were then photographed at 20X power using a Zeiss Axiophot Z microscope equipped with a Sony DXC-970MD 3CCD Color Vid Camera and an MCID Elite Stage, utilizing MCID (Imaging Research, Inc., Ontario, Canada) Analysis Software (Imaging Research, Inc.) that stitched individual images together to create a tile-field composite image of the entire retina. The images were viewed with

Adobe Photoshop, and a radial template overlay was used to define six equivalent and equally spaced regions of the retina. From each of these areas, the mean value from three separate ONL counts was determined, and these regional counts were then averaged to generate a value that represented the ONL thickness of the retina. Statistical comparisons between the transgenic and non-transgenic values were performed to generate P values using the paired, one-tailed Student's t-test feature of Exel spreadsheet software (Microsoft, Redmond, WA).

Results

Breeding Founder and Experimental Mice

A breeding pair of mrho+/- mice containing the hT17M transgene was kindly provided by Dr. Tiansen Li in 2002. However, this line had subsequently undergone a mating crisis due to poor fecundity and had become poorly characterized by the time these studies were initiated. It was uncertain which members of the colony actually contained the hT17M transgene, and of what respective mouse rhodopsin genotype those animals were. It was necessary to screen the entire colony by PCR for the hT17M transgene and then work from there. Several mice were found that contained the hT17M transgene; these animals were bred to mrho-/- mice, and their progeny were screened by PCR for the hT17M transgene, as well as for their respective genotype at the mouse rhodopsin locus. Eventually, mice were obtained that were heterozygous null for mouse rhodopsin (mrho-/-) and also contained the hT17M mutant rhodopsin transgene. Two mrho-/-; hT17M males were crossed to wild-type C57Bl6 female mice to breed the mrho+/-; hT17M animals used in these experiments. Concurrently, mrho-/-; hT17M females were crossed to mrho-/- males to maintain the hT17M transgene on a mouse rhodopsin null background.

ERG Natural History

Once these lines were breeding reliably, an ERG natural history study was conducted on the mrho+/-; hT17M mice and non-transgenic littermates. Two litters were genotyped for this study, producing eight mrho+/- animals and eight mrho+/-; hT17M siblings. These animals were subjected to ERG analysis every two weeks for the next six and a half months. Right and left eye amplitudes were averaged for each animal, and the averages of each group were plotted for each time point (Figures 2-4 and 2-5). Additionally, the ratio of the mrho+/- response to the mrho+/-; hT17M response for each time point was plotted (Figures 2-6 and 2-7).

There was a definite loss of both a- and b- wave responses over the life of the hT17M transgenic animals compared to their non-hT17M littermates. The a-wave response showed particularly early degradation, as the mutant response was only half that of the non-mutant siblings at one month of age. Mutant a-wave responses remained at around 50% of those of the non-transgenic animals for the next 2.5 months, when they again underwent a significant drop relative to their non-mutant siblings, to around 30% of non-mutant a-wave amplitude. The b-wave amplitudes of the transgenic animals were more robust, starting out at around 70 to 80% percent of the non-transgenic littermates and remaining so for the next 2.5 months, when they began to undergo steady a steady decrease in amplitude at around the time that the a-waves exhibited their drop to 30%.

Funduscopy

In order to see if the degeneration indicated by the ERG natural history study would be apparent upon funduscopic examination of the retina, two mrho+/- siblings, one of which contained the hT17M transgene, underwent ERG analysis at 6 months of age. The following day, fundus photographs were taken to visualize the retinas of these

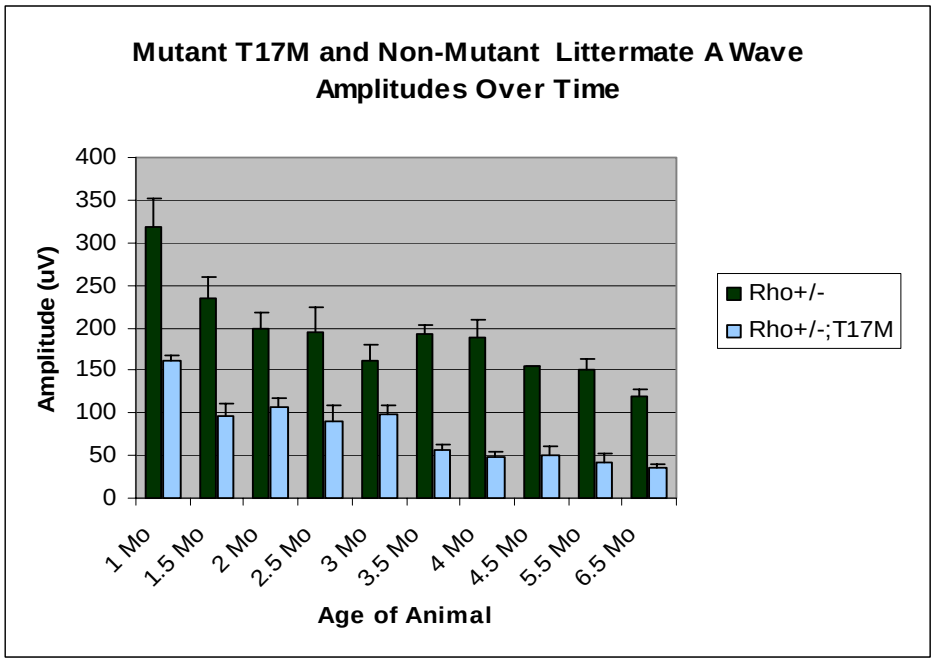

Figure 2-4. 10 dB intensity ERG a-wave natural history of mrho+/- and mrho+/-; hT17M mice.

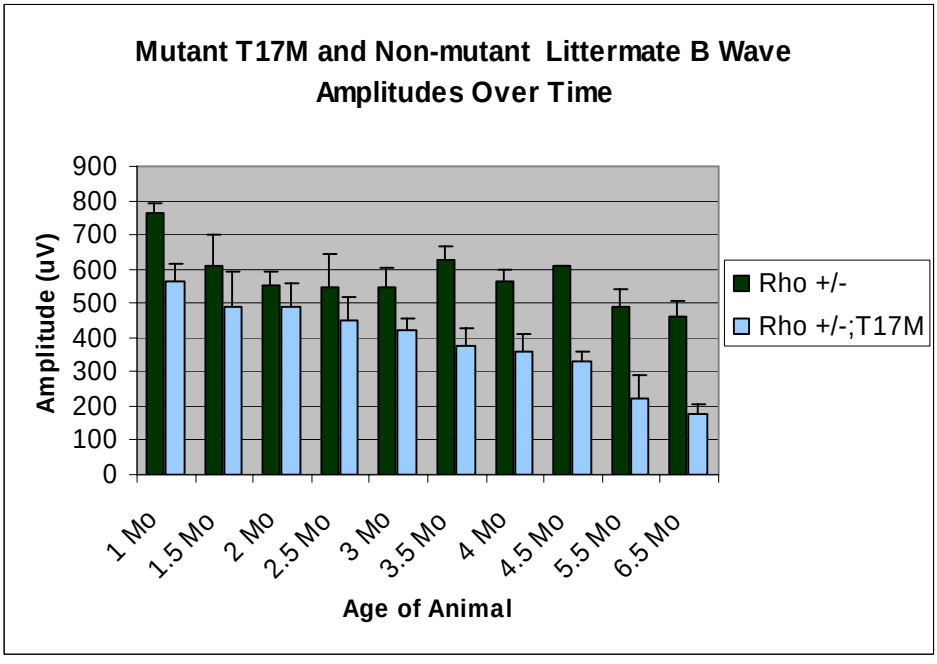

Figure 2-5. 10 dB intensity ERG b-wave natural history of mrho+/- and mrho+/-; hT17M mice. ERGs were performed at the 10dB light intensity.

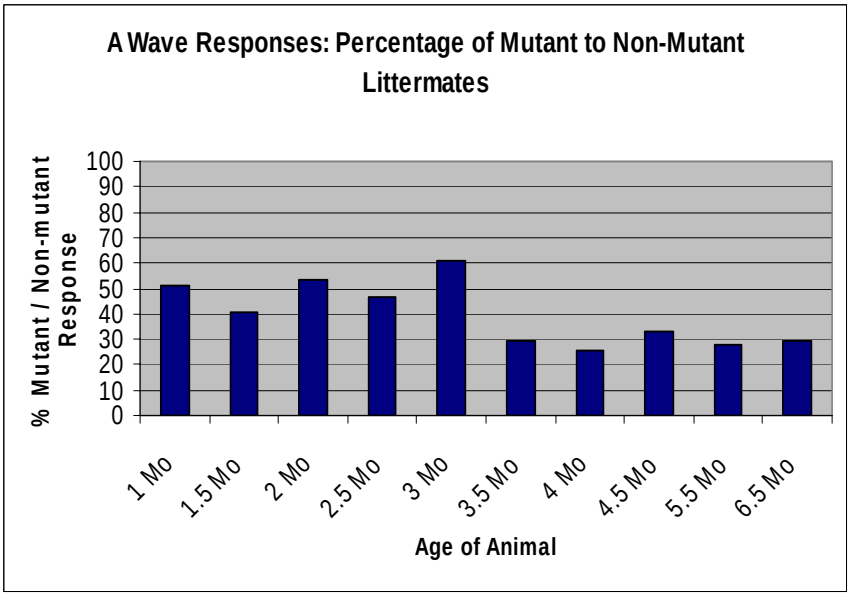

Figure 2-6. 10 dB intensity a-wave responses charted as a percentage of the average mrho+/-; hT17M response to the average response of the mrho+/- siblings at each time point.

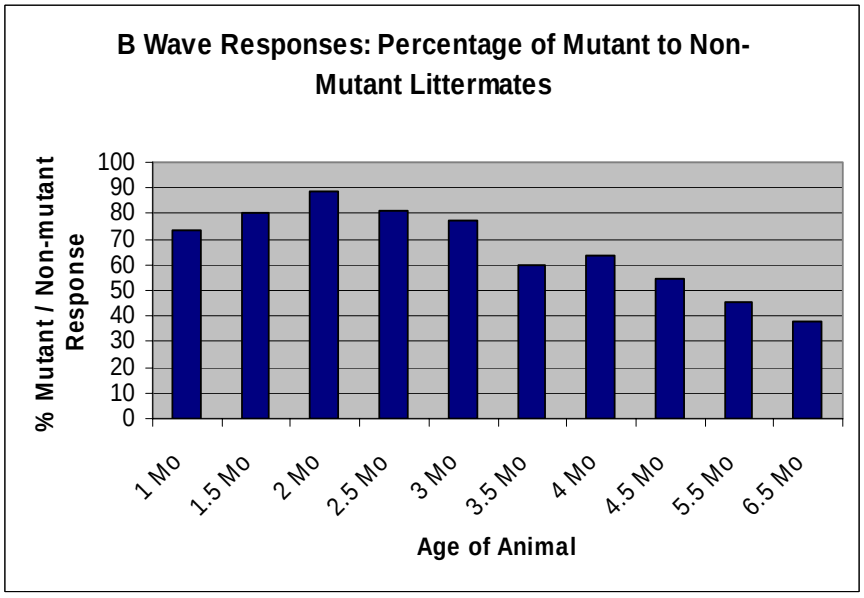

Figure 2-7. 10 dB intensity b-wave responses charted as a percentage of the average mrho+/-; hT17M response to the average response of the mrho+/- siblings at each time point.

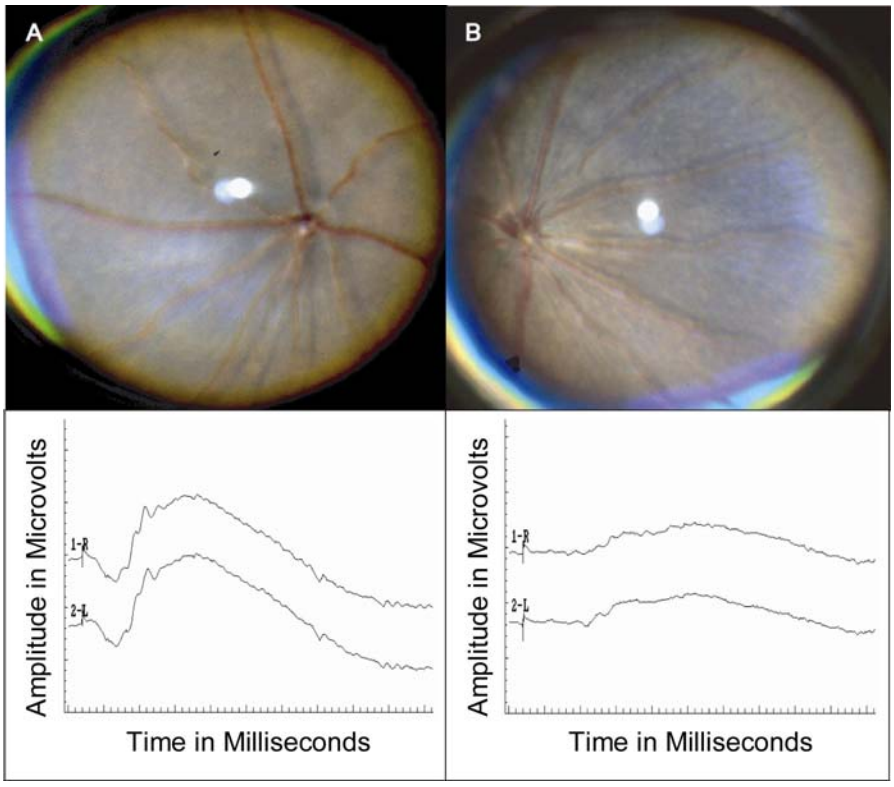

Figure 2-8. Fundus photographs and respective 10 dB intensity ERG tracings taken at 6 months of age. Photos and tracings from a mrho+/- animal are shown on the left (A), and those of its mrho+/-; hT17M littermate are shown on the right (B).

animals. The resultant images, matched with their respective ERG tracings, are shown in Figure 2-8. The fundus of the mrho+/- mouse looked normal, exhibiting relatively even pigmentation and healthy-appearing retinal morphology, and ERG analysis of this mouse showed robust a- and b-wave amplitudes. The hT17M sibling displayed a markedly depressed ERG tracing, as well as shadowy spotting in its fundus picture, indicating that the retina of this mutant animal had thinned as its photoreceptors degenerated.

Histology

Two of the animals (hT17M mutant and non-mutant sibling) from the natural history were sacrificed at 4 months of age to obtain an early look at the histological

results of the hT17M –mediated retinal degeneration. The rest of the mice were all sacrificed at 6.5 months, as the a- and b-wave loss seemed to plateau and it was feared that waiting longer would result in retinas that were too degraded to provide good sections. Representative sections from these animals showed severe, progressive degeneration of the outer nuclear layer (ONL) that is consistent with the loss of ERG response, both of which are hallmarks of retinitis pigmentosa. (Figure 2-9).

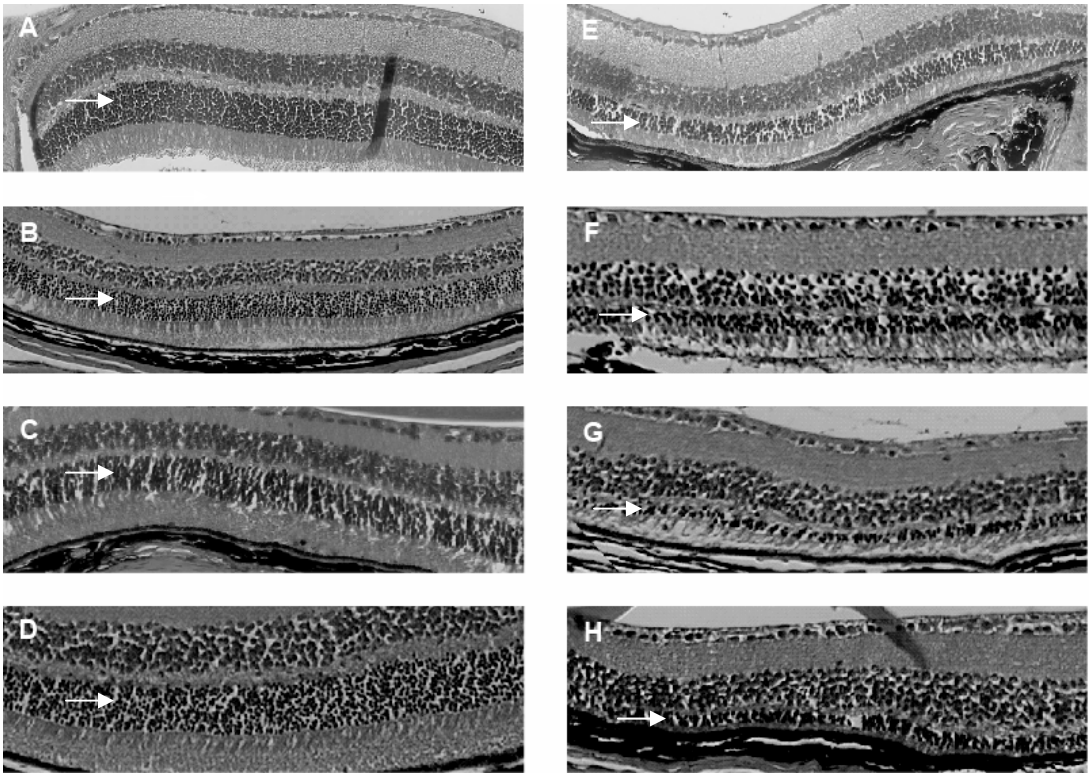

Figure 2-9. Representative sections of mrho+/- mice (A-D) and mrho+/-; hT17M siblings (E-H). Sections A and E are from animals sacrificed at 4 months of age, all other sections are from animals sacrificed at 6.5 months of age, at the completion of the natural history study. All hT17M animals (E-H) show severe degeneration of the outer nuclear layer (ONL). Arrows indicate ONL.

In order to obtain a more concrete idea of the extent of the ONL degeneration, tile field mapped images of the hT17m and non-hT17M retinas were examined. A semi-transparent template (Figure 2-10) was used to pinpoint eight areas of each retina from which ONL thickness could be measured (in numbers of nuclei) and averaged. The mean

of the counts taken from the six points was determined, and this number represents the average thickness of the ONL for that eye. For the animals sacrificed at 6.5 months of age, the ONL values from both eyes were averaged together, while only one eye from

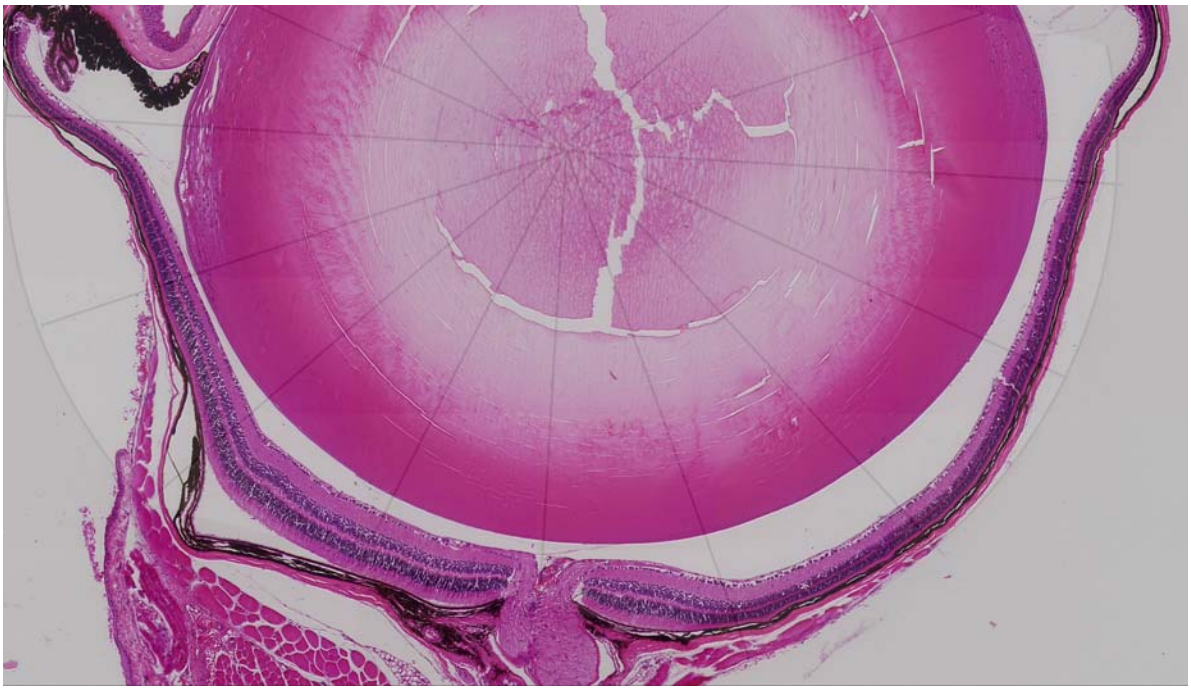

Figure 2-10. Tile-field mapped image of a mouse retina, with a translucent overlay that defines eight evenly-spaced sections of the retina from which outer nuclei counts can be obtained.

Table 2-1. ONL averages taken from mrho+/- and mrho+/-; hT17M mice sacrificed and analyzed at 4 and 6.5 months of age. ** indicates significant difference between mutant and non-mutant values with a P value of less than .001.

	mRho+/- mice	mrho+/-; hT17M mice
ONL Thickness at 4 months	8.8 Rows	5.9 Rows
ONL Thickness at 6.5 months	7.7 Rows**	2.4 Rows**

each animal at the 4 month time point was able to be analyzed. These results are summarized on Table 2-1. By this measure, hT17M mice exhibited significant thinning

of the outer nuclear layer when compared to their non-hT17M littermates sacrificed at the 6.5 month time point. hT17M mice sacrificed and analyzed at the 4 month time point also showed a reduction in the ONL thickness.

Discussion

The original mrho+/+; hT17M mouse line obtained from Dr. Tiansen Li provided a useful animal model for the study of retinal disease. These animals showed progressive photoreceptor loss that was accompanied by a loss of a- and b-wave ERG amplitudes, and experiments involving treatment of this mouse with vitamin A supplementation produced some compelling results. However, by the time we began these experiments, the line had become uncharacterized for reasons already described. A goal of the preceding experiments was to develop efficient methods for genotyping these mice and to breed the remaining hT17M positive animals to a final mrho-/- background. We then wanted to use these mrho-/-; hT17M mice both for maintenance of the transgenic line and for creation of a mrho+/-; hT17M transgenic line that would be useful in developing therapy for autosomal dominant retinal disease.

The PCR assays that we have developed to characterize these lines are simple and accurate. Use of the Quiagen DNeasy kit allows a researcher to easily purify substantial amounts of genomic DNA from small pieces of mouse tail in a short period of time. Two separate PCR reactions allow for determination of the endogenous mouse rhodopsin genotype (mrho+/+, mrho+/-, or mrho-/-), and to screen for the presence or absence of the T17M human mutant rhodopsin transgene. The line is now maintained on both the mrho-/- and mrho+/+ genetic background.

The retinal degeneration displayed by mrho+/-; hT17M transgenic line is an excellent model of the vision loss observed in human patients suffering from ADRP. Bi-

monthly ERG recordings demonstrated progressive loss of rod photoreceptors in the hT17M transgenic animals, culminating in a severe loss of visual response by six months of age, while the non-transgenic littermates retained normal visual function. The loss of ERG was accompanied by a progressive thinning of the ONL as determined from retinal sections, with mrho+/-; hT17M mice displaying a loss of 40% of their ONL by 4 months of age and a loss of 70% of their ONL by 6.5 months of age, as compared to their non-transgenic littermates. Funduscopic analysis of the transgenic animals revealed marked retinal thinning by 6 months of age, with non-transgenic littermates again displaying normal retinal morphology.

It is unfortunate that it has so far been impossible to breed the hT17M transgene to homozygosity. This is probably due to insertional inactivation of an unknown gene that is embryonic lethal if not present in at least one copy. The lines have been outbred for several years now since their arrival, and future attempts to breed the transgene to homozygosity could well meet with success. At present, our breeder mice are limited to one copy of the hT17M transgene, with the result being that, at most, around 75% hT17M transgenic mice can be produced from a breeding of two hT17M transgenic mice. As our breeders to date have consisted of one mrho-/-; hT17M transgenic mouse crossed with a wild-type C57BL6 mate, we have been producing litters composed of around 50% transgenic and 50% non-transgenic pups on an mrho+/- background. This is a drawback in terms of requiring twice as many mouse pups to provide sufficient numbers of transgenic animals for testing therapy for ADRP. However, this drawback has proven useful in that most experimental litters contain several non-transgenic control mice. In

fact, these non-transgenic littermates were essential in discovering an hT17M rhodopsin-mediated light sensitivity that will be discussed in future chapters.

Not all mouse models of retinal disease are practical for developing therapy. For example, one of the mouse lines created by Olsson et al. to express a human rhodopsin transgene containing the P23H mutation showed nearly complete photoreceptor degeneration by 20 days of age (Olsson et al., 1992). This is too rapid a degeneration to provide an effective test subject for all but the most rapidly acting therapies. On the other hand, an animal model that undergoes degeneration too slowly is also problematic because experiments utilizing the line can take a long time to provide useful data.

The hT17M human transgene expressed on an mrho+/+ background underwent a progressive loss of photoreceptors culminating in total loss of vision by around eight months of age. We decided to breed these animals to a mrho+/- background with the goal of both creating a mouse line that contained one copy each of mutant human and wild-type rhodopsin genes, and of developing a model that would undergo a more rapid retinal degeneration while still providing a therapeutic window for treatment. The resultant hT17M; mrho+/- animals did undergo a more rapid retinal degeneration, with almost complete loss of functional rod photoreceptors by around 6.5 months of age. Additionally, this line displayed a-wave and b-wave ERG responses of 100 μV and 400 μV, respectively, at 2.5 months of age. By 6.5 months of age these responses had degraded to an a-wave response of less than 50 μV and a b-wave response of less than 200 μV. Studies have shown that AAV pseudotype 2/5 can achieve significant transgene expression of mouse photoreceptor cells by twelve days following subretinal injection (Yang et al., 2002; Rabinowitz et al., 2002). Assuming that our hT17M transgenic mice

receive treatment at weaning (21 days of age), the line should retain ample photoreceptor function by the time one can expect expression of rAAV-delivered therapy designed to prolong retinal function. This therapeutic window should also be wide enough to be amenable to pharmacological treatment.

In conclusion, the hT17M transgene has been maintained and expressed on mrho+/+, mrho+/-, and mrho-/- backgrounds. This line undergoes a progressive photoreceptor degeneration that can be monitored by ERG measurements and that correlates with thinning of the ONL as visualized by funduscopy and by retinal histology. The degeneration of the mrho+/-; hT17M line is practically complete by 6.5 months; yet these mice retain sufficient retinal function and photoreceptor survival at early ages to make them amenable to therapeutic intervention.

CHAPTER 3
AAV-MEDIATED RIBOZYME TREATMENT OF MRHO+/-; hT17M MICE

Introduction

The hT17M mutant human rhodopsin transgene causes the autosomal dominant form of retinitis pigmentosa, meaning that expression of the mutant allele is responsible for the disease. One way to treat an autosomal dominant disorder is to selectively destroy the mRNA encoding the mutant allele – in theory this should abolish expression of the mutant protein and rescue the disease (Hauswirth et al., 2000). Mice bred to be hemizygous null at the rhodopsin allele (mrho+/-) show only slightly reduced ERG responses when compared to mice that contain two wild type copies of the gene (Humphries et al., 1997). Thus in our mrho+/-; hT17M line, removal of the mutant human mRNA while leaving the wild-type mouse message intact should protect against the vision loss associated with the mutant rhodopsin gene product.

Ribozymes are ideally suited for the treatment of autosomal dominant disease. As discussed before, the sequence specificity of ribozyme cleavage is stringent enough that a ribozyme can often be designed to discriminate between mutant and wild-type target RNAs that differ by a single nucleotide. This makes it feasible to treat certain dominant diseases arising from point mutations with ribozymes that selectively degrade the mutant RNA, thus selectively reducing or abolishing expression of the mutant protein. It was recently shown that the use of such a ribozyme that targeted the reduction of a P23H mutant rhodopsin message resulted in rescue of vision in a rat model of ADRP (Lewin et

al., 1998; LaVail et al., 2000; Drenser et al., 1998). We wanted to explore the efficacy of a similar ribozyme-mediated therapy for the threonine to methionine at position 17 (T17M) mutation carried in our rho+/-; hT17M mouse line.

To this end we designed ribozymes to selectively cleave human rhodopsin mRNAs. In most forms of ribozyme gene therapy for autosomal dominant disease, the ribozymes are designed to select between mutant and non-mutant messages because of sequence differences at the site of the causative mutation. This means that the therapeutic ribozyme must be specifically tailored to cleave the message at the mutation site, and often this target site is less than ideal for ribozyme-mediated cleavage, if it is susceptible to cleavage at all. In the hT17M transgenic mouse model, expression of a mutant human gene on a mouse genetic background is responsible for the disease, so we were able to design ribozymes that were targeted to ideal cleavage sites in the human rhodopsin gene that differed from the endogenous, wild-type mouse sequence, rather than having to design a ribozyme to a target site that was restricted to the site of the mutation. Using this strategy we were able to create two highly active ribozymes that cleaved the human rhodopsin message but should theoretically leave the mouse message intact.

Once an effective ribozyme has been created, the next step in developing a therapy for retinal disease is to deliver the ribozymes to the pertinent retinal cells. For this purpose we used recombinant adeno-associated virus (AAV) delivery vectors. As previously discussed, AAV is extremely well suited for retinal gene transfer (Flannery et al., 1997). For our experiments we decided to use AAV pseudotype 5, as this pseudotype has demonstrated preferentially high levels of transduction in photoreceptor cells, as well as a rapid onset of transgene expression (Yang et al., 2002). To drive the expression of

our human rhodopsin-specific ribozymes we chose the MOPS500 promoter, which has been shown to achieve impressive levels of transgene expression in the rod photoreceptors of rats and mice (Flannery et al., 1997). The combination of AAV pseudotype 5 vectors delivering ribozymes under the control of the MOPS500 promoter helps ensure high levels of ribozyme expression that are specific to the rod photoreceptors of treated animals.

In this chapter, I describe the creation and *in vitro* testing of two ribozymes designed to specifically cleave the human rhodopsin transgene. I will discuss how these ribozymes were cloned in specialized plasmids for packaging as recombinant AAV. Finally, I will detail the subretinal injection technique and the results of delivering this virus to the subretinal space of mrho+/-; hT17M transgenic animals.

Materials and Methods

RNA Oligonucleotides

RNA nucleotides were ordered from Dharmacon Research Inc. (Boulder, CO), at the 50 μmolar scale. The sequences were as follows:

Rz1: 5'-CCGAACUGAUGAGCCGUUCGCGGCGAAACGAAG-3'

Rz3: 5'-GUGAACUGAUGAGCCGUUCGCGGCGAAACGAGC-3'

Target1: 5'-CUUCGUCUUCGG-3'

Target 3: 5'-GCUCGUCUUCAC-3'

DNA Oligonucleotides

DNA oligonucleotides were obtained from Invitrogen at the 40 nmolar scale of preparation. Oligonucleotides used for cloning had 5' phosphate groups chemically added by the manufacturer, and were purified by desalting. Their sequences were as follows:

Rz1 Cloning Sense:

5'-**AGCTT**CCGAACTGATGAGCCGTTCGCGGCGAAACGAAG**ATGCA**-3'

Rz1 Cloning Antisense

5'-**T**CTTCGTTTCGCCGCGAACGGCTCATCAGTTCGG**A**-3'

Rz3 Cloning Sense

5'-**AGCTT**GTGAACTGATGAGCCGTTCGCGGCGAAACGAGC**ATGCA**-3'

Rz3 Cloning Antisense

5'-**T**GCTCGTTTCGCCGCGAACGGCTCATCAGTTCAC**A**-3'

Red nucleotides indicate restriction sites for HindIII (AAGCTT) and NsiI (ATGCAT).

Preparation of Synthetic RNA Ribozymes and Substrates

All hammerhead ribozymes as well as the substrate RNAs were purchased from Dharmacon Research, Inc. (Boulder, CO). The RNA oligonucleotides were chemically synthesized with an acid-labile orthoester protecting group (to reduce ribonuclease degradation) on the 2´-hydroxyl (2´-ACE) that must be deprotected by incubation at pH 3.8 at 60^{o}C according to the manufacturer's protocol prior to use. Deprotected RNA oligos were suspended at a final concentration of 300 picomoles per microliter.

5' End-labeling of Deprotected Target RNAs

Prior to in vitro kinetic analysis, the target RNAs were 5' end-labeled with [γ–^{32}P]-ATP (ICN, Irvine, CA) using T4 Polynucleotide Kinase (T4 PNK) (Promega, Madison, WI). A typical reaction contained: 2 µl target RNA oligo (20 picomoles total), 1 µl of 10X PNK Buffer [700 mM Tris-HCl (pH 7.6 at 25^{o}C), 100 mM $MgCl_2$], 1 µl RNasin

(Promega), 1 μl 0.1M DTT, 3 μl H_2O, 1 μl [γ–^{32}P]-ATP, and 1 μl T4 PNK. Reactions were incubated at 37°C for 30 minutes, and then 90 μl of H_2O was added. The mixture was then incubated at 65 for 5 minutes to inactivate the T4 PNK. Two Phenol:Chloroform:Isoamyl Alcohol extractions were then performed, and 90 μl of the aqueous phase was purified over a Sephadex G-25 Spin Column (Pharmacia, Piscataway, NJ) to separate the labeled target molecule from unincorporated radionucleotides. The resulting labeled target solution was at a final concentration of 0.2 picomoles per microliter.

In Vitro Ribozyme Time Course Analysis

Separate ribozyme and target mixes were made. The ribozyme mix consisted of: 13 μl 400 mM Tris-HCl (pH 7.45), 1 μl ribozyme (diluted to 2 pmol/μl), and 80 μl H_2O. The target mix consisted of 1μl radiolabeled target RNA, (diluted to 0.2 pmol/μl), 1 μl cold target RNA (diluted to 20 pmol/μl), and 8 μl of H_2O. After these two mixes were created, the ribozyme mix was heated to 65°C for two minutes, and then cooled to room temperature for at least ten minutes. 13 μl of a 1:10 RNasin:0.1M DTT mix and 13 μl of 50 mM $MgCl_2$ (for a final reaction concentration of 5 mM Mg Cl_2) were then added, and the solution was equilibrated at 37°C for ten minutes.

For the reaction, the 10 μl target mix was added to the ribozyme mix, the solution was mixed thoroughly by vigorous pipetting, and 10 μl of the reaction mix was immediately added to 10 ul formamide stop buffer (90% formamide, 50 mM EDTA, 0.05% bromophenol blue, and 0.05% xylene cyanol), and placed on ice (this was the 0 minute time point), and the remaining reaction mix was incubated at 37°C. At subsequent intervals of 1, 2, 4, 8, 16, 32, 64, and 128 minutes after the start of the

reaction 10 µl of the reaction mix was removed and likewise added to 10 µl formamide stop buffer and placed on ice.

The reaction/formamide stop buffer mix from each time point was then heat denatured at 95^{o}C for five to ten minutes, then placed on ice for five minutes, and then separated on a 10% polyacrylamide / 8M urea gel. The gel was fixed in 2 L of fixation solution (40% methanol, 10% acetic acid, 3% glycerol) for thirty minutes, dried, exposed to radioanalytic phosphorescent screens, and analyzed using a Molecular Dynamics PhosphoImager system and ImageQuant software (Molecular Dynamics, Sunnyvale, CA). The percentage of substrate cleaved in each sample was determined from the ratio of radioactivity in the 5'-end labeled cleavage product (P) to the sum of the radioactivity in the 5'-end labeled cleavage product and the substrate band (S): % Cleavage = P/P+S. Using Excel (Microsoft, Redmond, WA) the percentage substrate cleaved was then plotted as a function of time to generate a graphical representation of the cleavage time course.

Ligating Ribozyme Sequences into rAAV Packaging Vectors

Complementary DNA oligonucleotides encoding the sense and antisense strands of HRz1 and HRz3 were ordered. In addition to the ribozyme sequence these oligonucleotides contained sequences (shown above in red) appended to their 5' and 3' ends so that when they annealed they formed the sticky overhangs corresponding to HindIII at the 5' end and NsiI at the 3' ends. This allowed the oligonucleotides to be ligated into the rAAV packaging vector, pXX-GS-HP-MOPS500 (Figure 3-1) at a multiple cloning site containing a HindIII restriction site upstream of an NsiI restriction

site. The oligonucleotides came from the supplier with 5'-PO_4 groups already attached to allow immediate ligation into the packaging vector.

To linearize pXX-GS-HP-MOPS 500, 5μg of plasmid DNA was digested with HindIII for three hours at 37°C. The DNA was then ethanol precipitated, resuspended, and digested with NsiI for three hours at 37°C. After the two digestions were complete, the resultant fragment was run on a 1% agarose gel, and the digested plasmid band was visualized by ethidium bromide staining under UV illumination. The band was excised from the gel and the DNA was purified using a "freeze squeeze" technique (Sugden et al., 1975). In brief, the gel fragment was crushed and mixed in an equal volume of phenol in a 1.5 mL Eppendorf tube. The tube was then incubated at -80°C for 2 hours. Next the tube was spun at a speed of 13,000 rpm for 10 minutes, and the aqueous solution was removed. The aqueous solution was then extracted with an equal volume of phenol:chloroform:isoamyl alcohol, ethanol precipitated, and the resultant purified plasmid pellet resuspended at a concentration of 0.5 μg/μl.

To ligate the ribozyme-encoding oligonucleotides with the linearized packaging vector, the complementary oligonucleotides were mixed together for a final concentration of 20 picomoles each in a volume of 4 microliters. To facilitate proper annealing, the oligos were heated to 95°C for five minutes, and then allowed to slowly cool to room temperature. 0.5 μg of linearized plasmid (1 μl) was then added to the mixture along with 5 μl of 5X ligation buffer [250mM Tris (pH 7.5), 50 mM $MgCl_2$, 5mM ATP], 1 μl 25 mM DTT, 3 μl PEG 4000, 10 μl H2O, and 1 μl T4 DNA ligase (Promega). Reactions were incubated at 25°C overnight, and then 2 μl was transformed into 50 μl of electrocompetent *E. coli* by electroporation using a Bio-Rad Gene Pulser II

electroporation apparatus (Bio-Rad, Hercules, CA), utilizing 0.1 mm electroporation cuvettes (USA Scientific, Ocala, FL). The *E. coli* was plated on LB plates containing ampicillin, and the resultant transformants were picked, their DNA isolated, and sequenced for the proper ribozyme insert.

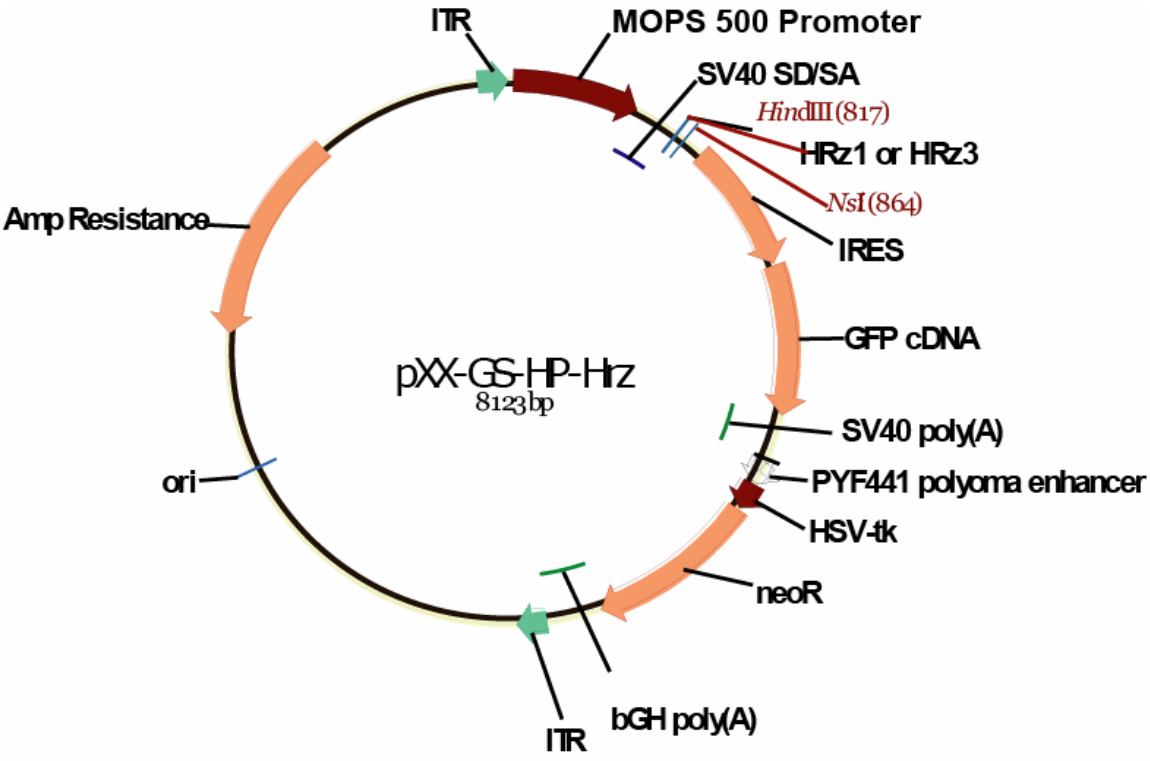

Figure 3-1. pXX-GS-HP MOPS 500 rAAV packaging plasmid. Human rhodopsin specific ribozymes were cloned into the HindIII-NsiI restriction sites as indicated.

Once each ribozyme was successfully cloned into pXX-GS-HP MOPS 500, 700ug of DNA was produced from a 1 L *E. coli* culture, purified via cesium banding on an ultracentrifuge, and finally packaged as recombinant AAV type 5 at the UF Ophthalmology Packaging Core.

Subretinal Injection of rAAV Ribozyme Delivery Vectors

At weaning age (21-24 days) litters were removed from their parents and their right eyes were dilated with 1% atropine sulfate solution (Bausch and Lomb, Tampa, FL). The next morning, the right eyes were again dilated with 1% atropine sulfate, and again an hour before the injection procedure, at which time the eyes also received a drop of 2.5% phenylephrine HCl and 0.5% proparacaine HCl. An hour after this final dilation, the animals were anesthetized by ketamine/xylazine injection and again treated with a drop each of 1% atropine sulfate, 2.5% phenylephrine HCl, and 0.5% proparacaine HCl. The right eyes of these animals then received a drop of 2.5% hypromellose to aid in retinal visualization and to help keep the retina hydrated. Injections were visualized with a Nikon SM2800 (Nikon, Melville, NY) dissecting microscope, with illumination provided by a Southern Micro Instruments 150 Watt fiber optic light source with Schott Fostec fiber optic arms (Southern Micron Instruments, Marietta, GA) (Figure 3-2), which at full power provided an intensity of illumination of around 10,000 lux. A hole was placed in the inferior cornea of the eye with a 28 gauge needle. A blunt 32 gauge needle was then inserted into the hole, the tip of the needle was rotated around the lens, and pushed through the retina until it came to rest at the sclera, which could be visualized by the eye sinking back into the socket. 0.5 μl of rAAV suspension was then slowly delivered into the subretinal space over a period of 20-30 seconds. This injection strategy is depicted in Figure 3-3. VPP antibiotic ointment (Akorn) was placed upon both eyes to maintain hydration and prevent infection in the injected eyes, and the animals were ear marked and 0.5 cm sections of tail tip were removed for genotyping as described previously. The animals were then allowed to recover on a warming plate at 37^{o}C.

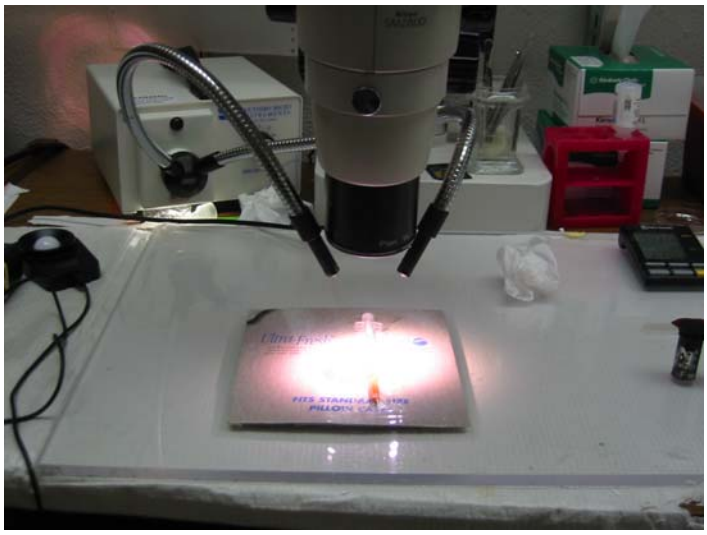

Figure 3-2. Dissecting scope and fiber optic light used during subretinal injections and experimental retinal illumination.

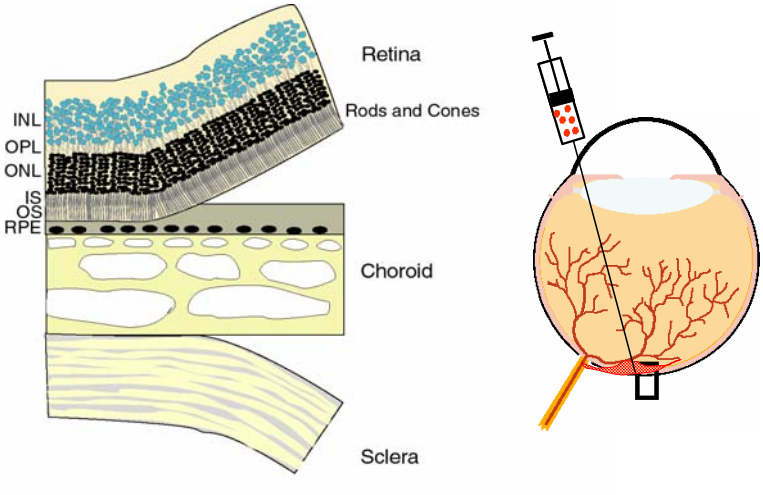

Figure 3-3. Cartoon depicting the subretinal injection. The blunt injection needle is shown passing through the cornea, around the lens, and into the subretinal space (right). Once positioned thus, the rAAV solution can be delivered to the subretinal space (left), resulting in a localized retinal detachment that resolves itself over time as the virus spreads laterally from the site of injection (red arrow). Figure courtesy of Dr. Lynn C. Shaw.

Electroretinography

Electroretinographic analysis of ribozyme-treated animals was performed as described above.

Results

Ribozyme Creation

Our therapeutic plan called for the creation of a ribozyme that would specifically cleave the mutant human rhodopsin mRNA while leaving the endogenous, wild-type mouse mRNA intact. A benefit of this strategy is that it allowed us to consider all possible ribozyme cleavage sites in areas of the human gene that showed polymorphisms with the mouse gene. We were also able to look for the specific cleavage site GUCUU. It has been consistently demonstrated that hammerhead ribozymes cleave more efficiently at the GUC target site than at any other (Shimayama et al., 1995). It has also been reported that hammerhead ribozyme cleavage can be enhanced when the triplet target sequence is followed by a UU or UA dinucleotide (Clouet-d'Orval and Uhlenbeck, 1997).

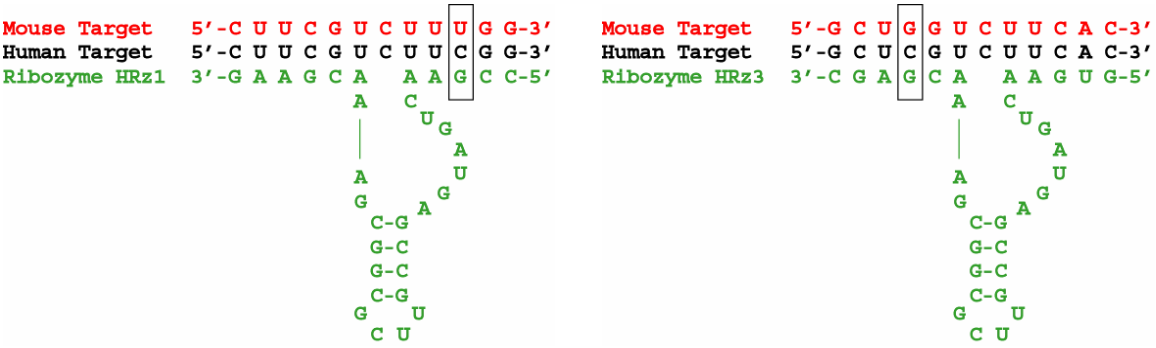

Figure 3-4. Primary structure of ribozymes HRz1 and HRz3 (green), shown paired with their human (black) and mouse (red) target sequences. Polymorphisms between the mouse and human rhodopsin genes are boxed.

The human rhodopsin gene contains 19 GUC sites in its reading frame. Of these, three contained a UU dinucleotide directly following the cleavage site, and two of these GUCUU sites contained single nucleotide polymorphisms between the endogenous mouse gene and the mutant human transgene. The first of these sites is a GUCUU site beginning at nucleotide 310 as measured from the start of the coding sequence for the

gene. The second of these begins at nucleotide 679. The predicted structure of these two areas of the mRNA showed no serious energetically favorable secondary structure that would inhibit proper ribozyme binding to their respective target sites. The two ribozymes, named HRz1 and HRz3, are illustrated in Figure 3-4.

In Vitro Time Course Analysis of HRz1 and HRz3

In vitro cleavage analysis showed HRz1 and HRz3 to be efficient at cleaving the human rhodopsin mRNA. Reactions were performed under a condition of 10-fold excess of substrate relative to ribozyme (10nM to 1nM). Both ribozymes achieved 20% substrate cleavage in one minute in a reaction mixture containing 20mM $MgCl_2$. Magnesium is necessary in cell free reactions to promote the folding of the ribozyme, but is not required in cells. Figure 3-5 shows a representative time course cleavage reaction performed by incubating the HRz1 RNA oligonucleotide with its 12 nucleotide, 5' end-labeled target as described. These reactions generate two bands when separated on polyacrylamide gels. The top band is the radioactively-labeled, uncut 12 nucleotide RNA target molecule, while the bottom band is the 7 nucleotide 5' cleavage product (as only the 5' end of the RNA target oligonucleotide was labeled, the 5 nucleotide 3' cleavage product was not detectable by autoradiography). Phosphorimager analysis was used to determine the relative intensity of these two bands, which in turn were used to calculate the time course cleavage rates as described. Identical time course reactions were performed using the HRz3 ribozyme/target combination (data not shown). Graphical representation of the time course reactions of HRz1 and HRz3, illustrated in Figure 3-6, confirmed the activity of our ribozyme selections and prompted us to initiate efforts to treat the hT17M mice with rAAV expressing these ribozymes.

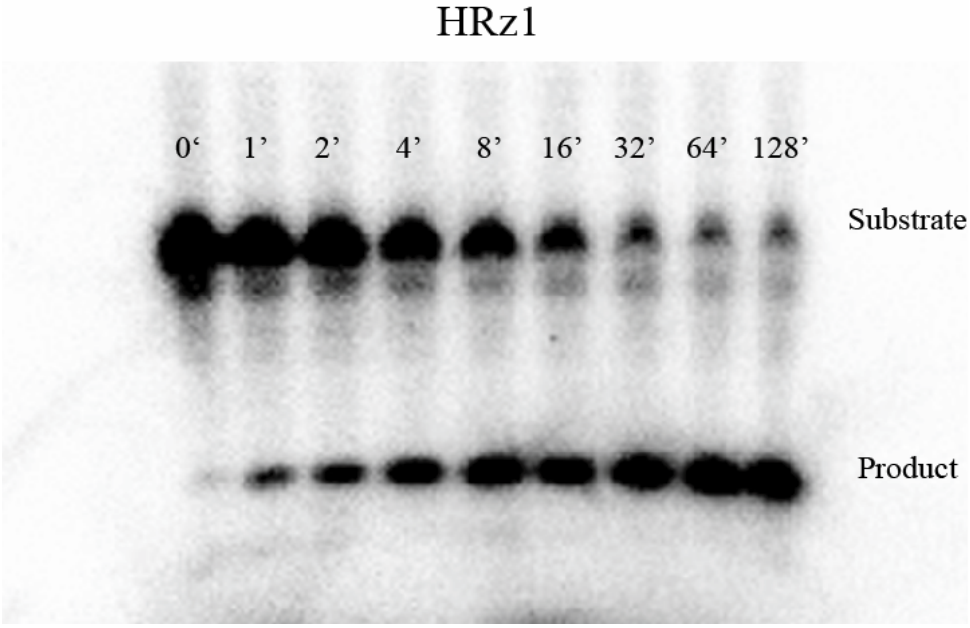

Figure 3-5. Representative PhosphorImager scan of a time course assay showing HRz1 cleavage of a 12 nucleotide synthetic human rhodopsin target RNA.

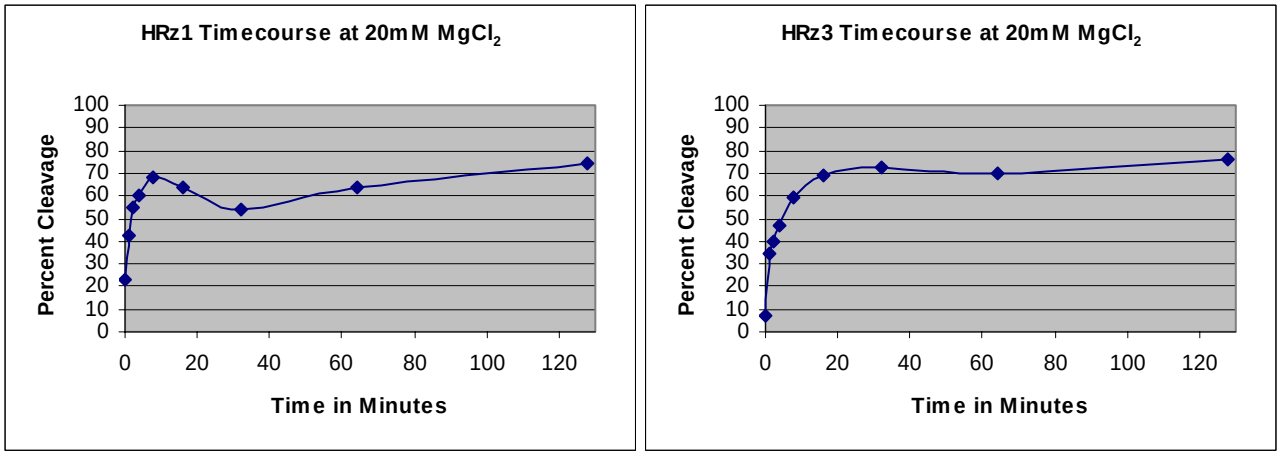

Figure 3-6. Time course of HRz1 and HRz3 cleavage. The percent cleavage of each 12 nucleotide synthetic target by its respective ribozyme is plotted as a function of time. Both ribozymes are able to achieve 20% cleavage in a minute or less in the presence of 20mM $MgCl_2$.

ERG Analysis of hT17M Transgenic Mice Treated With HRz1 and HRz3

Several features of the pXX-MOPS-GS-HP recombinant AAV packaging vector used in these studies merit attention (Figure 3-1). The plasmid contains a multiple cloning site under the control of the MOPS 500 promoter, which has been shown

previously to induce high levels of transgene expression in mouse and rat photoreceptor cells (Flannery et al., 1997). MOPS500 consists of 483 bp of the mouse opsin proximal promoter, including 70 bp of the 5' untranslated region of the mRNA coding sequence. Immediately following the promoter is an SV40 intron (SD/SA), which has also been shown to increase expression of RNAs by promoting nuclear export via the spliceosomal pathway (Bertrand et al., 1997). Next is the multiple cloning site, in which either HRz1 or HRz3 was inserted into the HindIII/NsiI junction as described. Following this is a downstream hairpin ribozyme that generates well-defined 3' ends for the ribozyme transcript, reducing the possibility of the ribozyme interacting with excess downstream sequence in such a way as to cause it to fold into an inactive or inaccessible (to the target mRNA) conformation (Altschuler et al., 1992).

The vector also contains an ampicillin antibiotic resistance gene to aid with bacterial cloning, a neomycin resistance gene enabling selection in mammalian cells using the antibiotic G418, and a GFP marker gene under the expression control of an internal ribosomal entry site (IRES). The entire ribozyme expression, GFP marker, and neomycin resistance cassettes are contained within inverted terminal repeat sequences (ITRs) that are necessary for these various elements to be packaged as recombinant AAV The resultant viruses were purified to a titer of $2x10^{13}$ genome copies/ml (HRz1) and $1x10^{13}$ genome copies/ml (HRz3).

Our initial treatment attempt involved subretinally injecting the right eyes of a litter consisting of five mrho+/-; hT17M transgenic mice and two mrho+/- siblings with 0.5 μl of rAAV expressing HRz1. The injections were performed at 21 days of age, and the animals underwent ERG analysis one and a half months later to assay rescue of the

injected eye. In all five hT17M mice, the injected eyes showed substantial ERG reduction relative to the uninjected eyes. The non-transgenic, mrho+/- siblings were not affected. These results are summarized in Figures 3-7 and 3-8. Injection of recombinant AAV expressing the HRz3 ribozyme produced similar results: significant depression of both a- and b-wave ERG responses in the injected eyes of the animals containing the hT17M transgene, but not in their non-transgenic littermates that were also injected.

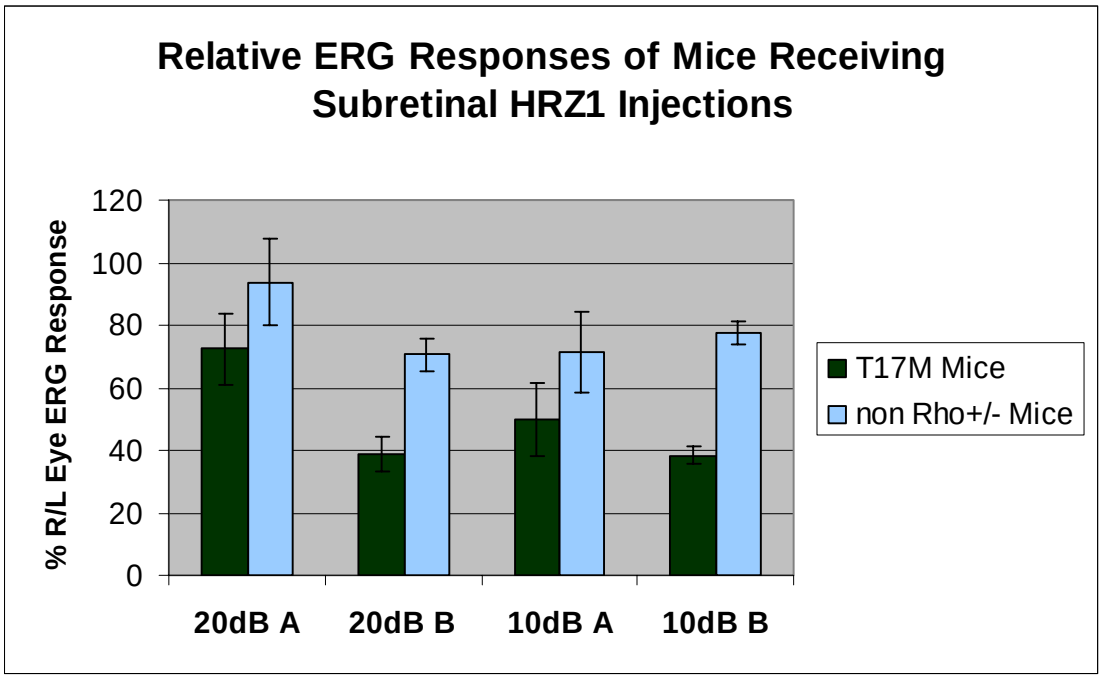

Figure 3-7. Relative ERG responses of a- and b-waves at 20 and 10dB flash intensities. Each bar represents the average of the ratio of right to left eye ERG responses for all animals in that group. These mice were analyzed at one month after subretinal injection of the right eye with 0.5 microliters of rAAV expressing HRz1. Subretinal injection led to significantly greater damage in the hT17M transgenic animals (dark green bars) than in their non-transgenic littermates (light blue bars).

Data generated during the creation of another mouse model of retinitis pigmentosa expressing a human rhodopsin transgene containing a P23H mutation demonstrated that such mice expressing two copies of wild type rhodopsin (mrho+/+) degenerated more slowly than those expressing only one copy (mrho+/-). This led us to attempt to treat the

hT17M model, which was expressed on a mrho+/- background, with recombinant AAV expressing wild-type mouse rhodopsin on the premise that increasing the level of normal rhodopsin might dilute the impact of the mutant transgene. These particular animals also received contralateral injections of recombinant AAV expressing only the GFP marker protein to control for any rescue that might result from an ocular response to injection damage. These injections led to ERG reductions in the mutant mice (Figure 3-9) that were similar to those seen with the ribozyme injections, only they were seen in both eyes of the hT17M transgenic animals, as both eyes were injected.

Discussion

We developed ribozymes with the ability to efficiently cleave the mRNA associated with a human rhodopsin transgene, which could be useful as therapeutic reagents for treatment of the hT17M mouse model of RP. The ribozymes were designed to allow them to discriminate between endogenous, wild-type mouse rhodopsin and the mutant human transgene in such a way as to abolish expression of the mutant RNA while leaving the wild-type RNA intact (Figure 3-4). HRz3 contained a mismatch with the mouse target at the first nucleotide upstream of the cleavage triplet, a site where mismatches between the ribozyme and its target sequence has been shown to abolish the catalytic step of hammerhead ribozyme cleavage *in vitro* (Werner and Uhlenbeck, 1995). HRz1 contained a mismatch with the mouse target that is located three nucleotides downstream of the cleavage triplet, and although sequence differences in this area are not though to severely reduce the catalytic step of ribozyme cleavage, they are thought to cause sufficient disruption of ribozyme binding to allow preferential cleavage of a perfectly matched target sequence. *In vitro* analysis showed these ribozymes to be catalytically efficient, with around 20% cleavage of a 12nt target RNA sequence

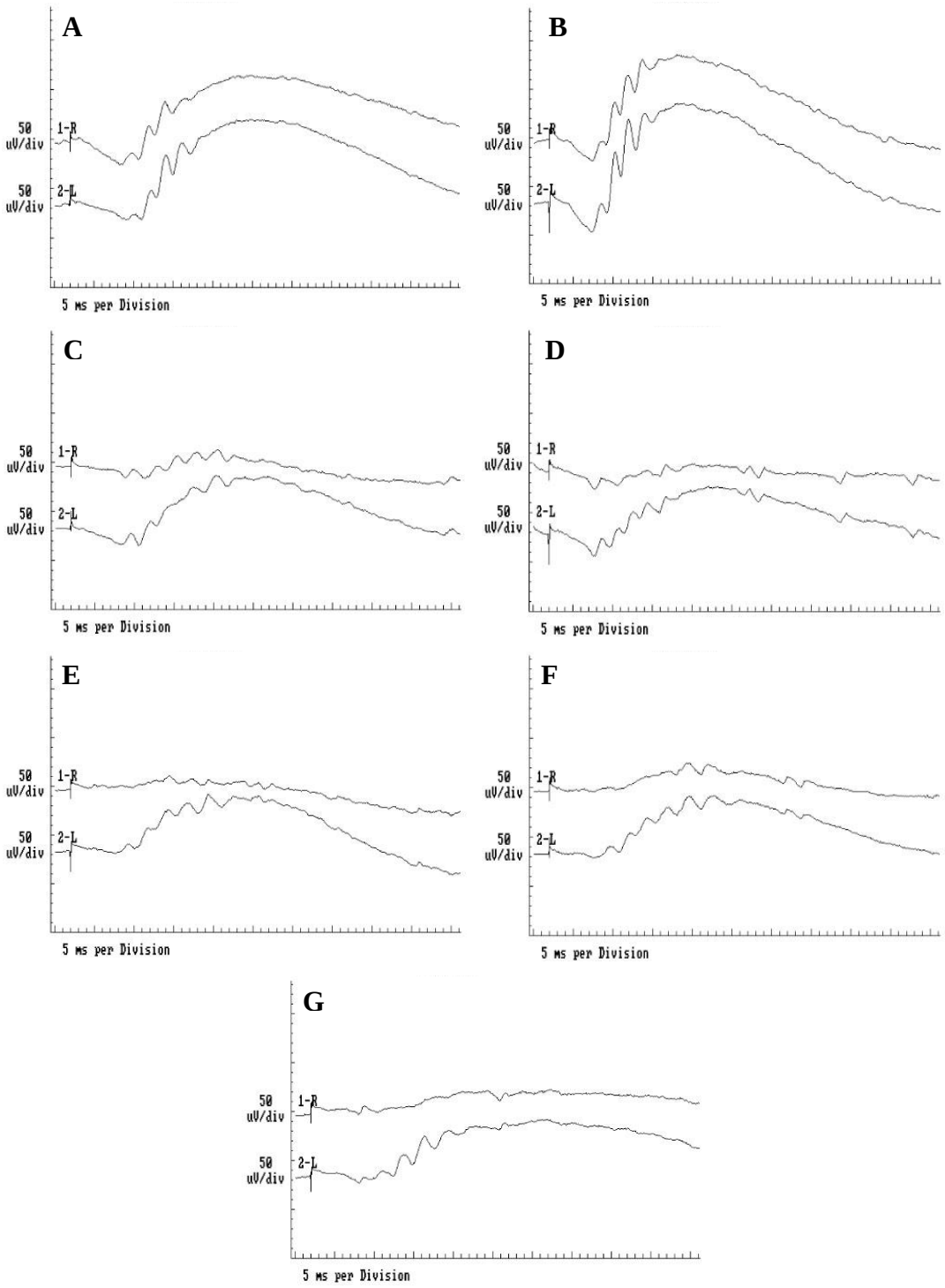

Figure 3-8. 10dB intensity ERG tracings from mice receiving subretinal injections of their right eyes with rAAV expressing HRz1. mrho+/- mice (A and B) show normal ERG responses in both left and right eyes, while the mrho+/-; hT17M transgenic mice (C-G) show substantial reduction in the ERG response of the injected eye. These tracings were used to generate the data in Figure 3-7.

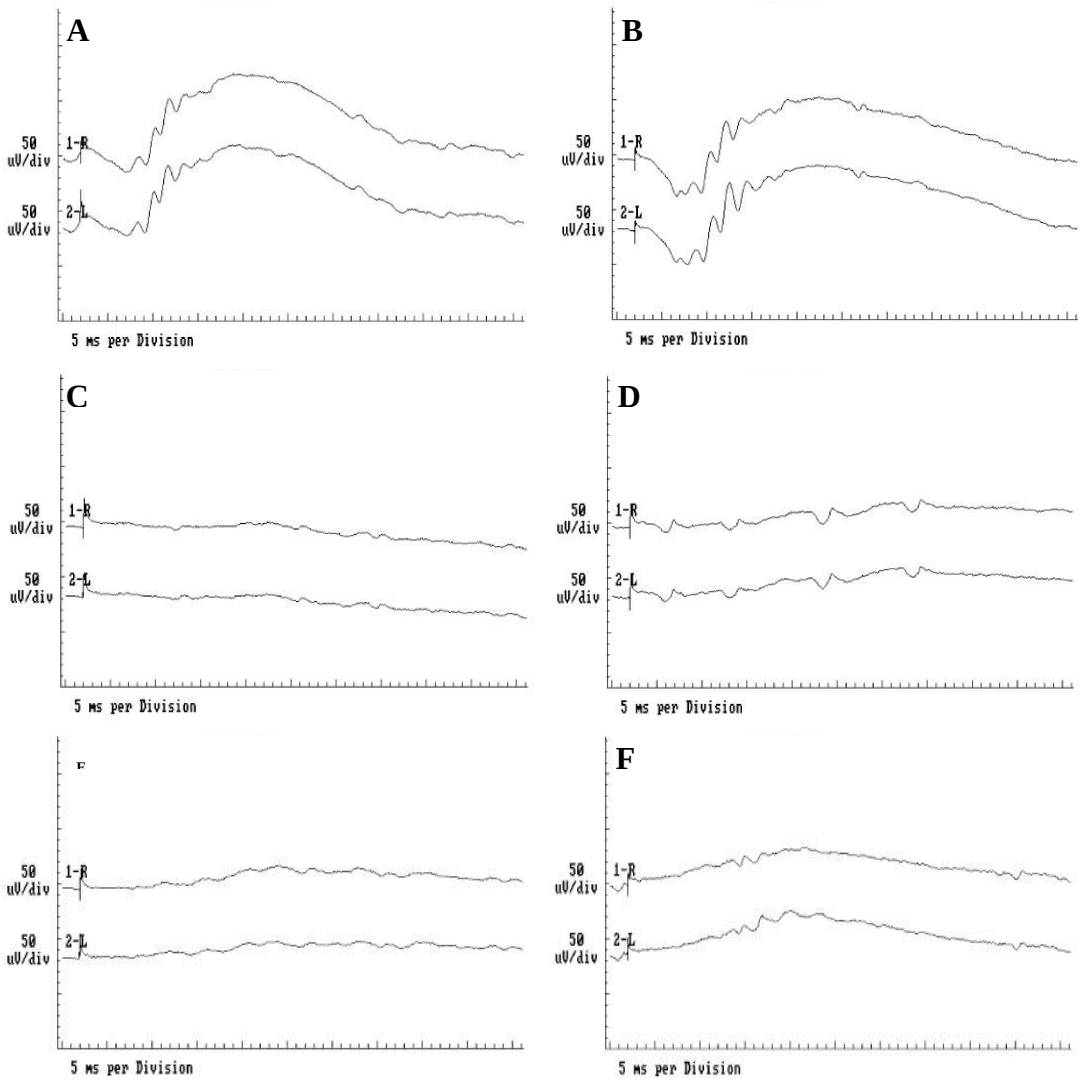

Figure 3-9. 10dB intensity ERG tracings from mice receiving subretinal injections of both eyes. The right eyes were injected with rAAV delivering a wild type mouse rhodopsin transgene, while the left eyes were injected with control rAAV delivering the GFP marker gene. mro+/- mice (A and B) show normal ERG responses in both left and right eyes, while the mrho+/-; hT17M transgenic mice (C,D,E, and F) show substantial reduction in the ERG response of the injected eyes.

observed at the one minute time point at a $MgCl_2$ concentration of 20mM. This time course cleavage rate was comparable to that demonstrated by other hammerhead ribozymes in our laboratory that have been shown to be effective in animal models (Lewin et al., 1998; Fritz et al., 2002; Liu et al., 2005; Gorbatyuk et al., 2005).

The ribozymes were cloned and packaged as recombinant AAV (rAAV), with expression controlled by a rhodopsin-specific promoter sequence. Ancillary sequences were included in these viral vectors that should allow for efficient expression of ribozyme molecules in the target photoreceptor cells. Downstream, self-cleaving ribozyme sequences were also included to generate precise 3' ends for the therapeutic ribozymes. rAAV viral vectors expressing both ribozymes were purified to a high titer, and injections were performed to deliver 0.5 µl of the HRz1-expressing virus (1.0×10^{10} genome copies per injection) to the subretinal space of mrho+/-; hT17M transgenic animals, along with their non-transgenic littermates. Subsequent PCR genotyping was performed to determine the mrho and hT17M genotype of each animal.

Unfortunately, these injections actually resulted in significant retinal damage instead of the intended rescue. ERG analysis of mice containing the mutant human transgene performed one month post-injection revealed severe attenuation of both a- and b- wave ERG responses (Figure 3-8). The non-transgenic littermates were unaffected. Repetition of these experiments with several subsequent litters using either HRz1 or HRz3 as the delivered ribozyme produced the same results - severe damage to the retina as determined by ERG analysis one month after injection. An attempt was also made to achieve treatment by injecting vectors designed to produce a surplus of wild-type rhodopsin in the retinas of the hT17M transgenic animals. This experiment utilized a

control injection of rAAV designed to deliver a GFP marker protein to the photoreceptors of the contralateral eye. This paired injection experiment led to severe ERG attenuation of BOTH eyes of the transgenic animals, while again the non-transgenic littermates were unaffected (Figure 3-9).

These results were surprising. Although a slight amount of ERG attenuation is often seen in animals following subretinal injection, it is usually neither as severe nor as prolonged as the reduction observed in these experiments (Timmers et al., 2001). Occasionally bad injections are accidentally performed that can cause severe retinal damage, but these are rare when the technique is performed, as ours was, by experienced personnel. Attempts to treat our hT17M transgenic mouse line invariably resulted in grossly high failure rates, and it eventually became evident that the severe injection damage was always seen in mice containing the hT17M transgene and not in their non-transgenic littermates. This led us to suspect a defect in injection tolerance in the hT17M mice and to design experiments to determine which aspects of the subretinal injection technique were responsible for such a severe loss of ERG response.

CHAPTER 4
INCREASED LIGHT SENSITIVITY IN mRHO+/-; hT17M MICE

Introduction

Repeated attempts were made to treat hT17M-mediated retinal degeneration in mice with subretinal injection of rAAV delivering either human rhodopsin-specific ribozymes or wild-type mouse rhodopsin transgenes. Analysis of treated animals showed severely reduced ERG responses in the injected eyes. At first this was thought to be the result of injection damage, but it was soon observed that the ERG reduction was seen only in mice carrying the hT17M mutant rhodopsin transgene. After this trend was shown to repeat itself in several experimental groups, we hypothesized that the mechanism of injection itself was detrimental to the visual response of the hT17M mutant animals and not to their non-transgenic siblings. The subretinal injection technique had two components that seemed likely candidates for the damage: the introduction of a virus-containing solution into the subretinal space and the use of bright fiber optic light to illuminate the extremely dilated eyes of these animals during the actual procedure.

Subretinal injection is known to create a retinal detachment that resolves itself over time as the injected solution (in this case containing rAAV expressing the human rhodopsin-specific ribozyme) is removed from the eye (Timmers et al., 2001). If the technique is not performed properly, it is possible to damage the retina so severely that the visual response is affected. It is also possible that mice expressing hT17M mutant rhodopsin are for some reason unable to resolve their retinal detachments, leading to

decreased ERG response following what would normally have been a successful subretinal injection. Injecting the transgenic mice with saline solution resulted in a reduction in the ERG response similar to that observed following subretinal injections of rAAV solutions, suggesting retinal damage (data not shown).

Light-mediated retinal damage (LMD) has been studied extensively since the first reports of its occurrence in laboratory rats four decades ago (Noell et al., 1966). It has since been documented in various other laboratory animals, including pigmented and non-pigmented fish (Penn, 1985), mice (LaVail et al., 1987), rabbits (McKechnie and Johnson, 1977), dogs (Cideciyan et al., 2005), and monkeys (Lawwill et al., 1980). In many instances, simply maintaining these animals under continuous room-level illumination can lead to severely attenuated ERG responses that correlate with a loss of rod photoreceptor cells. Although the phenomenon has been extensively studied, the exact mechanism by which light damage leads to photoreceptor cell death is still not fully understood (Wenzel et al., 2005). All forms of light-induced retinal damage have two things in common: rhodopsin is the initial effector molecule, and the ultimate fate of the damaged photoreceptor cells is death by apoptosis.

There is significant evidence to demonstrate the involvement of rhodopsin in LMD. Studies of the RPE65 knockout mouse model show that this mouse is completely resistant to light damage. Since RPE65 is involved in regeneration of 11-*cis* retinal from all-*trans* retinal, this observation led researchers to conclude that reconstituted rhodopsin (i.e. opsin bound to the 11-*cis* retinal chromophore) is the initial mediator of LMD (Grimm et al., 2000b). Protection against light damage can also be achieved by inhibiting rhodopsin reconstitution through pharmacological means. Intravitreal

treatment with 11-*cis* retinoic acid, which presumably competes with 11-*cis* retinal binding to RPE-65 and thus inhibits reconstitution of active rhodopsin, has been shown to protect against light damage in rats (Sieving et al., 2001). Administration of halothane anesthesia has also been shown to block regeneration of 11-*cis* retinal, and such treatment prior to light damaging light exposure can prevent LMD in albino rats and mice (Keller et al., 2001).

Apoptotic involvement in light mediated retinal damage was convincingly demonstrated in albino rats through TUNEL labeling of fragmented DNA in the affected retinas (Aonuma et al., 1999). In 1998, studies involving p53 knockout mice demonstrated that they were not resistant to LMD, indicating that the gene was not involved in the light-induced apoptotic pathway (Lansel et al., 1998). Subsequent studies reported involvement of the apoptotic effector molecule c-fos, which is a member of the AP1 transcription factor complex, in light-mediated apoptosis, and elevated levels of AP1 have been demonstrated in several models of acute LMD (Reme et al., 1998; Wenzel et al., 2002; Naash et al., 1996; Cideciyan et al., 2005).

Genetic mutations have been shown to increase light sensitivity in the retina. In 1987, LaVail and coworkers reported increased light sensitivity in Balb/c mice as compared to C57BL6 mice (LaVail et al., 1987). Matings between the two strains produced F1 progeny that showed an intermediate phenotype, demonstrating a segregating genetic trait as the mediator of light sensitivity. It is now known that this is the RPE65 gene, and that a polymorphism at codon 450 (leucine in Balb/c mice and methionine in C57BL6 mice) leads to increased RPE65 activity in the leucine variant, leading to accelerated rhodopsin regeneration which, as discussed above, leads to

increased susceptibility to light damage (Wenzel et al., 2001b; Danciger et al., 2004). However, these results could not be duplicated in rat models of LMD (Beatrice et al., 2003). Mice with mutations in the SOD 1 gene also show increased susceptibility to light damage (Mittag et al., 1999), suggesting a role for reactive oxygen species as mediators of damage.

As it has been demonstrated that rhodopsin is the initial mediator of retinal light damage, it is perhaps unsurprising that mutations affecting this gene have been associated with increased susceptibility to such damage. Both the P23H and S334ter rhodopsin mutations have been associated with increased light sensitivity in rat and mouse models of ADRP (Ranchon et al., 2003; Wang et al., 1997). Indeed, dark-reared mice containing the P23H mutation show substantial reduction in the rate of retinal degeneration when compared to P23H litters raised in normal cyclic light, suggesting that cell death as a result of ADRP could share at least some apoptotic mechanisms with certain forms of light-induced damage (Naash et al., 1996).

Recently a dog model of human retinitis pigmentosa containing a tyrosine to arginine mutation at rhodopsin codon 4 has been associated with an extreme sensitivity to light damage (Cideciyan et al., 2005). These animals were subjected to focused retinal light exposures with light intensities that were 1500 to 6000 times less intense than those typically used in animal models of LMD. The researchers reported significant loss of retinal thickness at the site of light exposure, as measured by optical coherence tomography. This result is intriguing, as both T4R and T17M mutations have been shown to affect glycosylation at the amino terminus of rhodopsin (Kaushal et al., 1994; Zhu et al., 2004).

Given the association of rhodopsin mutations with LMD, and considering that the subretinal injection technique utilized in our studies involved shining bright fiber optic light into the severely dilated retinas of anesthetized animals, experiments were designed to test whether this intense exposure to light could have a damaging effect on the retinas of mice containing the hT17M mutant rhodopsin transgene. This chapter describes those experiments.

Materials and Methods

Retinal Illumination

Breedings were arranged as described above to create mrho+/- litters, of which a portion would also contain the hT17M mutant rhodopsin transgene. At weaning age (21-24 days) these litters were removed from their parents and their right eyes were dilated with 1% atropine. The next morning, the right eyes were again dilated with 1% atropine, and again an hour before the illumination procedure, at which time the eyes also received a drop of 2.5% phenylephrine and 0.5% proparacaine HCl. An hour after this final dilation, the animals were anesthetized and again treated with a drop each of 1% atropine, 2.5% phenylephrine, and 0.5% proparacaine HCl. The right eyes of these animals then received a drop of 2.5% hypomellose to aid in retinal visualization and to help keep the retina hydrated, and were illuminated with a Southern Micro Instruments 150 Watt fiber optic light source with Schott Fostec fiber optic arms at an intensity of 10,000 or 5,000 lux for a period of 2.5 minutes. Light intensities were measured with an Extech Data Logging Light Meter (Extech, Waltham, MA). Retinas were visualized under a dissecting microscope, as described previously for the subretinal injections, to ensure that the pupils remained dilated and that the light remained focused on the retina throughout the duration of the experiment. Both eyes of the animals then received smears of VPP

ointment, and the mice were allowed to recover on a warming tray. This experiment was designed to closely mimic the subretinal injection protocol in all ways except for the actual injection.

Genotyping

Tail snips were taken from the mice while they were anesthetized for retinal illumination, funduscopy, or in the case of the animals used for histological examination, after they were sacrificed. Genomic DNA isolation and PCR analysis was performed as described above to identify animals containing the hT17M mutant human rhodopsin transgene.

Electroretinography

Electroretinography was performed as described above. Statistical comparisons between the illuminated and non-illumated eyes were performed to generate P values using the paired, one-tailed Student's t-test feature of Exel spreadsheet software (Microsoft, Redmond, WA).

Funduscopy

Funduscopy was performed as described above.

Histology

Animals were sacrificed by overdose of Isoflurane, followed by cervical dislocation. Eyes were enucleated, and a small hole was placed in the cornea with an insulin needle. They were then fixed overnight at 4^{o}C in freshly-made 4% paraformaldehyde. The next day they were incubated in solutions of sucrose diluted in phosphate buffer (pH 7.4) at concentrations of 7% (2 hours at 4^{o}C), 15% (2 hours at 4^{o}C), and 30% (overnight at 4^{o}C), for cryoprotection. After the final incubation, the eyes were

suspended in 15x15x5mm disposable base molds (Electron Microscopy Sciences, Ft. Washington, PA) in Tissue Tek OCT Compound Embedding Medium (Sakura Finetek, Torrance, CA) such that the cornea and optic nerve formed an axis parallel to the bottom of the mold, with the cornea to the front. The blocks were then frozen in isopentane at a temperature of -40^{o}C. Frozen eyes were stored at -80^{o}C. 12-14 micron retinal sections were then obtained from these frozen eyes using a Microm H550 (Microm, Walldorf, Germany) cryostat, with particular care taken to obtain sections around the optic nerve. Fisherbrand (Fisher Scientific, Pittsburgh, PA) Superfrost Plus microscope slides of size 75x25x1.0mm were used to collect the sections, which were stored at -80^{o}C.

TUNEL Visualization of Apoptosis

DNA fragmenting, a characteristic of apoptosis, was detected using a terminal deoxynucleotide-mediated nick end-labeling (TUNEL) assay. For these experiments, the *In Situ* Cell Death Detection Kit, TMR red (Roche Applied Science, Mannheim Germany) was used, as per the manufacturer's instructions. In brief, sections were thawed for twenty minutes, and then washed twice for five minutes in room temperature 1X PBS. Next, the sections were permeablized in a solution of 0.1% sodium citrate and 0.1% Triton X-100 detergent for two minutes on ice. The sections were then washed twice for ten minutes with 1X PBS at room temperature. A hydrophobic slide marker pen (Daido Sangyo Co., Ltd., Tokyo, Japan) was used to surround the retinal sections so that the TUNEL reagents would not leak off. TUNEL label mix was subsequently added to the slides as per the manufacturer's instructions. Cover slips (size 24x60mm, Fisher Scientific) were added, and the sections incubated in the dark at 37 ^{o}C in a humid chamber. After an hour, the cover slips were gently removed, the sections were rinsed three more times in room temperature 1X PBS for 10 minutes each wash, dried briefly,

mounted with Vectashield Mounting Medium with DAPI (Vector Laboratories, Burlingame, CA), and re-covered. Cover slips were sealed to the slides with Sally Hansen Double Duty Nail Polish (Del Laboratories, Inc., Farmingdale, NY). Apoptotic cells fluoresced red when visualized and photographed on a Zeiss Axiokop 2 mot plus microscope utilizing Axiovision 4 software (Zeiss International).

Results

High Intensity Illumination

The right eyes of an experimental group consisting of six mrho+/- mice and six mrho+/-; hT17M mice, aged 21-23 days, were illuminated as described with light of 10,000 lux intensity for 2.5 minutes. A period of 2.5 minutes was chosen for the illumination because it is the approximate time an animal is exposed during an actual injection procedure. Electroretinographic analysis was then performed on the mice at intervals of 1, 3, and 5 weeks, and the results plotted (Figures 4-1 and 4-2). The results demonstrate a significant decrease of around 30% in both a- and b-wave responses at each time point in the illuminated eyes of animals containing the hT17M transgene, but not their non-transgenic siblings.

Low Intensity Illumination

One possible way to reduce the damage caused by retinal illumination during subretinal injections would be to reduce the intensity of the fiber optic light used to visualize the retina. To test whether a reduction in intensity could decrease or eliminate light-induced retinal degeneration, nine mrho+/- and eight mrho+/-; hT17M mice were subjected to illumination as described, with the intensity of illumination reduced to 5,000 lux. Electroretinographic analysis was performed on the mice at intervals of 1, 3, and five weeks after illumination, and the results plotted (Figures 4-3 and 4-4). Low intensity

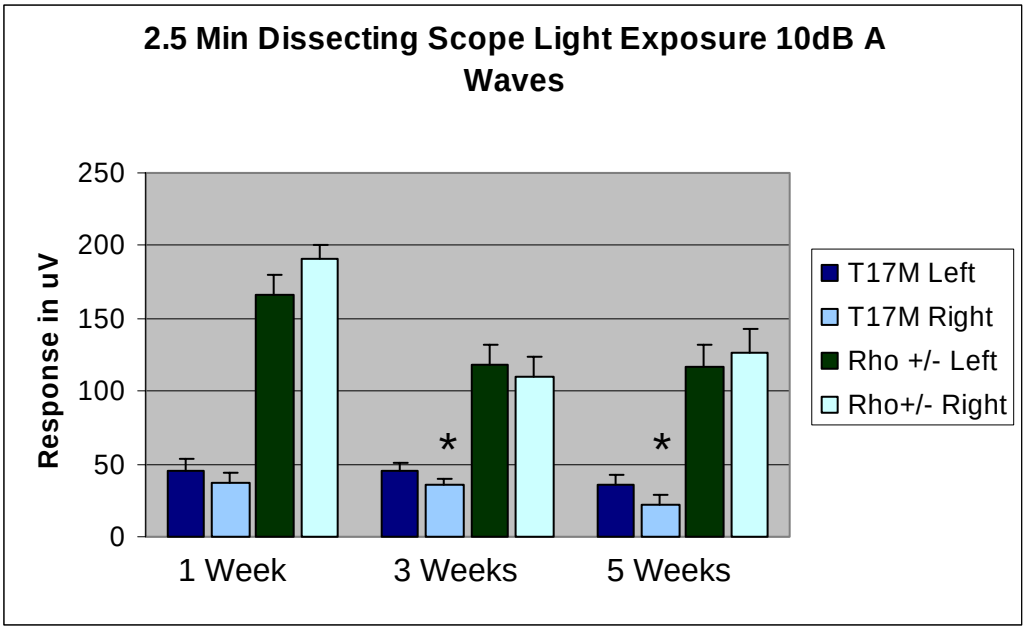

Figure 4-1. A-wave ERG responses at one, three, and five weeks after 10,000 lux intensity, 2.5 minute illumination of mrho+/- and mrho+/-;T17M mice. Asterisks indicate a difference between the right eye and the left eye with a P value of less than 0.05.

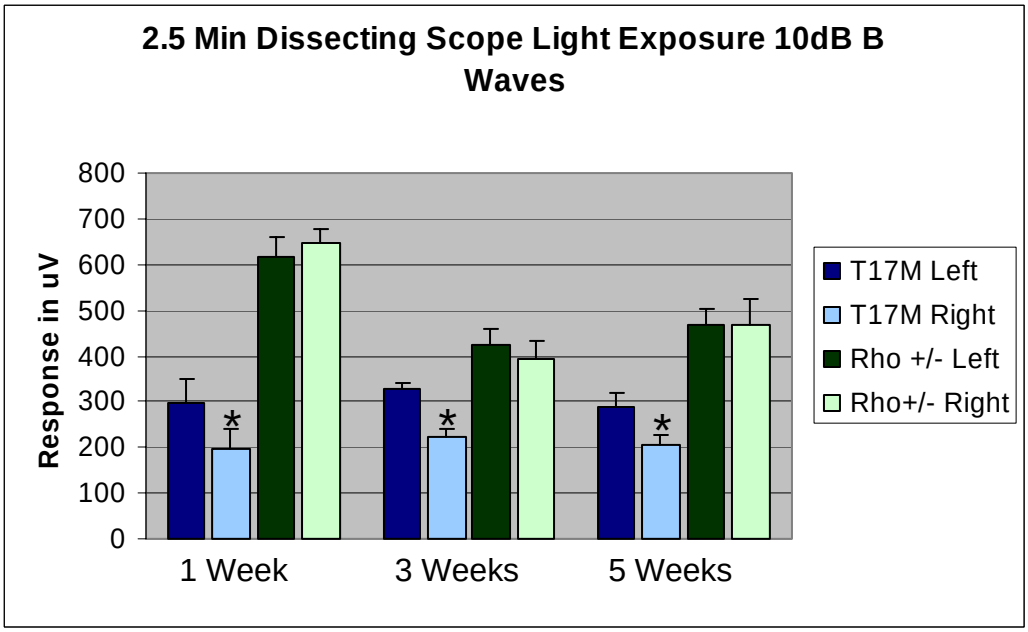

Figure 4-2. B-wave ERG responses at one, three, and five weeks after 10,000 lux intensity, 2.5 minute illumination of mrho+/- and mrho+/-;T17M mice. Asterisks indicate a difference between the right eye and the left eye with a P value of less than 0.05.

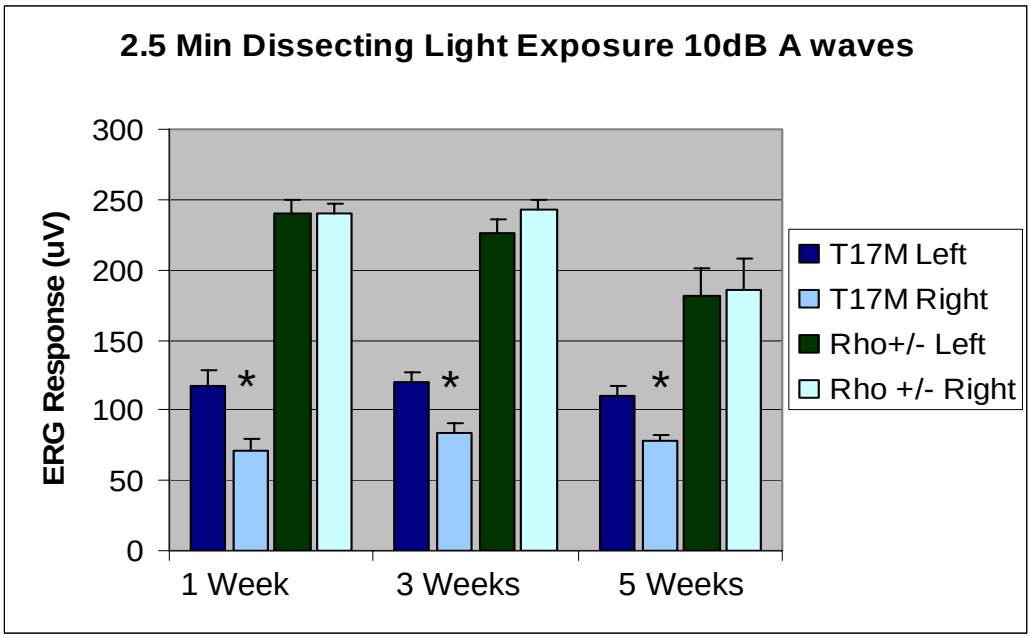

Figure 4-3. A-wave ERG responses at one, three, and five weeks after 5,000 lux intensity, 2.5 minute illumination of mrho+/- and mrho+/-;T17M mice. Asterisks indicate a difference between the right eye and the left eye with a P value of less than 0.05.

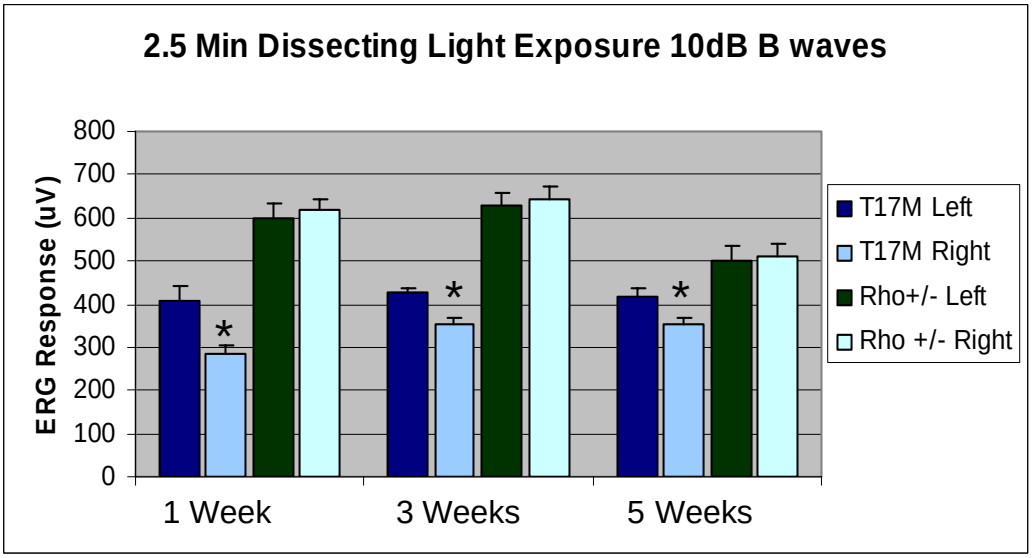

Figure 4-4. B-wave ERG responses at one, three, and five weeks after 5,000 lux intensity, 2.5 minute illumination of mrho+/- and mrho+/-;T17M mice. Asterisks indicate a difference between the right eye and the left eye with a P value of less than .05.

illumination led to a 20-30% decrease in both a- and b-wave amplitudes at all three time points. These results closely resembled the results observed after the similar, high-intensity illumination experiments.

Apoptosis in Retinas Damaged by Low Intenisty Illumination

Light damage to the retina has been extensively studied. It has been demonstrated that light-induced retinal damage is caused by apoptosis of photoreceptor cells (Hao et al., 2002; Farrar et al., 2002). It is this cell death that is responsible for the depressed ERG responses that are seen in light-damaged animals. To test whether apoptotic cell death was the cause of the ERG reduction that was seen in the retinal illumination experiments, two mrho+/- and three mrho+/-; hT17M mice were subjected to 5000 lux illumination as described previously. The animals were sacrificed after 24 hours, their eyes were fixed and sectioned, and TUNEL labeling was used to visualize apoptosis. The results, shown in Figures 4-5 and 4-6, show evidence of intense photoreceptor cell death in the illuminated retinas of the animals containing the hT17M transgene, but not in their non-transgenic littermates.

In order to document the extent of photoreceptor apoptosis, pan-retinal images were obtained from the TUNEL stained sections using tile-field mapping of 20X images on a Zeiss Axiophot Z microscope equipped with a Sony DXC-970MD 3CCD Color Vid Camera and an MCID Elite Stage, utilizing MCID (Imaging Research, Inc., Ontario, Canada) Analysis Software (Imaging Research, Inc.). The results, shown in Figure 4-6, show that the photoreceptor damage is pan-retinal, rather than tightly localized.

Funduscopic Illumination

Funduscopic examination is one of the most common ophthalmologic procedures, often performed either as part of a routine physical or complete eye examination to detect

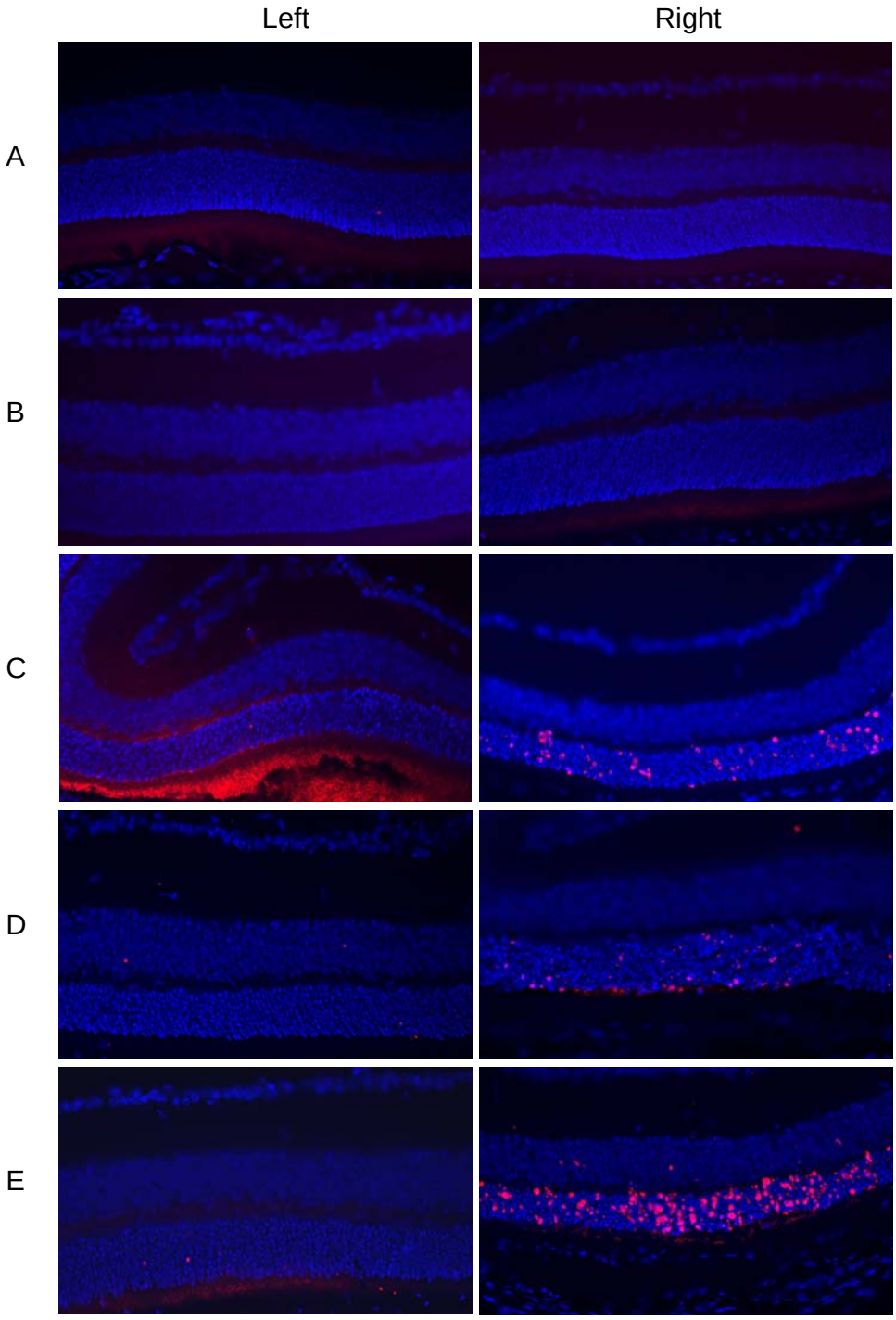

Figure 4-5. TUNEL stained retinal sections from mrho+/- and mrho+/-; hT17M mice whose right eyes were illuminated with 5000 lux white light for 2.5 minutes. Sections of mrho+/- mice (rows A and B) show no evidence of apoptosis, while sections from mrho+/-; hT17M mice (rows C, D, and E) show extensive apoptosis, as evidenced by large numbers of red-labeled photoreceptor nuclei. In each row, left and right eye sections are from the same experimental animal.

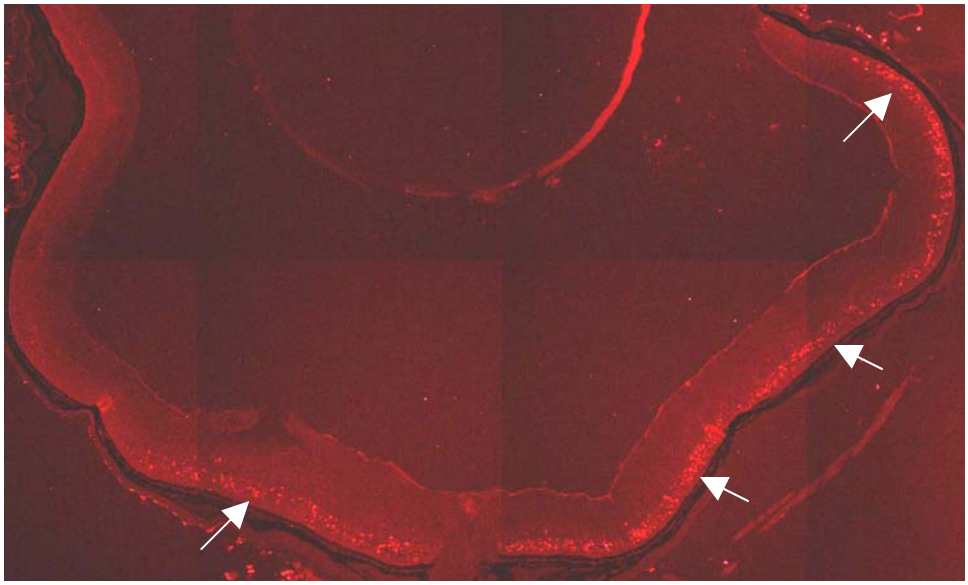

Figure 4-6. Tile-field mapped image of the TUNEL stained retina of an eye from a mrho+/-; hT17M animal that was illuminated for 2.5 minutes with 5,000 lux light. Arrows indicate pan-retinal red fluorescence indicative of apoptotic photoreceptors.

and evaluate symptoms of eye disease, such as glaucoma or retinal detachment, or if diabetes, hypertension, or other vascular disease is suspected. The characteristic "bone spicule" deposits associated with retinitis pigmentosa are among the indicators that a patient presenting with reduced visual fields and impaired night vision is actually suffering from RP. During this procedure, the back of the retina is visualized through the dilated iris of the patient using a bright white light. If photographs of the retina are taken, they too must utilize intense flashes of light to record their images. It has been demonstrated that funduscopic examination is damaging to the retinas of dogs containing a T4R rhodopsin mutation (Cideciyan et al., 2005).

In order to determine if funduscopic examination and photography of the retinas of mice carrying the hT17M human mutant rhodopsin transgene was harmful, eight mrho+/- mice, four with the hT17M transgene and four that were non-transgenic, had two fundus pictures taken of their right eyes at three and six weeks of age. One week after each set

of photographs, electroretinography was performed as described, and the results averaged and plotted (Figure 4-7). These ERG recordings show clearly depressed a- and b-wave amplitudes in the hT17M transgenic mice following both sets of funduscopic photography, while their non-transgenic littermates were unaffected.

The first set of fundus pictures show no evidence of retinitis pigmentosa in either the mrho+/- mice or their mrho+/-; hT17M littermates. However the second set of fundus images, taken at six weeks of age, reveal punctate regions of the retina in the hT17M transgenic animals, suggesting loss of pigment in the retina. The images of the non-transgenic mice looked normal. These results are summarized in Figure 4-8.

Apoptosis in Retinas Damaged by Fundus Photography

It seemed reasonable to assume that the depression of ERG response seen in hT17M transgenic mice following fundus photography would be accompanied by photoreceptor apoptosis, as was noted with the animals damaged by low-intensity fiber optic illumination. In order to confirm this, two mrho+/- littermate mice, one containing the hT17M mutant rhodopsin transgene and one that was non transgenic, were subjected to fundus photography of the right eye at 21 days of age. One day later, the animals were sacrificed, and their eyes were enucleated, fixed and sectioned. Sections containing the optic nerve were then TUNEL stained to visualize apoptotic cells, with DAPI counterstain to reveal retinal morphology. The results, illustrated in Figure 4-9, show that fundus photography clearly induced apoptosis in the rod photoreceptor cells of mrho+/-; hT17M mice, but not in their non-hT17M littermates.

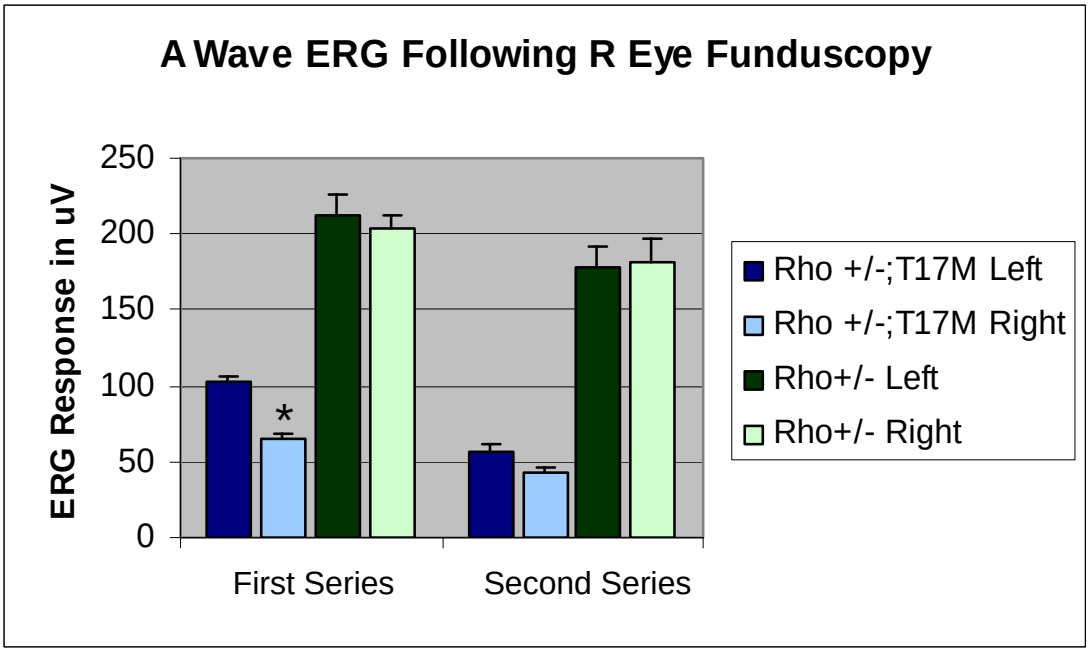

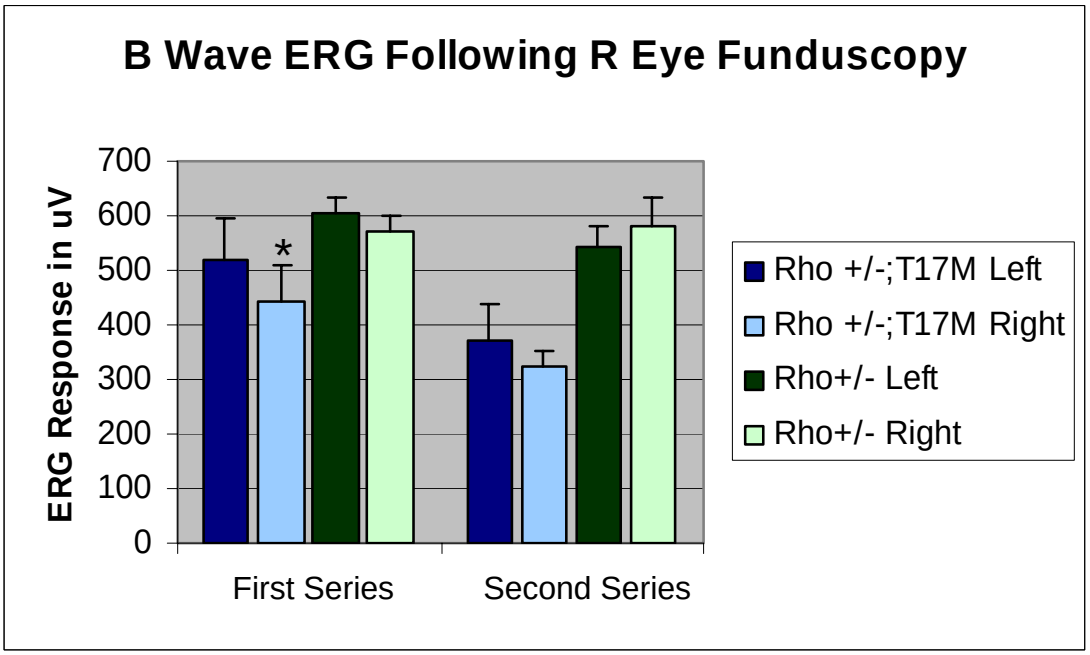

Figure 4-7. A and b-wave ERG responses of mrho+/- and mrho+/-; hT17M mice subjected to fundus photography at 3 weeks (first series) and 6 weeks (second series) of age. * indicates significant difference between right and left eyes with a P value of less than 0.05.

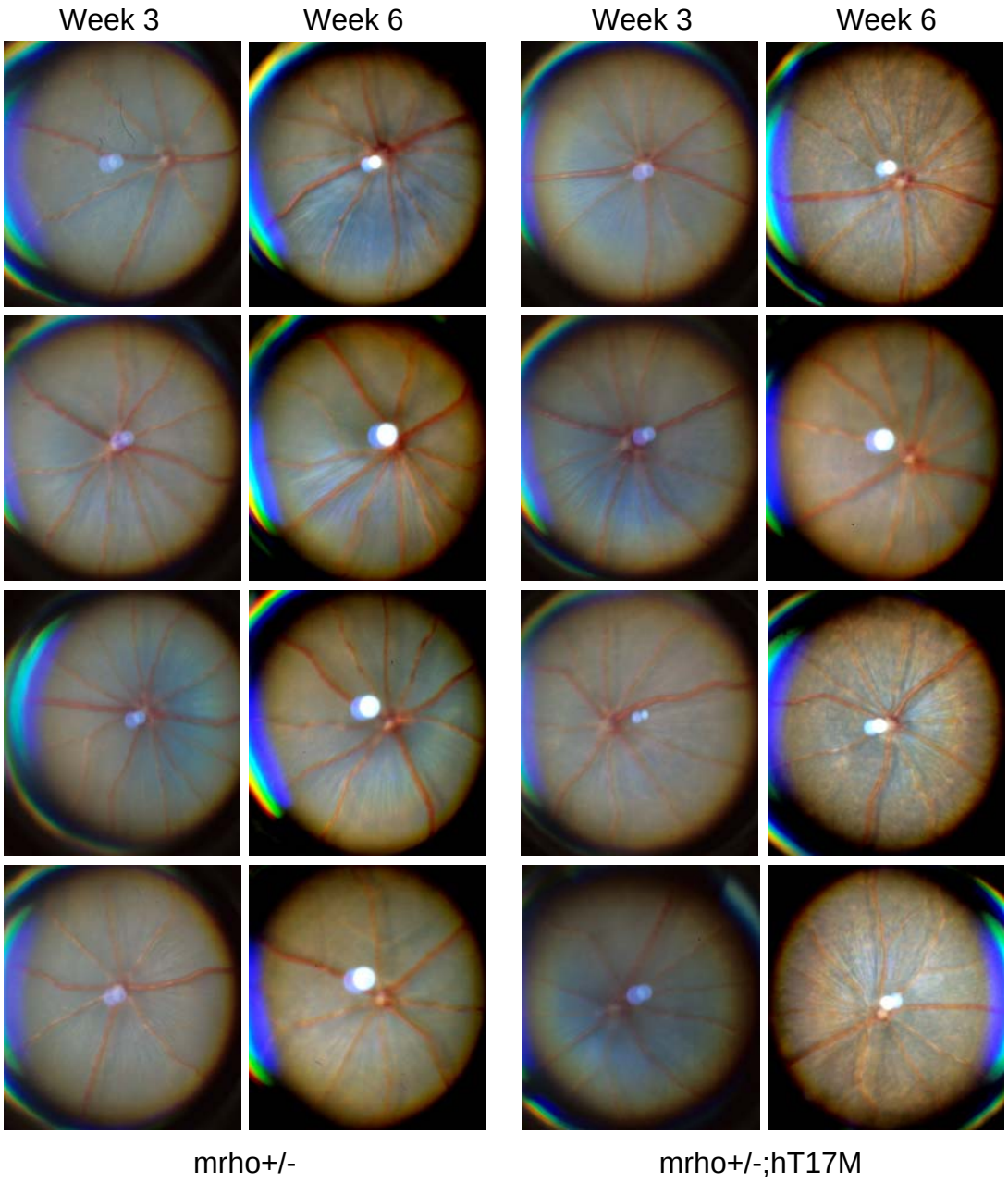

Figure 4-8. Fundus pictures of mrho+/- (left sets) and mrho+/-; hT17M (right sets) mice at three and six weeks of age. Evidence of retinal degeneration is seen in the six week set of hT17M transgenic mice.

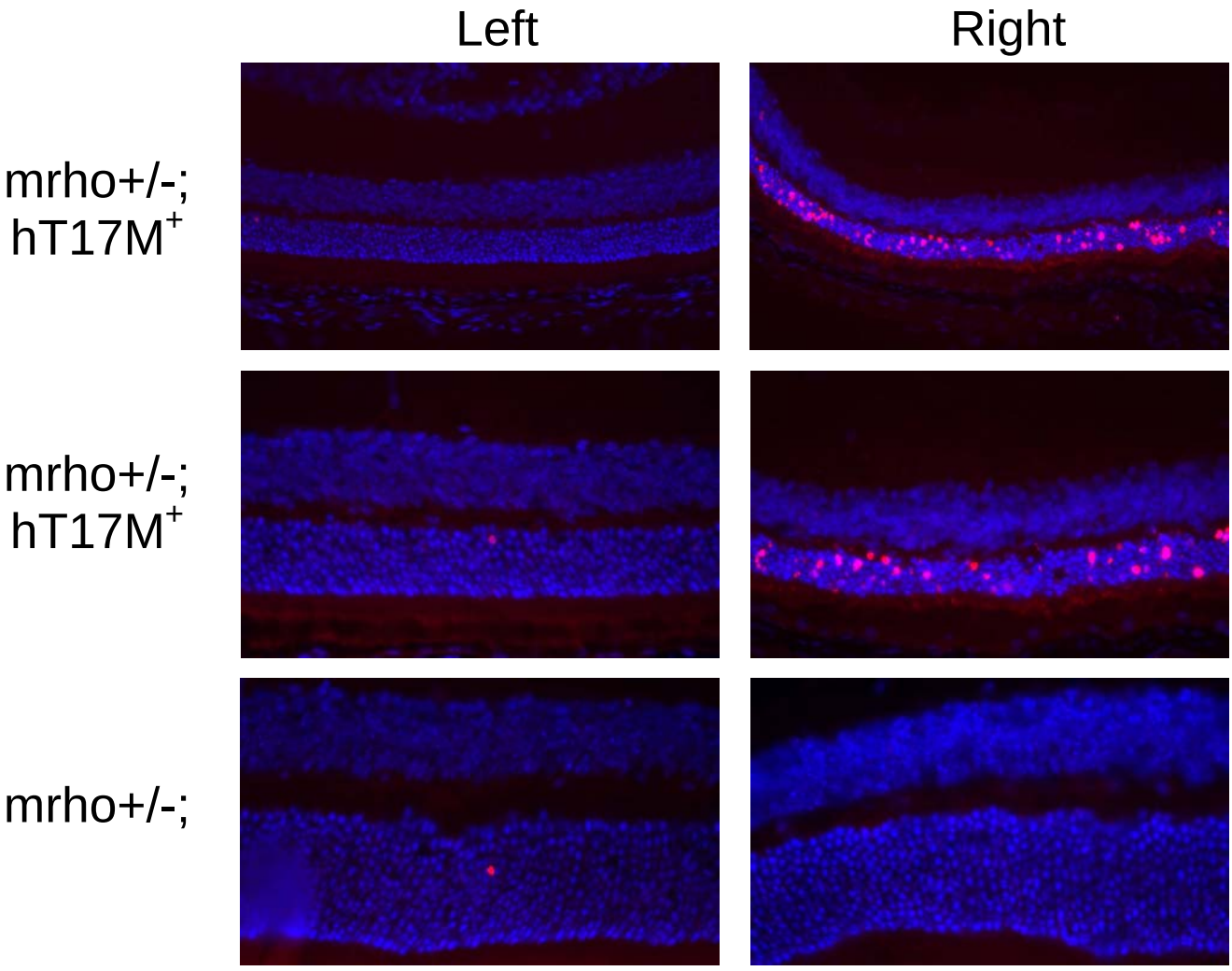

Figure 4-9. TUNEL labeling of retinal sections from mice whose right eyes underwent fundus photography at 21 days of age. Sections of mrho+/- mice (bottom row) show no evidence of apoptosis, while sections from mrho+/-; hT17M mice (top rows) show extensive apoptosis, as evidenced by large numbers of red-labeled photoreceptor nuclei. Images in the top row were taken at 20X magnification; those in the bottom two rows were taken at 40X magnification.

ERG Analysis of hP23H Mice After High Intensity Illumination

As has been discussed, rats and mice containing a human rhodopsin transgene that contains a proline to histidine mutation at codon 23 have been extensively used to study and model retinal disease. Mice that are bred to be hemizygous null at the mouse rhodopsin locus and that also contain the hP23H transgene undergo rapid retinal

degeneration with concomitant photoreceptor loss, culminating with a 60% loss of ERG response at three months of age. This model has been successfully treated with ribozymes designed to specifically cleave the mutant human transgene (F. Fritz UF doctoral dissertation and unpublished results).

Since procedures used for subretinal injection of both lines of mice are identical, it was important to explore the effect of focused fiber optic light on the retinas of mice containing the hP23H transgene. If the hP23H mice showed light sensitivity similar to the hT17M transgenics, it could have a negative impact on the ultimate success of treatment with subretinal ribozyme injections. It was also of interest to determine whether these two closely located mutations, which lead to different rates of retinal degeneration, would respond differently to intense retinal illumination.

Our initial experiments examined the effect of high intensity fiber optic light on the ERG responses of mrho+/-;hP23H mice. Eight rhodopsin hemizygous mice containing the hP23H transgene and their five non-transgenic siblings were exposed in their right eyes to 2.5 minutes of 10,000 lux intensity light, as described above. The animals then underwent ERG analysis at one, three, and five weeks post-illumination to determine the effect of the light exposure upon their visual response. These data are summarized in Figure 4-10.

Although there were significant depressions of a- and b- wave ERG amplitudes in the hP23H transgenic mice after illumination, the differences averaged around a 10% reduction of a- and b- wave responses at 1 week after illumination, as compared to around 26% depression in the hT17M transgenic mice. Furthermore, the hT17M mice continued to exhibit reduction in a- and b-wave ERG responses at five weeks post

illumination, while the hP23H transgenic mice showed only a statistically insignificant 5% depression of both a- and b- wave amplitudes at this time point. Additionally, the non-transgenic littermates used in these experiments also exhibited an initial ERG reduction of around 5 to 10%, one of which was actually statistically significant, at the initial ERG time point (Table 4-1). The fact that the hP23H transgenic animals were not more sensitive to high intensity retinal illumination than their non-transgenic littermates taken together with the transient, moderate severity of the phenotype when compared to the hT17M transgenic mice seems to indicate that the hP23H mutation does not confer profound sensitivity to high intensity retinal irradiation of the type used to facilitate subretinal injections or fundus photography.

Table 4-1. Percent reduction in eyes illuminated 10,000 lux white light. Illumination effects are shown for mrho+/-; hP23H mice (left sets), mrho+/-; hT17M mice (center sets), and mrho+/- littermates (right sets). Numbers represent the percent difference between the right (illuminated) and left (unilluminated) eyes. A "+" sign indicates that the right eye response was greater than the left eye response. * indicates significant differences with a P-value of less than 0.05.

	mho+/-; hP23H[§]		mrho+/-; hT17M[€]		mrho+/-[Δ]	
	a-wave	b-wave	a-wave	b-wave	a-wave	b-wave
1 Week	14%*	7%*	22%	29%*	+4%	+2%
3 Weeks	14%*	7%*	20%*	32%*	1%	4%
5 Weeks	4%	+3%	43%*	28%*	+5%	0%

[§]n=8, [€]n=6, [Δ]n=11

Apoptosis in hP23H Mouse Retinas After High Intensity Illumination

The results discussed above seemed to demonstrate that hP23H transgenic mice were not susceptible to light damage in a manner similar to mice containing the hT17M transgene. To confirm this result, histology and TUNEL staining were performed as described previously on four mrho+/-;hP23H and one mrho+/- mice were illuminated with 10,000 lux fiber optic light in their right eyes for 2.5 minutes. hP23H transgenic mice exhibited no increase in apoptosis in their illuminated eyes either compared to their own unilluminated left eyes, or the illuminated right eye of a non transgenic littermate (Figure 4-11). A positive control involving DNase treatment prior to TUNEL labeling was performed on a section from a non transgenic, non-illuminated eye in order to ensure that the lack of TUNEL-positive photoreceptors was not due to any problems with the TUNEL kit itself. These results support the conclusion that hP23H transgenic mice are not as sensitive to retinal light damage as their hT17M transgenic cousins.

Discussion

Investigation of the injection damage phenomenon observed in the hT17M transgenic mouse line led to the discovery of an acute light sensitivity in these transgenic animals. Illumination for 2.5 minutes with both 10,000 and 5,000 lux white fiber optic light caused severe attenuation of the ERG response in these mice, with around a 30% reduction seen in both a- and b-waves out to five weeks post-illumination. Histological analysis followed by TUNEL labeling revealed significant amounts of apoptosis localized to the photoreceptor cells of the ONL in the illuminated eyes of hT17M mice. This result supports the conclusion that light exposure of the duration and intensity used for subretinal injections caused apoptotic photoreceptor cell death.

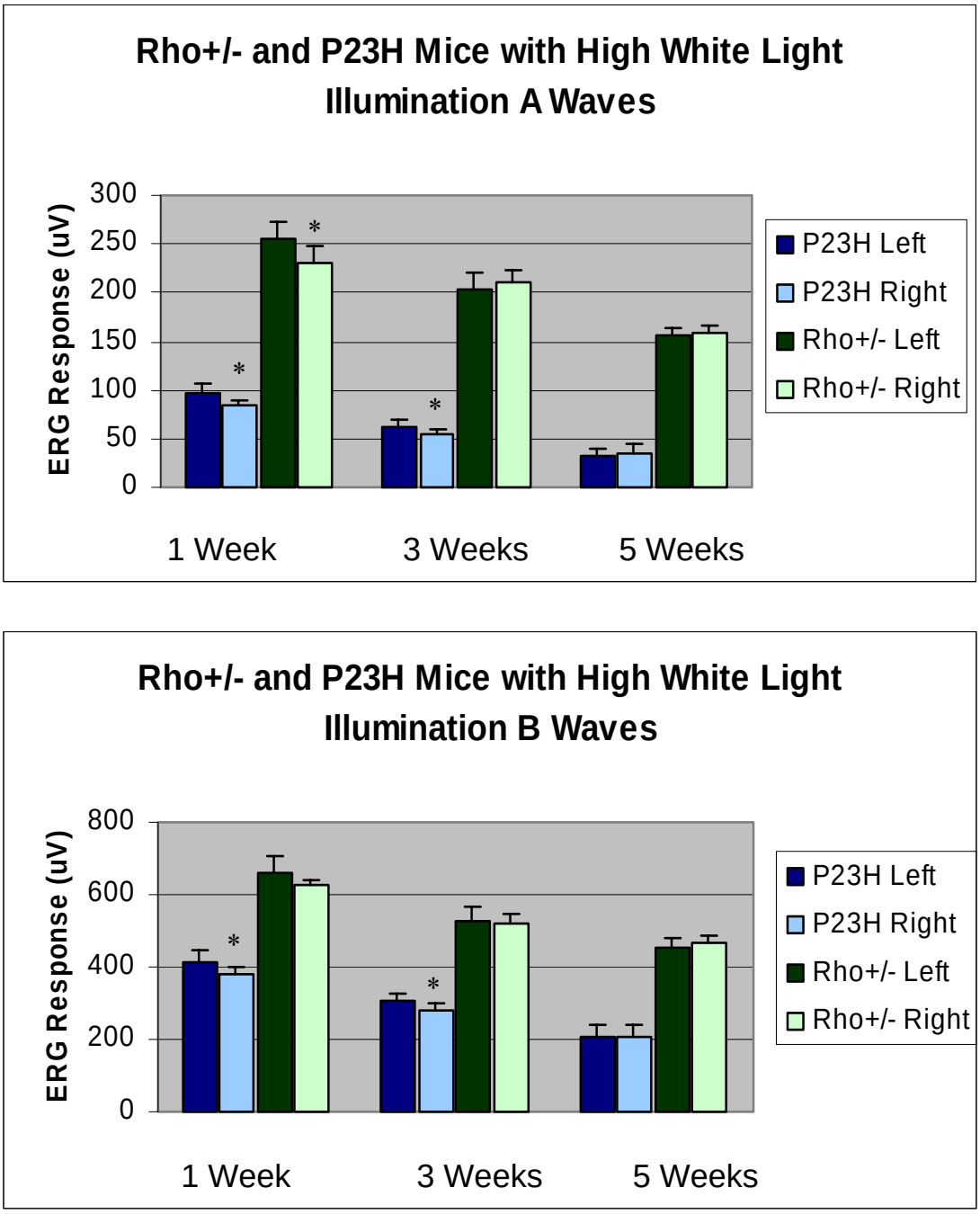

Figure 4-10. 10dB intensity a- and b-wave ERG responses at one, three, and five weeks after 2.5 minute, 10,000 lux illumination of mrho+/- and mrho+/-;hP23H mice. * indicates a right to left eye difference with a P value of less than 0.05.

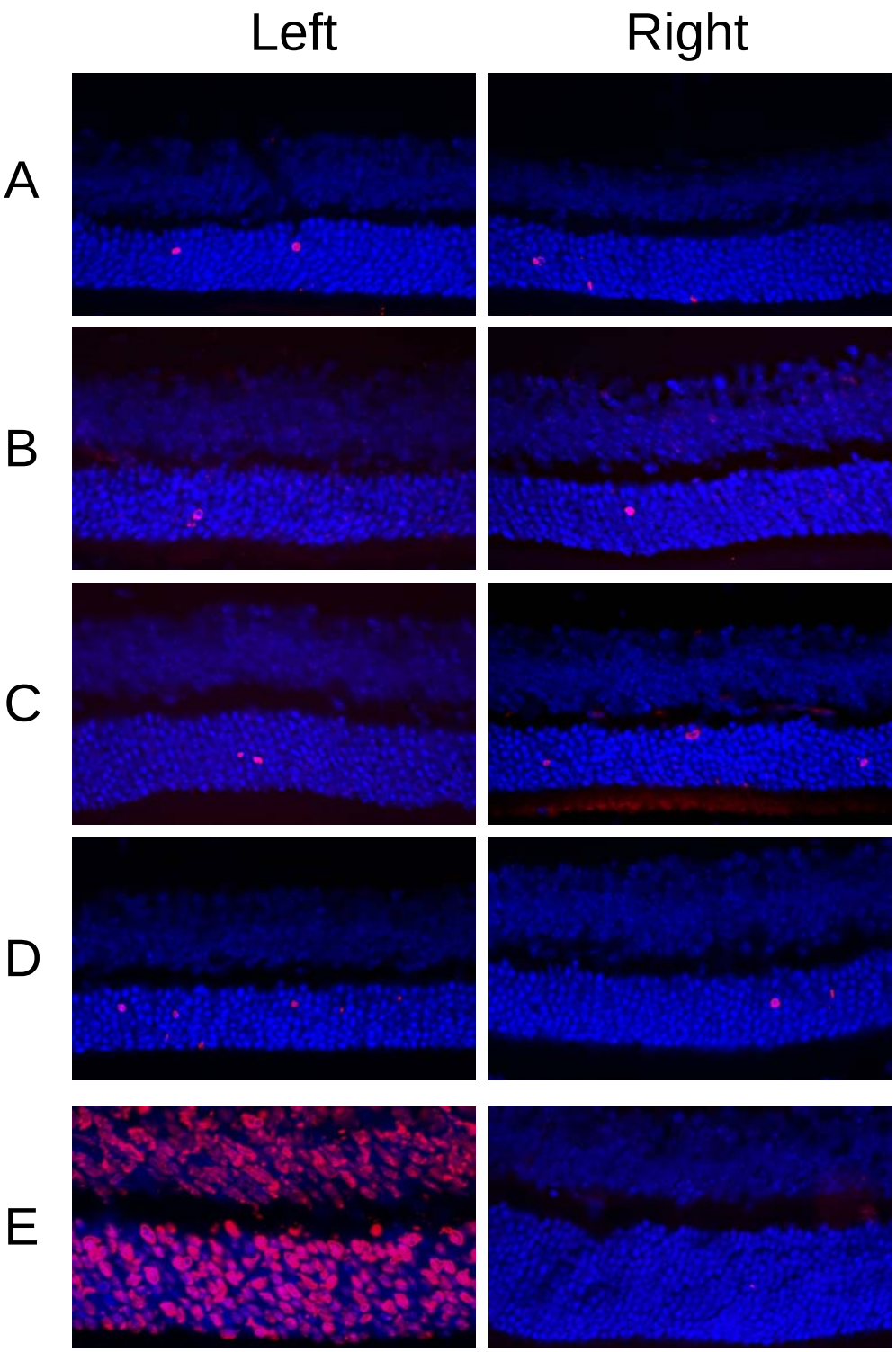

Figure 4-11. TUNEL labeling of mouse retinal sections from mice that were irradiated in the right eye with 10,000 lux white fiber optic light at 21 days of age. Rows A-D are from mrho+/-;hP23H mice. Row E contains (left) a DNase treated positive control eye from an mrho+/-;hP23H mouse and (right) a TUNEL labeled, illuminated right eye from a non-hP23H mouse.

In 1978, researchers reported retinal damage in owl monkeys resulting from intraocular illumination with fiber optic white light similar to that used to perform vitrectomies in human patients (Fuller et al., 1978). These findings coupled with other examples of light-mediated damage in normal, healthy animals, led to concerns that other common ophthalmologic techniques that involved retinal illumination, such as funduscopic examination and photography, could also be damaging (Lanum, 1978). Fundus photography is a routine procedure that involves photographing the retina through the magnifying lens of an apparatus called a funduscope. As the procedure involves bright flashes of white light focused on a dilated retina, we explored the possibility that this procedure could cause damage in the light sensitive hT17M mice. ERG analysis confirmed that fundus photography resulted in significant photoreceptor damage in the hT17M transgenic mice, but not in their non-transgenic littermates. Analysis of TUNEL stained retinal sections following the procedure revealed that this damage was the result of widespread photoreceptor apoptosis.

We also wanted to explore whether this light sensitivity would be observed in a mouse model of ADRP that contained a P23H mutant human rhodopsin transgene. ERG analysis demonstrated that this was not the case, as the hP23H transgenic animals showed only a 5% decrease in the a-wave and b-wave responses of the illuminated eyes after 2.5 minute illumination of 10,000 lux intensity white fiber optic light at one week after the procedure. There was no significant a- or b-wave difference between illuminated and non-illuminated eyes observed at five weeks after the procedure. Analysis of TUNEL stained retinal sections from hP23H mice 24 hours post-illumination revealed no

significant photoreceptor apoptosis, supporting the ERG results. These experiments suggest that the extreme light sensitivity observed in the hT17M transgenic mice is not common to all rhodopsin mutants. Analysis of other rhodopsin mutants using these illumination parameters would be helpful in determining whether this is a rare or common feature of mutations that cause ADRP.

This light sensitivity, while intriguing from a scientific point of view, presents a problem for our therapeutic strategy. Previous results of rAAV-delivered, ribozyme-mediated therapy for ADRP in a rat model containing a P23H mutant human rhodopsin transgene resulted in a 30% rescue of ERG response. Such a therapeutic outcome, if it could be achieved in our hT17M mouse line, would be completely masked by the retinal damage produced by the light exposure associated with our subretinal injection technique. Reducing the intensity of illumination by 50% (from 10,000 to 5,000 lux) did not alleviate the damage, and after damage was seen in the hT17M mice following the incredibly brief light flashes associated with fundus photography, it became clear that special measures would be required to overcome this therapeutic obstacle.

CHAPTER 5
RED FILTERED LIGHT FOR INJECTIONS PROTECTS AGAINST LIGHT DAMAGE IN THE mrho+/-; hT17M MOUSE

Introduction

Results from the previous chapter clearly demonstrate a mutation-specific sensitivity to light exposure in hT17M transgenic animals. This sensitivity lead to a 20-30% decrease in ERG amplitudes after exposure to white light of the type used to visualize the retina during subretinal injection of therapeutic rAAV. Lowering the intensity of this light did not protect against retinal damage. Since our ability to treat these animals with ribozyme-expressing, recombinant AAV depends upon a subretinal injection protocol that is not harmful to the visual response, we decided to explore ways to modify our current injection technique to make it less harmful to the hT17M transgenic mice.

Rhodopsin absorbs light at a peak wavelength of 500nm. As one moves towards longer or shorter wavelengths of light, the ability of rhodopsin to absorb light decreases markedly (Figure 5-1). Red filtered light contains primarily wavelengths above 600nm, which do not activate rhodopsin, or activate it only poorly (Figure 5-1). This is the rationale behind using red-filtered headlamps while handling dark-adapted animals that are to undergo ERG analysis. As mentioned before, several studies have implicated rhodopsin as the effector molecule in animal models of light-mediated retinal damage. The damage we have described in the preceding chapters affected only mice expressing

mutant rhodopsin; it therefore seemed reasonable to assume that activation of mutant rhodopsin by light was the key causative agent of LMD in the rho+/-; hT17M mice. In order to create an injection protocol that would allow us to visualize the injected eye while not activating the mutant rhodopsin, we decided to filter the light we used for subretinal injections like that used in our darkroom headlamps, so that it contained wavelengths longer than 600nm.

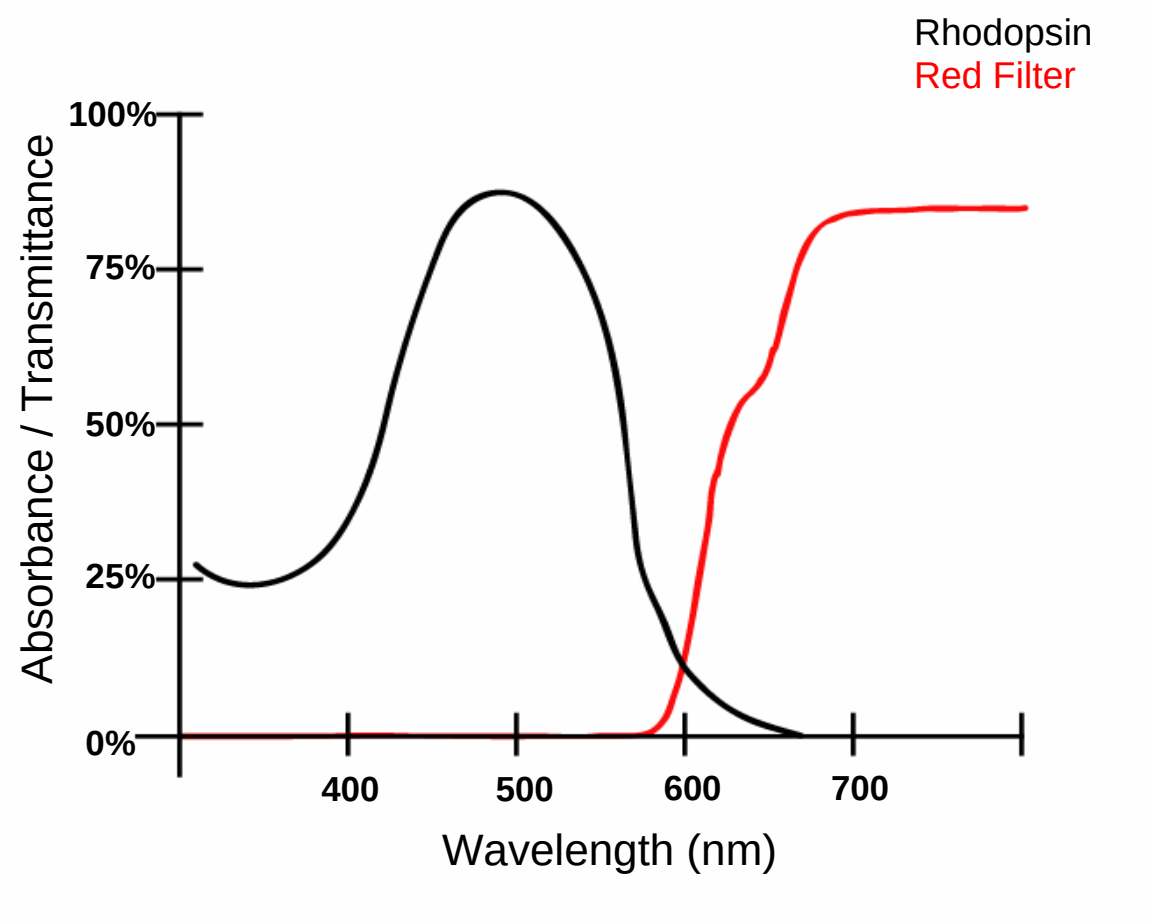

Figure 5-1. Absorbance spectrum of rhodopsin (black), shown together with the measured transmittance spectrum of the red plastic used to create the 600nm red light filters. Note the small overlap of spectra at around 600nm.

This chapter describes the creation and characterization of 600nm red light filters for use in subretinal injections of animals sensitive to light damage. The architecture and

absorbance characteristics of the filters will be discussed, as will experiments designed to test the new filters for their ability to illuminate the retina sufficiently for successful subretinal injections while reducing or eliminating the retinal damage associated with exposure to unfiltered fiber optic light.

Materials and Methods

Creation of 600nm Filters

Plastic photographic filters of the Cokin 003 variety were obtained from a local photographic supply store. The filters were analyzed in a Hewlett-Packard 8452A Diode Array Spectrophotometer (Hewlett-Packard Company, Palo Alto, CA) to determine their absorbance/transmittance spectrum, which is shown in Figure 5-1. A Dremel Minimite model 750 modeling tool (Dremel, Racine, WI) was used to excise sections of these filters that were around 2cm in diameter. These sections were then glued to cylindrical sections cut from 15 ml plastic test tubes (Sarstedt Inc., Newton, N.C.). The resulting filters, shown in Figure 5-2 (left image), could then be attached to the ends of the arms of

Figure 5-2. 600nm red light filters (left) are attached to the fiber optic light sources used for subretinal injections to create an apparatus (right) that filters out harmful wavelengths of light during subretinal injections.

the fiber optic light source used for subretinal injections, creating an apparatus that gave proper injection illumination while filtering out light with wavelengths below 600nm (Figure 5-2, right image).

Retinal Illumination

Although the red filters reduced the intensity of transmitted light, at full power they were still able to produce illumination of an intensity of 5,000 lux. This intensity was used for retinal illumination as described previously, with the right eyes of the experimental mice exposed to 5,000 lux intensity red-filtered (greater than 600nm wavelength) light for a duration of 2.5 minutes.

Electroretinography

Electroretinography was performed as described above. Statistical comparisons between the illuminated and non-illumated eyes were performed to generate P values using the paired, one-tailed Student's t-test feature of Exel spreadsheet software (Microsoft, Redmond, WA).

Histology

Histology was performed as described above.

TUNEL Visualization of Apoptosis

TUNEL labeling of retinal sections and visualization of apoptotic photoreceptor cell death was performed as described above.

Test Injections Using 600nm Filtered Light

Injection procedures were as described, with the exception that the 600nm red filters were attached to the fiber optic light source as depicted in Figure 5-2. Mice of

weaning age (21-24 days of age) received 0.5µl subretinal injections of Lactated Ringers solution (Abbott Laboratories, Abbott Park, IL).

Results

Spectrophotometric Analysis of 600nm Filters

In order to ensure that the red photographic plastic we obtained for the purpose of creating our injection filters actually filtered out light below 600nm, the transmittance spectrum of the plastic was determined. The results, which are shown merged with the known absorbance spectrum of rhodopsin in Figure 5-1, indicate that they efficiently excluded light with wavelengths below 600nm. Most importantly, the spectrum contained no "holes" below 600nm, which would appear as spikes of light at selected wavelengths below 600nm, and would indicate imperfections of the filters that would pass light of wavelengths which could activate rhodopsin (and thus damage the retina). Additionally, the 600nm transmittance cutoff was a sharp, almost vertical line, as opposed to a gradual curve up to a 600nm cutoff, which shows that these filters only pass a small amount of light with wavelengths below immediately below 600nm that can overlap with the rhodopsin absorbance spectrum (and thus activate rhodopsin).

ERG Analysis After 600nm Retinal Illumination

After determining the transmittance characteristics of and building the 600nm red light filters, the effects of red-shifted illumination on the retinas of mice containing the hT17M transgene were tested. The intensity of light transmitted through the filters when the source was turned to full power was 5,000 lux. Therefore, using the red filters at the full power setting created illumination conditions that were identical to those in the low white light study that led to retinal damage, with the exception that all the light in this study was filtered to be of a wavelength greater than 600nm.

A large number of experimental animals were used in these experiments in order to ensure that any protective effect seen from light filtration was reproducible and statistically significant. Thirty four mice were analyzed in all, of which fourteen were mrho+/-; hT17M mutant animals and twenty were mrho+/- control siblings. The animals were subjected as described to 2.5 minute illumination in the right eye with 5,000 lux

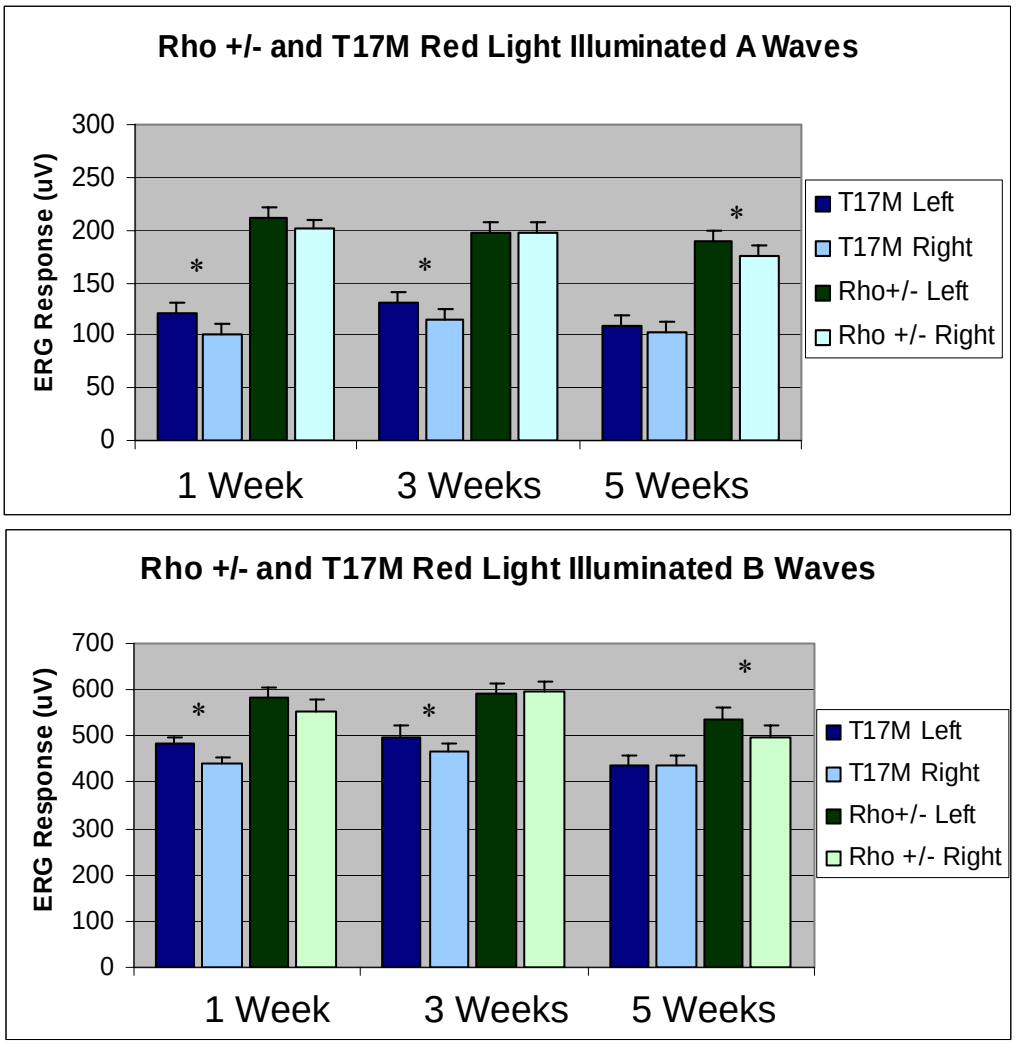

Figure 5-3. A wave (top) and B wave (bottom) amplitudes at one, three, and five weeks after right eye illumination with 600nm filtered light. 14 hT17M transgenic mice and 20 non-transgenic littermates were analyzed. Asterisks indicate difference between right and left eyes with a P value of less than 0.05.

intensity light passed through the 600nm filters. The animals then underwent ERG analysis at one, three, and five weeks after illumination, and the average a- and b-wave maximum amplitudes were graphed and compared between hT17M and non-hT17M sets.

The results, shown in figure 5-3, demonstrate that the 600nm filters provide substantial protection against light induced damage in the hT17M transgenic mice. Although there was a statistically significant reduction in a- and b-wave amplitudes at one and three weeks post illumination, these effects were not as substantial (an average of 15% difference in a-wave responses and 8% difference in b-wave responses) when compared to the previously described effect of 5,000 lux illumination with unfiltered light in the same line, which resulted in an average a-wave reduction of 35% and an averate b-wave reduction of 24% at these time points. The damage was also transient, and at the five week ERG measurement the right and the left eye of the hT17M transgenic animals showed identical a- and b-wave ERG responses (Table 5-1).

Apoptosis in Retinas Exposed to 600nm Illumination

In order to ensure that the protection seen at the ERG level was mirrored by a corresponding lack of apoptosis in rod photoreceptors, histological sectioning and TUNEL labeling was performed. Five mrho+/-; hT17M mice and one mrho+/- littermate underwent 2.5 minute right eye illumination with 5,000 lux of 600nm filtered light, as described above. A day later, the animals were sacrificed, their eyes fixed and sectioned, and sections containing the optic nerve were TUNEL labeled as described in order to identify apoptotic photoreceptors. The results of this experiment, illustrated in Figure 5-4, demonstrate that 600nm illumination does not lead to a substantial increase of apoptotic photoreceptor cells in the illuminated right eyes of hT17M transgenic mice.

Test Injections Using 600nm Filtered Light

Having demonstrated through ERG analysis and TUNEL labeling of retinal sections the protective effect of filtering wavelengths below 600nm from the light used for retinal illumination, we decided to attempt test injections under the red-filtered retinal illumination. Five mice received subretinal injections of 0.5 µl Lactated Ringers solution under these conditions. Tail snips were obtained while the animals were under anesthesia for the procedure. Subsequent DNA isolation and genotyping showed that three of the

Table 5-1. Percent reduction in eyes illuminated with red or white light. Illumination effects are shown for both mrho+/- mice (left sets) and mrho+/-; hT17M littermates (right sets). Numbers represent the percent difference between the right (illuminated) and left (unilluminated) eyes. A "+" sign indicates that the right eye response was greater than the left eye response. * indicates significant differences with a P-value of less than 0.05.

	mrho+/-				mrho+/-; hT17M			
	white[§] a-wave	red[∂] a-wave	white[§] b-wave	red[∂] b-wave	white[Δ] a-wave	red[Ω] a-wave	white[Δ] a-wave	red[Ω] a-wave
1 Week	0%	4%	+4%	4%	39%*	16%*	30%*	9%*
3 Weeks	+8%	0%	+3%	+1%	31%*	13%*	18%*	6%*
5 Weeks	+5%	5%*	+3%	7%*	28%*	1%	15%*	+2%

[§]n=9, [∂]n=20, [Δ]n=14, [Ω]n=8

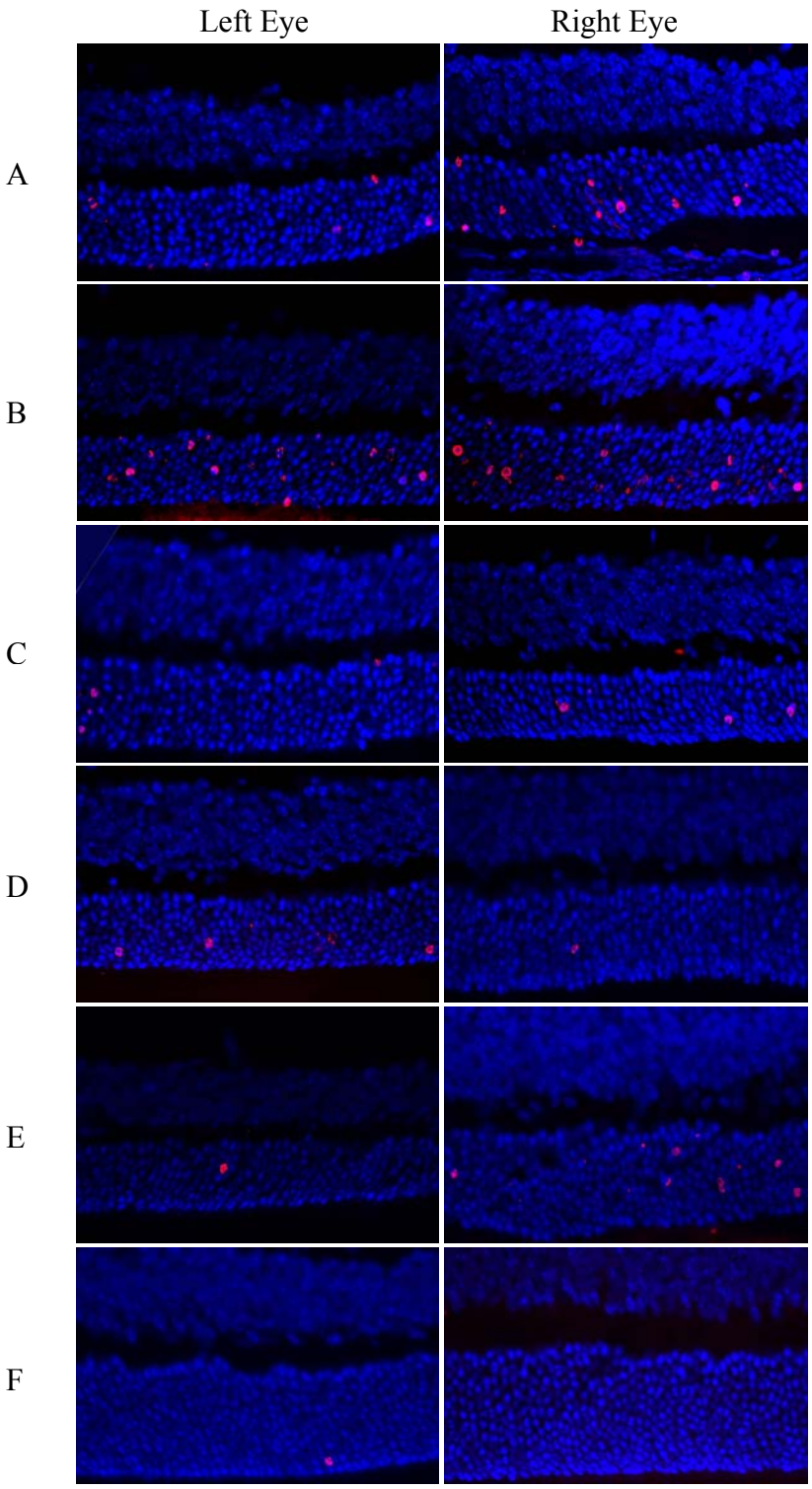

Figure 5-4. TUNEL labeled right and left eye sections from eyes that were subjected to 2.5 minute illumination with 5000 lux, 600nm filtered light. Images in rows A-E are from mrho+/-; hT17M mice; images in row F are from a mrho+/- non transgenic littermate control mouse. Refer to chapter 4 for comparison with images from hT17M mouse eyes illuminated with unfiltered light.

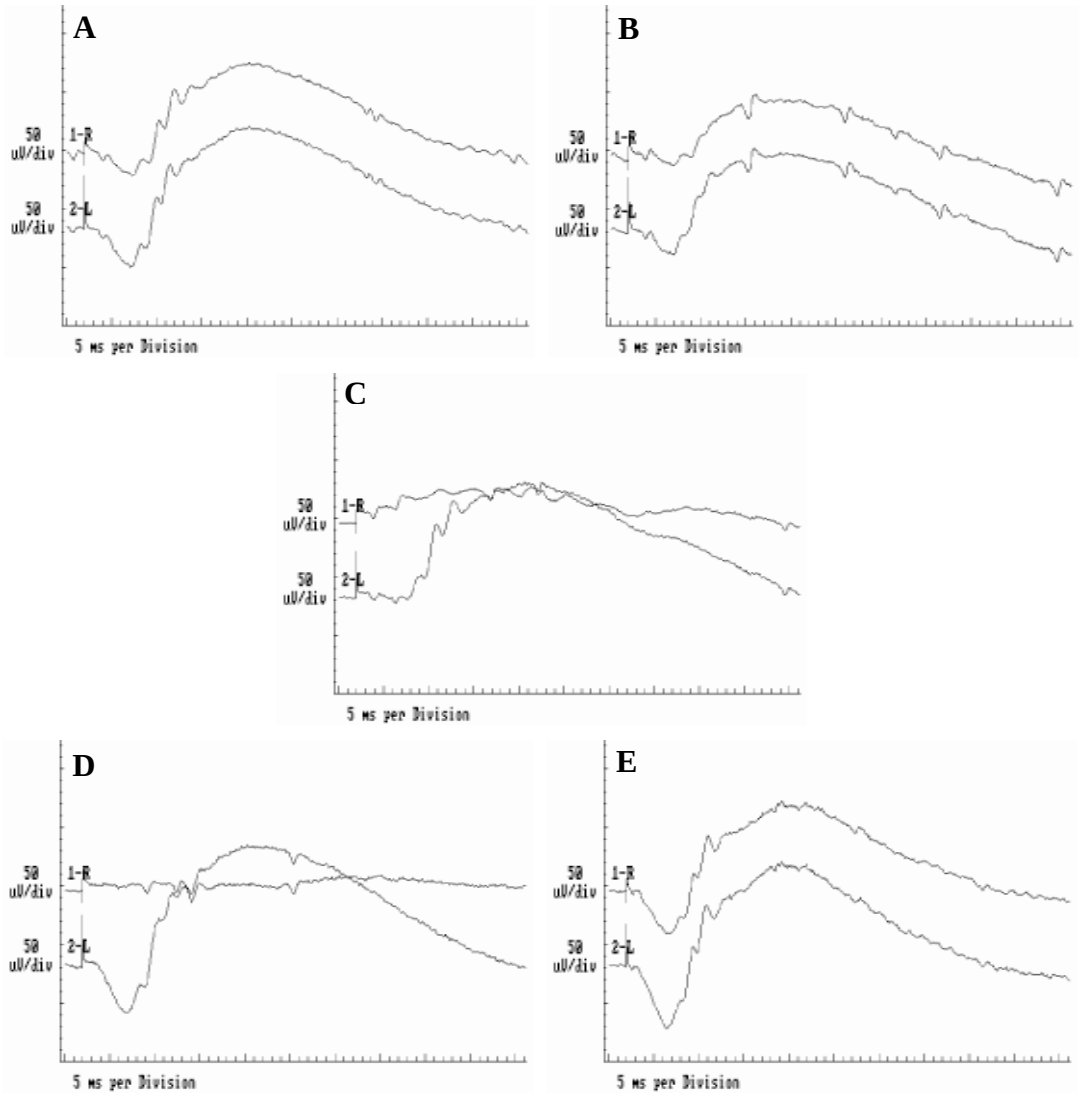

Figure 5-5. ERG responses measured two weeks after subretinal test injections performed under 600nm filtered fiber optic illumination. A-C are tracings from mrho+/-; hT17M transgenic mice. D and E are from non-transgenic littermates. Although the injections shown in panels C and D appeared to be failures, meaning that the procedure itself caused physical damage that resulted in a total loss of a- and b-wave responses by two weeks, the rest, including two performed upon hT17M transgenic mice, were well-tolerated.

five animals were mrho+/-; hT17M transgenic animals, while the other two did not contain the mutant human transgene. ERG analysis was performed two weeks after injection. The results, illustrated in Figure 5-5, demonstrate the feasibility of performing subretinal injections under this type of illumination. Although there were two failed injections that led to total loss of ERG response, these were seen in only two of the fiveanimals, and involved both an hT17M transgenic mouse and a non-transgenic littermate. Most importantly, two of the hT17M transgenic mice tolerated subretinal injection with preservation of ERG response that was far better than that seen using unfiltered white light.

Discussion

In 1977, Adrian et al. described the creation of "a brownish ophthalmic filter which absorbs the short wavelengths preferentially, thus protecting the rods primarily" in an attempt to protect RP patients from light-mediated damage (Adrian et al., 1977). The authors go on to state "Whether or not use of these filters will be efficacious has yet to be determined and will require careful experimentation and the accumulation of clinical experience." Almost thirty years later, we can say that in the case of the damage resulting from retinal illumination in the hT17M transgenic mouse model of ADRP, such filtration can be very effective.

We created filters using photographic plastic that would only pass red-shifted light, containing wavelengths longer than 600nm. The 600nm filters passed light of a sufficient level to allow an experienced researcher to perform a subretinal injection. However, red light illumination at the 5,000 lux intensity did not result in persistent electroretinographic a- or b-wave attenuation. Additionally, the retinal histology of animals illuminated with this type of light appeared normal at 24 hours following the

procedure, and there was little increase in apoptotic photoreceptors relative to the unilluminated eye, as assayed by TUNEL labeling of retinal sections.

We utilized these filters to provide illumination during a preliminary experiment involving subretinal Lactated Ringers injections in five mice, three of which contained the hT17M transgene. ERG analysis performed two weeks after the injection revealed that although there were two failed injections, one in a mutant animal and one in a non-transgenic littermate, the other three mice, of which two contained the hT17M transgene, maintained good a- and b-wave responses relative to the uninjected eye. This is an important result, as these are the first subretinal injections in this line that did not result in substantial retinal damage. The results demonstrate the usefulness of the 600nm filters in preventing the damage caused by intense retinal illumination during subretinal injection. Future experiments will use these filters to facilitate subretinal injections of rAAV delivering ribozyme therapy in an attempt to treat the hT17M-mediated retinal degeneration.

At least one other rhodopsin mutation, tyrosine to arginine at position four, has been shown to confer light sensitivity in dogs that is similar to that seen in our hT17M mouse line (Cideciyan et al., 2005). This is intriguing because of the fact that both mutations result in abolished N-termial rhodopsin glycosylation (Kaushal et al., 1994; Zhu et al., 2004). It would be interesting to see if the filters developed in our laboratory would protect against light damage observed in the T4R dog model. It remains to be seen if other rhodopsin mutations will behave similarly, although it does not appear that all will do so, as demonstrated by the experiments involving hP23H transgenic mice detailed in the previous chapter. However, given the large number of rhodopsin mutations

associated with ADRP, coupled with the range of degenerative phenotypes conferred by them, it seems reasonable to predict that some of these mutations will also confer some degree of light sensitivity.

Here we have described the creation of filters designed to prevent the light-mediated retinal damage associated with subretinal injections. The filters are inexpensive, simple to create, and provide sufficient illumination for successful subretinal injection. Given that the goal of gene therapy for retinal disease is to effect the preservation of rod and cone photoreceptors, the use of such filters when attempting subretinal injections intended to treat animal models of ADRP that involve rhodopsin mutations would seem a useful and desirable precautionary measure.

CHAPTER 6
DISCUSSION

Summary

The preceding chapters detailed the creation of a novel hT17M transgenic mouse model of retinitis pigmentosa. Although the hT17M transgene had been previously studied in a mouse background containing two copies of nonmutant rhodopsin (mrho+/+), to our knowledge this was the first examination of a mouse line in which the transgene was expressed on a hemizygous null rhodopsin background (mrho+/-). Expressing the mutant human rhodopsin transgene in the presence of only one wild type mouse rhodopsin allele provides a closer approximation of autosomal dominant retinitis pigmentosa as it occurs in human populations, in which patients will most often present with one normal and one mutant copy of the rhodopsin gene.

The mrho+/-; hT17M mice in this study showed significant reduction in the outer nuclear layer (ONL), with concomitant reduction of a- and b-wave ERG amplitudes to almost undetectable levels by around six and a half months. Significant drop in ERG amplitudes was seen as early as 1 month of age. Furthermore, evidence of retinal damage was noted as early as three months of age when fundus photography was used to visualize the retinal morphology of the mutant mice. However, substantial ERG response and ONL thickness was still seen at 4.5 months, providing a window for therapeutic intervention that should have made the mrho+/-; hT17M line a good candidate model for testing recombinant AAV-delivered ribozyme therapy. It was unfortunate that after

creating a pair of highly active hammerhead ribozymes targeted to the mutant human transgene, packaging them and purifying and concentrating them as high-titer recombinant AAV, we were unable to test the effectiveness of this therapy because of the significant damage caused during vector delivery. However, exploring possible reasons for mutation-specific sensitivity to subretinal injection damage led us to discover the extreme light sensitivity of the mice in question. This was an intriguing phenomenon in its own right, and one that may have significant therapeutic implications, as will be discussed.

The hT17M transgenic mice showed significant reduction in both a- and b-wave amplitudes of eyes that were illuminated with either 5,000 or 10,000 lux intensity white light for a period of 2.5 minutes. This reduction was seen as early as one week and persisted for at least five weeks following illumination. Non-transgenic, mrho+/- littermate mice were unaffected by this light exposure. Light exposure due to fundus photography of the mutant mice likewise led to a reduction of ERG amplitude in the photographed eyes, while again the non-transgenic mice showed no measurable ill effects from this procedure. TUNEL analysis of retinal sections from mutant mice exposed to both fiber optic illumination and funduscopic examination and photography revealed that there was significant photoreceptor apoptosis that was accompanied by a decrease in ONL thickness by as early as 24 hours following either procedure. These assays revealed no apoptosis in non-transgenic littermates subjected to identical retinal illumination. These observations strongly support the conclusion that the hT17M mutant rhodopsin gene confers significant light sensitivity to transgenic mice that express it.

These observations caused us to explore ways to more successfully perform subretinal injections of hT17M transgenic mice without causing light-mediated retinal damage. As the mutant rhodopsin transgene was required for the damage to occur, it seemed reasonable to assume that it was the absorption of light by the mutant rhodpsin molecule that was the cause of the damage. Since rhodopsin absorbs in the visible spectrum with a peak exhaustion coefficient of 500nm, we decided to illuminate our hT17M mice with 2.5 minutes of 5,000 lux intensity light that was filtered to pass no wavelengths below 600nm. Transgenic mice that were illuminated in this manner showed little or no ERG damage, and this was reflected by a lack of significant apoptosis in the illuminated retinas, as assayed by TUNEL labeling of retinal sections. The red-filtered light affords sufficient retinal visualization for experienced personnel to perform subretinal injections with no loss of speed, although the efficacy of injections performed under this type of illumination remains to be demonstrated. Recently, a mixed litter of mrho+/- and mrho+/-; hT17M mice was injected with lactated ringer's solution, and although two animals (one transgenic, one nontransgenic) received significant injection damage, the other five animals, including two hT17M transgenic mice, showed good ERG responses relative to their uninjected eyes when analyzed at 2 weeks post injection.

Light sensitivity also appeared to be mutation specific. A second mouse model of ADRP was available for study, this one engineered to express a P23H mutant human rhodopsin transgene on an mrho+/- genetic background. Despite exhibiting what seemed to be a more severe form of ADRP, the hP23H transgenic mice were not susceptible to light-induced retinal damage when exposed to 10,000 lux fiber optic illumination for 2.5 minutes, as measured by both ERG analysis and TUNEL labeling of retinal sections.

To summarize, we have bred the hT17M human rhodopsin transgene onto a hemizygous null (mrho+/-) mouse rhodopsin background. ERG and histological analysis of this line show it to be a good model of autosomal dominant retinitis pigmentosa, with significant photoreceptor degeneration by 6.5 months that is preceded by preservation of retinal function for a duration sufficient to provide a good therapeutic window for treatment. While the difficulties caused by illumination with intense white light during subretinal injection were unfortunate, these setbacks allowed us to identify an extreme light sensitivity associated with the hT17M transgene. The use of 600nm red filters during subretinal injection of hT17M transgenic mice prevents the light-mediated damage, and will facilitate future experiments designed to introduce rAAV-delivered, ribozyme-mediated therapy to the retinas of these animals.

Mechanism of Light-Induced Photoreceptor Apoptosis

Light-mediated retinal damage is a phenomenon that has received considerable study. Although there are many different theories as to the exact mechanism of LMD, all share two central points: first, rhodopsin is the initial mediator of the damage (Grimm et al., 2000b; Sieving et al., 2001; Keller et al., 2001) and, second, apoptotic cell death is the ultimate fate of the affected photoreceptors (Aonuma et al., 1999). Apoptotic cell death is also the causative event in the retinal degeneration seen in patients suffering from ADRP arising from mutations in the rhodopsin gene. This has led researchers to study the pathways involved in light-mediated photoreceptor apoptosis, with the goal of achieving a better understanding of apoptotic photoreceptor death in patients suffering from rhodopsin-mediated ADRP.

In 2002, Hao and coworkers reported evidence for at least two apoptotic pathways involved in light-mediated retinal degeneration. One pathway, termed the “acute”

pathway, was induced by 10 minute illumination of Balb/c mice with white light at an intensity of 5,000 lux, and was shown to be independent of transducin activity, meaning that the phototransduction cascade was not required for the induction of apoptosis observed in photoreceptor layers of these mice. They reasoned the acute pathway is caused by activated rhodopsin or its photo-bleached products, based on the fact that mice deficient in both rhodopsin kinase and arrestin, which are involved in the inactivation of rhodopsin, are extremely sensitive to acute light exposure. This type of apoptosis was also found to be dependent upon expression of the transcription factor AP-1. A second light damage pathway, termed the "low-intensity" pathway, was noted in animals with defects in either arrestin or rhodopsin kinase, which are involved in inactivation of photoactivated rhodopsin; these mice were shown to undergo retinal degeneration upon prolonged exposure to normal, cyclic room light. In contrast to the "acute" pathway, transducin activity was central to the "low-intensity" apoptotic pathway, and mice lacking a functional transducin gene were protected from this form of LMD. AP-1 expression was shown to be uninvolved with the low-intensity pathway (Hao et al., 2002).

A possible mechanism for photoreceptor apoptosis resulting from the low-intensity pathway can be found in the "equivalent-light hypothesis" of Fain and Lisman, who postulated that photoreceptor apoptosis resulting from ADRP could be the result of constant activation of the visual cycle in both the presence and absence of light (Fain and Lisman, 1993). Such a defect would result in depressed intracellular levels of Ca^{2+}, which has been shown to cause death in cultured neuronal cells (Woodruff et al., 2004; Fain and Lisman, 1999). Although the equivalent-light hypothesis cannot explain all

forms of light-mediated apoptosis, as evidenced by the transducin-independent apoptosis seen in the "acute" model of Hao and colleagues, it is possible that depressed Ca^{2+} levels are involved in the transducin-dependent photoreceptor apoptosis observed in the low intensity pathway. This is supported by experiments showing that "low-intensity" light-induced apoptosis in Balb/c mice is blocked by treatment with the calcium channel-blocker D-*cis*-diltiazem, which presumably prevents efflux of Ca^{2+} from the cell via the Na^{2+} / C^{2+} exchanger following constitutive loss of cGMP-mediated Ca^{2+} influx (Woodruff et al., 2004; Donovan and Cotter, 2002).

AP-1 is a transcription factor involved in light-mediated retinal apoptosis, and exists as a heterodimer with proteins from the Jun/ Fos families. Retinal exposure to damaging white light has been shown to lead to increased levels of mRNA for two of these proteins, c-Fos and c-Jun in mice (Grimm et al., 2000a). Experiments utilizing DNA microarrays to analyze retinal gene expression following light exposure have similarly confirmed upregulation of AP-1 (Chen et al., 2004). In other work, transgenic *c-fos* knockout mice (*c-fos*-/-) were shown to be highly resistant to light damage (Hafezi et al., 1997). AP-1 upregulation is also noted in the "acute" light damage model of Hao et al. (Hao et al., 2002), and following damaging retinal illumination in the T4R dog (Cideciyan et al., 2005). It remains to be determined if a similar AP-1 induction can be observed following light damage in the mrho+/-; hT17M mouse line.

As discussed earlier, apoptotic pathways can also be classified as caspase-dependent or caspase-independent. Caspase-dependent pathways involve the activation of caspase proteins, which normally exist in an inactive form termed "procaspases". These are cleaved by activated caspases into smaller, active subunits which in turn cleave

and activate other caspases in a highly organized cascade that leads to photoreceptor cell death. The caspase-dependent pathway has been shown to result from both an extrinsic pathway, which is initiated by the binding of extracellular ligands to membrane receptors such as Fas/CD95 or TNFα, and an intrinsic pathway involving mitochondrial release of cytochrome *c* (Wenzel et al., 2005). Caspase-independent apoptosis describes apoptotic pathways in which involvement of caspases has not been demonstrated. Components of the caspase-independent pathway include cathepsins, calpains, granzymes A and B, and serine proteases like AP24 (Wenzel et al., 2005). Both pathways have been observed in animal models of retinal degeneration (Doonan et al., 2003), and it would be interesting to determine which is operating in photoreceptors of the mrho+/-; hT17M mouse in response to light damage.

Numerous attempts have been made to overcome light-induced apoptosis with pharmacological agents (for an excellent review, see Wenzel et al., 2005). Dexamethasone treatment, which results in induction of glucocorticoid activity, has shown to lower AP-1 levels and rescue light-induced damage in the "acute" model of Hao et al.(Wenzel et al., 2001a; Hao et al., 2002). Administration of halothane anesthesia, which has been shown to limit rhodopsin regeneration following photoactivation, is also protective against light-mediated damage in albino mice and rats (Keller et al., 2001). In 2001, Cao et al. reported the protective effect of intravitreal injection of pigment epithelium-derived growth factor and basic fibroblast growth factor in albino Sprague-Dawley rats (Cao et al., 2001). Intraperitoneal injection of phenyl-N-tert-butylnitrone, which is known to possess antioxidant properties, also prevented light damage in Sprague-Dawley rats (Ranchon et al., 2001), but such treatment was unable to

rescue photoreceptor degeneration in rat models of ADRP that were transgenic for P23H or S334ter mutant rhodopsin(Ranchon et al., 2003). In fact, although many agents are known to prevent the retinal degeneration induced by light damage, none of these treatments to date has been successful at additionally preventing retinal degeneration in animal models of retinitis pigmentosa (Wenzel et al., 2005). It is possible that further understanding of the apoptotic pathways involved in photoreceptor death resulting from both light-induced damage and retinitis pigmentosa will lead to the discovery of agents or combinations of agents that can perform both therapeutic functions.

The experiments described above provide insight into possible means of unraveling the mechanism of apoptotic cell death induced by light exposure in the mrho+/-; hT17M transgenic mice. Crossing this line with transducin knockout mice, for example, would enable us to determine whether the damage was transducin-dependent, and possibly Ca2+ related, as seen in the "low-intensity" pathway of Hao et al. On the other hand, the observation of elevated levels of the AP-1 transcription factor or rescue by dexamethasone would lead to the classification of the hT17M-mediated light sensitivity as more of an "acute" model of light-induced photoreceptor apoptosis. If the hT17M degeneration involves the "acute" pathway, then crossing this line to the RPE65 knockout mouse line would be expected to reduce or prevent retinal light damage. Similarly, the success or failure of treatment with pharmacological agents such as D-*cis*-diltiazem, phenyl-N-tert-butylnitrone, halothane, or 13-*cis* retinoic acid at preventing light damage would assist in understanding this apoptotic pathway, contributing to the overall understanding of the mechanisms of photoreceptor apoptosis and possibly leading, as discussed, to more effective treatments for retinitis pigmentosa.

On the other hand, it is possible that the aforementioned experiments would have little success in elucidating the mechanism of the light sensitivity conferred by hT17M transgene expression. The evidence described here indicates that hT17M transgene expression results in one of the most light-sensitive mouse retinal phenotypes yet described. To illustrate this point, consider the Balb/c model of light sensitivity, which owes its phenotype to the leucine at the polymorphic codon 450 of the RPE65 gene (Wenzel et al., 2001b). The threshold of light-mediated damage in this animal, as measured by nucleosome release, is between 10 and 15 minutes of exposure to white light of 13,000 lux intensity (Wenzel et al., 2005). In our model of light-mediated damage, significant apoptosis was observed after a much less intense light exposure of 5,000 lux for 2.5 minutes. Additionally, we observed significant photoreceptor apoptosis in the hT17M mice that resulted from the extremely brief light exposure associated with fundus photography. The severity of the light sensitivity seen in the hT17M mouse line raises the possibility that it is the result of apoptotic pathways that differ from those previously described.

It is intriguing that the T17M rhodopsin mutation abolishes the glycosylation site at position 15 of rhodopsin (Kaushal et al., 1994). It shares this feature with the T4R rhodopsin mutation, which has been also been associated with extreme sensitivity to light-mediated retinal damage in a dog model of ADRP (Cideciyan et al., 2005; Zhu et al., 2004). Experiments involving the inhibition of rhodopsin glycosylation have been shown to lead to defects in the morphogenesis of photoreceptor outer segments (Fliesler et al., 1985). It seems reasonable to postulate that inhibition of rhodopsin glycosylation by the T4R or T17M mutations results in a protein that is uniquely affected by light

exposure, leading to photoreceptor cell death. It is possible that light exposure increases the rate of aberrant disc morphogenesis in these animals, which would be expected to lead to result in photoreceptor cell death (Mendes et al., 2005; Besharse and Wetzel, 1995). Light-induced, toxic accumulation of non-glyosylated rhodopsin could also trigger the unfolded-protein or ER-stress response, which has been shown to lead to apoptosis (Mendes et al., 2005; Rutkowski and Kaufman, 2004).

When considering other possible mechanisms for light-mediated photoreceptor damage in the hT17M transgenic mice, it bears repeating that Sung and coworkers note that their class II rhodopsin mutations show retention/mislocalization to the endoplasmic reticulum similar to that seen with other disease-causing mutant proteins such as Class II low density lipoprotein receptors and cystic fibrosis transmembrane conductance regulator proteins (Sung et al., 1991; Sung et al., 1994). As T17M was characterized as a class II mutation in those studies, it is quite possible that the mutant rhodopsins expressed by our mrho+/-; hT17M mice are improperly retained in the inner segments of rod photoreceptor cells. Rhodopsin, as was mentioned, is a G-coupled receptor protein, and it is possible that photoactivated rhodopsin is able to interact with other heterotrimeric G proteins besides transducin. In response to certain intensities of illumination, these mislocalized T17M rhodopsins could be responsible for widespread activation of heterotrimeric G proteins in improper cellular locations, with possible deleterious consequences for the photoreceptor cell. At least one such G protein has been shown to exist in the outer segment (Peng et al., 1997).

Ironically, the very light sensitivity that has slowed our efforts to treat the hT17M mouse line with rAAV-delivered, ribozyme mediated gene therapy could make this an

excellent model for the rapid identification of compounds that are able to inhibit or prevent the retinal degeneration associated with ADRP. Accumulation of misfolded protein and the ultimate apoptosis of affected photoreceptors are two targets for potential pharmacological intervention with either anti-apoptotic treatments or agents that can accelerate the clearance of misfolded proteins. If such drugs could be shown to be effective for long term prevention of retinal degeneration in the mrho+/-; hT17M line, as assayed by periodic electroretinograpic and histologic examination, there is the possibility that their introduction could also rescue the acute light sensitivity seen in these animals. If such is the case, then the effectiveness of similar types of drugs could be rapidly screened in the mrho+/-; hT17M line in a matter of days rather than the months it would take to observe rescue of the ADRP-mediated degeneration. The presence or absence of light-induced photoreceptor apoptosis following retinal light exposure can be determined by TUNEL labeling of histological sections in around a week. More quantitative results could be obtained in around 48 hours by using the nucleosome release assay described by Hao et al.(Hao et al., 2002). Indeed, we plan to employ this assay for future experiments involving light-mediated retinal damage in the mrho+/-; hT17M line because of its speed and the quantitative nature of the data that it generates. These experiments will hopefully increase our understanding of the apoptotic mechanisms involved in retinal degeneration.

Clinical Impact

Mutation-specific light damage is an important concern for clinical practitioners advising and treating patients with retinitis pigmentosa. Funduscopic examination is one of the simplest and most common of all ophthalmologic techniques, and the data reported here indicate that it is likely that this type of examination could result in retinal

illumination with intensities of white light that are extremely deleterious to the visual acuity of RP patients containing certain rhodopsin mutations, like T17M. Retinal surgery to resolve cataracts, detached retinas, or perform vitrectomies can also expose the retina to intense white light of the type shown here to cause retinal damage and exacerbation of RP photoreceptor degeneration (Lawwill et al., 1980; Michels et al., 1987; Meyers and Bonner, 1982; McKechnie and Ghafour, 1982).

The fact that some forms of rhodopsin RP mutations, like P23H, exhibit no increased sensitivity to "acute" light damage while others, like the T17M and T4R mutation show exquisite sensitivity, make it all the more necessary for the vision research community to urge extreme caution when dealing with light exposure for RP patients. The fact that an ophthalmologist or optometrist has seen no ill effects following funduscopy or other procedures involving patients with retinitis pigmentosa does not mean that the light exposure was harmless, or if it was harmless, that it will not be damaging to future RP patients with different rhodopsin mutations. In fact, there could be many who would experience severe visual impairment following these examinations. Because of the heterogeneous nature of RP and the varying rates with which it affects different patients with the same rhodopsin mutations it would be easy for a clinician to conclude that a large drop in visual acuity reported by an RP patient following ophthalmologic procedures involving intense retinal illumination was the result of the patient suffering a "rapid onset" form of the disease rather than damage incurred from the examination procedure(s). Without prospective studies aimed at determining whether human patients suffering from RP caused by certain "extreme light sensitive" rhodopsin

Figure 6-1. Eye from a human who suffered from ADRP caused by the T17M rhodopsin mutation. The eye is oriented with the superior portion at the top of the photograph. Evidence of retinitis pigmentosa, including bone spicule deposits and drusen bodies are located almost exclusively in the inferior retina(Li et al., 1994).

mutations suffer greater retinal damage from such procedures than patients with other rhodopsin mutations, as we have shown to be the case in the mouse lines used in these experiments, this question cannot be clearly answered.

In any event, patients with RP and other types of retinal degeneration should be encouraged to avoid light exposure whenever possible by staying indoors on sunny days and wearing personal eye protection in the form of sunglasses or hats whenever outdoor activity cannot be avoided. The importance of incidental light exposure in ADRP associated with the T17M mutation is driven home by its clinical presentation: Retinal

degeneration is frequently observed primarily in the inferior retina (Figure 6-1). The image shown in this figure is of an eye excised from a deceased human patient who suffered from ADRP caused by the T17M rhodopsin mutation. This eye exhibits severe photoreceptor damage resulting from ADRP, as evidenced by the multitude of bone spicule deposits and drusen bodies. Interestingly, these telltale signs of retinitis pigmentosa are located almost exclusively in the inferior portion of the retina, while the superior retina appears relatively normal. Lifelong exposure to sunlight and overhead illumination specifically irradiated the inferior portion of the patient's retina and may thus have accelerated the rate of degeneration in that portion of the eye. It is difficult to overstate the importance of limiting retinal illumination by intense white light in patients suffering from autosomal dominant retinitis pigmentosa and other forms of retinal disease.

LIST OF REFERENCES

Acland,G.M., Aguirre,G.D., Bennett,J., Aleman,T.S., Cideciyan,A.V., Bennicelli,J., Dejneka,N.S., Pearce-Kelling,S.E., Maguire,A.M., Palczewski,K., Hauswirth,W.W., and Jacobson,S.G. (2005). Long-Term Restoration of Rod and Cone Vision by Single Dose rAAV-Mediated Gene Transfer to the Retina in a Canine Model of Childhood Blindness. Mol. Ther.

Acland,G.M., Aguirre,G.D., Ray,J., Zhang,Q., Aleman,T.S., Cideciyan,A.V., Pearce-Kelling,S.E., Anand,V., Zeng,Y., Maguire,A.M., Jacobson,S.G., Hauswirth,W.W., and Bennett,J. (2001). Gene therapy restores vision in a canine model of childhood blindness. Nat. Genet. *28*, 92-95.

Adamus,G., Sugden,B., Shiraga,S., Timmers,A.M., and Hauswirth,W.W. (2003). Anti-apoptotic effects of CNTF gene transfer on photoreceptor degeneration in experimental antibody-induced retinopathy. J. Autoimmun. *21*, 121-129.

Adrian,W., Everson,R.W., and Schmidt,I. (1977). Protection against photic damage in retinitis pigmentosa. Adv. Exp. Med. Biol. *77*, 233-247.

Ali,R.R., Sarra,G.M., Stephens,C., Alwis,M.D., Bainbridge,J.W., Munro,P.M., Fauser,S., Reichel,M.B., Kinnon,C., Hunt,D.M., Bhattacharya,S.S., and Thrasher,A.J. (2000). Restoration of photoreceptor ultrastructure and function in retinal degeneration slow mice by gene therapy. Nat. Genet. *25*, 306-310.

Altschuler,M., Tritz,R., and Hampel,A. (1992). A method for generating transcripts with defined 5' and 3' termini by autolytic processing. Gene *122*, 85-90.

Aonuma,H., Yamazaki,R., and Watanabe,I. (1999). Retinal cell death by light damage. Jpn. J. Ophthalmol. *43*, 171-179.

Auricchio,A., Behling,K.C., Maguire,A.M., O'Connor,E.M., Bennett,J., Wilson,J.M., and Tolentino,M.J. (2002). Inhibition of retinal neovascularization by intraocular viral-mediated delivery of anti-angiogenic agents. Mol. Ther. *6*, 490-494.

Auricchio,A., Kobinger,G., Anand,V., Hildinger,M., O'Connor,E., Maguire,A.M., Wilson,J.M., and Bennett,J. (2001). Exchange of surface proteins impacts on viral vector cellular specificity and transduction characteristics: the retina as a model. Hum. Mol. Genet. *10*, 3075-3081.

Auricchio,A., and Rolling,F. (2005). Adeno-associated viral vectors for retinal gene transfer and treatment of retinal diseases. Curr. Gene Ther. *5*, 339-348.

Beatrice,J., Wenzel,A., Reme,C.E., and Grimm,C. (2003). Increased light damage susceptibility at night does not correlate with RPE65 levels and rhodopsin regeneration in rats. Exp. Eye Res. *76*, 695-700.

Bence,N.F., Sampat,R.M., and Kopito,R.R. (2001). Impairment of the ubiquitin-proteasome system by protein aggregation. Science *292*, 1552-1555.

Bennett,J. (2003). Immune response following intraocular delivery of recombinant viral vectors. Gene Ther. *10*, 977-982.

Bennett,J., Tanabe,T., Sun,D., Zeng,Y., Kjeldbye,H., Gouras,P., and Maguire,A.M. (1996). Photoreceptor cell rescue in retinal degeneration (rd) mice by in vivo gene therapy. Nat. Med. *2*, 649-654.

Berson,E.L. (1996). Retinitis pigmentosa: unfolding its mystery. Proc. Natl. Acad. Sci. U. S. A *93*, 4526-4528.

Bertrand,E., Castanotto,D., Zhou,C., Carbonnelle,C., Lee,N.S., Good,P., Chatterjee,S., Grange,T., Pictet,R., Kohn,D., Engelke,D., and Rossi,J.J. (1997). The expression cassette determines the functional activity of ribozymes in mammalian cells by controlling their intracellular localization. RNA. *3*, 75-88.

Berzal-Herranz,A., Joseph,S., Chowrira,B.M., Butcher,S.E., and Burke,J.M. (1993). Essential nucleotide sequences and secondary structure elements of the hairpin ribozyme. EMBO J. *12*, 2567-2573.

Besharse,J.C., and Wetzel,M.G. (1995). Immunocytochemical localization of opsin in rod photoreceptors during periods of rapid disc assembly. J. Neurocytol. *24*, 371-388.

Blouin,V., Brument,N., Toublanc,E., Raimbaud,I., Moullier,P., and Salvetti,A. (2004). Improving rAAV production and purification: towards the definition of a scaleable process. J. Gene Med. *6 Suppl 1*, S223-S228.

Bosch,A., Perret,E., Desmaris,N., and Heard,J.M. (2000). Long-term and significant correction of brain lesions in adult mucopolysaccharidosis type VII mice using recombinant AAV vectors. Mol. Ther. *1*, 63-70.

Bownds,D. (1967). Site of attachment of retinal in rhodopsin. Nature *216*, 1178-1181.

Bowne,S.J., Sullivan,L.S., Blanton,S.H., Cepko,C.L., Blackshaw,S., Birch,D.G., Hughbanks-Wheaton,D., Heckenlively,J.R., and Daiger,S.P. (2002). Mutations in the inosine monophosphate dehydrogenase 1 gene (IMPDH1) cause the RP10 form of autosomal dominant retinitis pigmentosa. Hum. Mol. Genet. *11*, 559-568.

Bradley,D.G., Farrar,G.J., Sharp,E.M., Kenna,P., Humphries,M.M., McConnell,D.J., Daiger,S.P., McWilliam,P., and Humphries,P. (1989). Autosomal dominant retinitis pigmentosa: exclusion of the gene from the short arm of chromosome 1 including the region surrounding the rhesus locus. Am. J. Hum. Genet. *44*, 570-576.

Bredesen,D.E., Mehlen,P., and Rabizadeh,S. (2005). Receptors that mediate cellular dependence. Cell Death. Differ. *12*, 1031-1043.

Burger,C., Gorbatyuk,O.S., Velardo,M.J., Peden,C.S., Williams,P., Zolotukhin,S., Reier,P.J., Mandel,R.J., and Muzyczka,N. (2004). Recombinant AAV viral vectors pseudotyped with viral capsids from serotypes 1, 2, and 5 display differential efficiency and cell tropism after delivery to different regions of the central nervous system. Mol. Ther. *10*, 302-317.

Buzayan,J.M., Feldstein,P.A., Segrelles,C., and Bruening,G. (1988). Autolytic processing of a phosphorothioate diester bond. Nucleic Acids Res. *16*, 4009-4023.

Cao,W., Tombran-Tink,J., Elias,R., Sezate,S., Mrazek,D., and McGinnis,J.F. (2001). In vivo protection of photoreceptors from light damage by pigment epithelium-derived factor. Invest Ophthalmol. Vis. Sci. *42*, 1646-1652.

Cech,T.R. (1988a). Conserved sequences and structures of group I introns: building an active site for RNA catalysis--a review. Gene *73*, 259-271.

Cech,T.R. (1988b). Ribozymes and their medical implications. JAMA *260*, 3030-3034.

Chang,B., Hawes,N.L., Hurd,R.E., Davisson,M.T., Nusinowitz,S., and Heckenlively,J.R. (2002). Retinal degeneration mutants in the mouse. Vision Res. *42*, 517-525.

Chen,L., Wu,W., Dentchev,T., Zeng,Y., Wang,J., Tsui,I., Tobias,J.W., Bennett,J., Baldwin,D., and Dunaief,J.L. (2004). Light damage induced changes in mouse retinal gene expression. Exp. Eye Res. *79*, 239-247.

Choi,V.W., McCarty,D.M., and Samulski,R.J. (2005). AAV hybrid serotypes: improved vectors for gene delivery. Curr. Gene Ther. *5*, 299-310.

Cideciyan,A.V., Jacobson,S.G., Aleman,T.S., Gu,D., Pearce-Kelling,S.E., Sumaroka,A., Acland,G.M., and Aguirre,G.D. (2005). In vivo dynamics of retinal injury and repair in the rhodopsin mutant dog model of human retinitis pigmentosa. Proc. Natl. Acad. Sci. U. S. A *102*, 5233-5238.

Citti,L., and Rainaldi,G. (2005). Synthetic hammerhead ribozymes as therapeutic tools to control disease genes. Curr. Gene Ther. *5*, 11-24.

Clouet-d'Orval,B., and Uhlenbeck,O.C. (1997). Hammerhead ribozymes with a faster cleavage rate. Biochemistry *36*, 9087-9092.

Conrad,C.K., Allen,S.S., Afione,S.A., Reynolds,T.C., Beck,S.E., Fee-Maki,M., Barrazza-Ortiz,X., Adams,R., Askin,F.B., Carter,B.J., Guggino,W.B., and Flotte,T.R. (1996). Safety of single-dose administration of an adeno-associated virus (AAV)-CFTR vector in the primate lung. Gene Ther. *3*, 658-668.

Daiger,S.P., Sullivan,L.S., and Rodriguez,J.A. (1995). Correlation of Phenotype with Genotype in Inherited Retinal Degeneration. Behavioral and Brain Sciences *18*, 452-467.

Danciger,M., Lyon,J., Worrill,D., Hoffman,S., Lem,J., Reme,C.E., Wenzel,A., and Grimm,C. (2004). New retinal light damage QTL in mice with the light-sensitive RPE65 LEU variant. Mamm. Genome *15*, 277-283.

Diager, S. P., Sullivan, L. S., and Browne, S. J. RetNet. internet . 1-11-2005.

Ref Type: Electronic Citation

Dinculescu,A., Glushakova,L., Min,S.H., and Hauswirth,W.W. (2005). Adeno-associated virus-vectored gene therapy for retinal disease. Hum. Gene Ther. *16*, 649-663.

Donovan,M., and Cotter,T.G. (2002). Caspase-independent photoreceptor apoptosis in vivo and differential expression of apoptotic protease activating factor-1 and caspase-3 during retinal development. Cell Death. Differ. *9*, 1220-1231.

Donsante,A., Vogler,C., Muzyczka,N., Crawford,J.M., Barker,J., Flotte,T., Campbell-Thompson,M., Daly,T., and Sands,M.S. (2001). Observed incidence of tumorigenesis in long-term rodent studies of rAAV vectors. Gene Ther. *8*, 1343-1346.

Doonan,F., Donovan,M., and Cotter,T.G. (2003). Caspase-independent photoreceptor apoptosis in mouse models of retinal degeneration. J. Neurosci. *23*, 5723-5731.

Drenser,K.A., Timmers,A.M., Hauswirth,W.W., and Lewin,A.S. (1998). Ribozyme-targeted destruction of RNA associated with autosomal-dominant retinitis pigmentosa. Invest Ophthalmol. Vis. Sci. *39*, 681-689.

Dryja,T.P., McGee,T.L., Reichel,E., Hahn,L.B., Cowley,G.S., Yandell,D.W., Sandberg,M.A., and Berson,E.L. (1990). A point mutation of the rhodopsin gene in one form of retinitis pigmentosa. Nature *343*, 364-366.

Fain,G.L., and Lisman,J.E. (1993). Photoreceptor degeneration in vitamin A deprivation and retinitis pigmentosa: the equivalent light hypothesis. Exp. Eye Res. *57*, 335-340.

Fain,G.L., and Lisman,J.E. (1999). Light, Ca2+, and photoreceptor death: new evidence for the equivalent-light hypothesis from arrestin knockout mice. Invest Ophthalmol. Vis. Sci. *40*, 2770-2772.

Farber,D.B., Flannery,J.G., Bird,A.C., Shuster,T., and Bok,D. (1987). Histopathological and biochemical studies on donor eyes affected with retinitis pigmentosa. Prog. Clin. Biol. Res. *247*, 53-67.

Farrar,G.J., Kenna,P.F., and Humphries,P. (2002). On the genetics of retinitis pigmentosa and on mutation-independent approaches to therapeutic intervention. EMBO J. *21*, 857-864.

Fisher,K.J., Jooss,K., Alston,J., Yang,Y., Haecker,S.E., High,K., Pathak,R., Raper,S.E., and Wilson,J.M. (1997). Recombinant adeno-associated virus for muscle directed gene therapy. Nat. Med. *3*, 306-312.

Flannery,J.G., Farber,D.B., Bird,A.C., and Bok,D. (1989). Degenerative changes in a retina affected with autosomal dominant retinitis pigmentosa. Invest Ophthalmol. Vis. Sci. *30*, 191-211.

Flannery,J.G., Zolotukhin,S., Vaquero,M.I., LaVail,M.M., Muzyczka,N., and Hauswirth,W.W. (1997). Efficient photoreceptor-targeted gene expression in vivo by recombinant adeno-associated virus. Proc. Natl. Acad. Sci. U. S. A *94*, 6916-6921.

Fliesler,S.J., Rayborn,M.E., and Hollyfield,J.G. (1985). Membrane morphogenesis in retinal rod outer segments: inhibition by tunicamycin. J. Cell Biol. *100*, 574-587.

Flotte,T.R. (2005). Recent developments in recombinant AAV-mediated gene therapy for lung diseases. Curr. Gene Ther. *5*, 361-366.

Fritz,J.J., White,D.A., Lewin,A.S., and Hauswirth,W.W. (2002). Designing and characterizing hammerhead ribozymes for use in AAV vector-mediated retinal gene therapies. Methods Enzymol. *346*, 358-377.

Fu,H., Samulski,R.J., McCown,T.J., Picornell,Y.J., Fletcher,D., and Muenzer,J. (2002). Neurological correction of lysosomal storage in a mucopolysaccharidosis IIIB mouse model by adeno-associated virus-mediated gene delivery. Mol. Ther. *5*, 42-49.

Fuller,D., Machemer,R., and Knighton,R.W. (1978). Retinal damage produced by intraocular fiber optic light. Am. J. Ophthalmol. *85*, 519-537.

Gao,G., Vandenberghe,L.H., and Wilson,J.M. (2005). New recombinant serotypes of AAV vectors. Curr. Gene Ther. *5*, 285-297.

Gao,G.P., Alvira,M.R., Wang,L., Calcedo,R., Johnston,J., and Wilson,J.M. (2002). Novel adeno-associated viruses from rhesus monkeys as vectors for human gene therapy. Proc. Natl. Acad. Sci. U. S. A *99*, 11854-11859.

Gigout,L., Rebollo,P., Clement,N., Warrington,K.H., Jr., Muzyczka,N., Linden,R.M., and Weber,T. (2005). Altering AAV tropism with mosaic viral capsids. Mol. Ther. *11*, 856-865.

Gorbatyuk,M.S., Pang,J.J., Thomas,J., Jr., Hauswirth,W.W., and Lewin,A.S. (2005). Knockdown of wild-type mouse rhodopsin using an AAV vectored ribozyme as part of an RNA replacement approach. Mol. Vis. *11*, 648-656.

Goto,Y., Peachey,N.S., Ripps,H., and Naash,M.I. (1995). Functional abnormalities in transgenic mice expressing a mutant rhodopsin gene. Invest Ophthalmol. Vis. Sci. *36*, 62-71.

Goto,Y., Peachey,N.S., Ziroli,N.E., Seiple,W.H., Gryczan,C., Pepperberg,D.R., and Naash,M.I. (1996). Rod phototransduction in transgenic mice expressing a mutant opsin gene. J. Opt. Soc. Am. A Opt. Image Sci. Vis. *13*, 577-585.

Grimm,C., Wenzel,A., Hafezi,F., and Reme,C.E. (2000a). Gene expression in the mouse retina: the effect of damaging light. Mol. Vis. *6*, 252-260.

Grimm,C., Wenzel,A., Hafezi,F., Yu,S., Redmond,T.M., and Reme,C.E. (2000b). Protection of Rpe65-deficient mice identifies rhodopsin as a mediator of light-induced retinal degeneration. Nat. Genet. *25*, 63-66.

Grimm,D. (2002). Production methods for gene transfer vectors based on adeno-associated virus serotypes. Methods *28*, 146-157.

Grimm,D., and Kay,M.A. (2003). From virus evolution to vector revolution: use of naturally occurring serotypes of adeno-associated virus (AAV) as novel vectors for human gene therapy. Curr. Gene Ther. *3*, 281-304.

Grum-Tokars,V., Milovanovic,M., and Wedekind,J.E. (2003). Crystallization and X-ray diffraction analysis of an all-RNA U39C mutant of the minimal hairpin ribozyme. Acta Crystallogr. D. Biol. Crystallogr. *59*, 142-145.

Guerrier-Takada,C., and Altman,S. (1984). Catalytic activity of an RNA molecule prepared by transcription in vitro. Science *223*, 285-286.

Guerrier-Takada,C., Gardiner,K., Marsh,T., Pace,N., and Altman,S. (1983). The RNA moiety of ribonuclease P is the catalytic subunit of the enzyme. Cell *35*, 849-857.

Guy,J., Qi,X., Muzyczka,N., and Hauswirth,W.W. (1999). Reporter expression persists 1 year after adeno-associated virus-mediated gene transfer to the optic nerve. Arch. Ophthalmol. *117*, 929-937.

Hafezi,F., Steinbach,J.P., Marti,A., Munz,K., Wang,Z.Q., Wagner,E.F., Aguzzi,A., and Reme,C.E. (1997). The absence of c-fos prevents light-induced apoptotic cell death of photoreceptors in retinal degeneration in vivo. Nat. Med. *3*, 346-349.

Hao,W., Wenzel,A., Obin,M.S., Chen,C.K., Brill,E., Krasnoperova,N.V., Eversole-Cire,P., Kleyner,Y., Taylor,A., Simon,M.I., Grimm,C., Reme,C.E., and Lem,J. (2002). Evidence for two apoptotic pathways in light-induced retinal degeneration. Nat. Genet. *32*, 254-260.

Hargrave,P.A., and Mcdowell,J.H. (1992). Rhodopsin and Phototransduction - A Model System for G-Protein-Linked Receptors. Faseb Journal *6*, 2323-2331.

Haseloff,J., and Gerlach,W.L. (1988). Simple RNA enzymes with new and highly specific endoribonuclease activities. Nature *334*, 585-591.

Hauswirth,W.W., LaVail,M.M., Flannery,J.G., and Lewin,A.S. (2000). Ribozyme gene therapy for autosomal dominant retinal disease. Clin. Chem. Lab Med. *38*, 147-153.

Hauswirth,W.W., and Lewin,A.S. (2000). Ribozyme uses in retinal gene therapy. Prog. Retin. Eye Res. *19*, 689-710.

Hauswirth,W.W., Li,Q., Raisler,B., Timmers,A.M., Berns,K.I., Flannery,J.G., LaVail,M.M., and Lewin,A.S. (2004). Range of retinal diseases potentially treatable by AAV-vectored gene therapy. Novartis. Found. Symp. *255*, 179-188.

Hennig,A.K., Ogilvie,J.M., Ohlemiller,K.K., Timmers,A.M., Hauswirth,W.W., and Sands,M.S. (2004). AAV-mediated intravitreal gene therapy reduces lysosomal storage in the retinal pigmented epithelium and improves retinal function in adult MPS VII mice. Mol. Ther. *10*, 106-116.

Hermonat,P.L., Quirk,J.G., Bishop,B.M., and Han,L. (1997). The packaging capacity of adeno-associated virus (AAV) and the potential for wild-type-plus AAV gene therapy vectors. FEBS Lett. *407*, 78-84.

Hernandez,Y.J., Wang,J., Kearns,W.G., Loiler,S., Poirier,A., and Flotte,T.R. (1999). Latent adeno-associated virus infection elicits humoral but not cell-mediated immune responses in a nonhuman primate model. J. Virol. *73*, 8549-8558.

Hildinger,M., Auricchio,A., Gao,G., Wang,L., Chirmule,N., and Wilson,J.M. (2001). Hybrid vectors based on adeno-associated virus serotypes 2 and 5 for muscle-directed gene transfer. J. Virol. *75*, 6199-6203.

Hims,M.M., Diager,S.P., and Inglehearn,C.F. (2003). Retinitis pigmentosa: genes, proteins and prospects. Dev. Ophthalmol. *37*, 109-125.

Huang,P.C., Gaitan,A.E., Hao,Y., Petters,R.M., and Wong,F. (1993). Cellular interactions implicated in the mechanism of photoreceptor degeneration in transgenic mice expressing a mutant rhodopsin gene. Proc. Natl. Acad. Sci. U. S. A *90*, 8484-8488.

Humphries,M.M., Rancourt,D., Farrar,G.J., Kenna,P., Hazel,M., Bush,R.A., Sieving,P.A., Sheils,D.M., McNally,N., Creighton,P., Erven,A., Boros,A., Gulya,K., Capecchi,M.R., and Humphries,P. (1997). Retinopathy induced in mice by targeted disruption of the rhodopsin gene. Nat. Genet. *15*, 216-219.

Humphries,P., Kenna,P., and Farrar,G.J. (1992). On the Molecular-Genetics of Retinitis-Pigmentosa. Science *256*, 804-808.

Illing,M.E., Rajan,R.S., Bence,N.F., and Kopito,R.R. (2002). A rhodopsin mutant linked to autosomal dominant retinitis pigmentosa is prone to aggregate and interacts with the ubiquitin proteasome system. J. Biol. Chem. *277*, 34150-34160.

Jomary,C., Vincent,K.A., Grist,J., Neal,M.J., and Jones,S.E. (1997). Rescue of photoreceptor function by AAV-mediated gene transfer in a mouse model of inherited retinal degeneration. Gene Ther. *4*, 683-690.

Joseph,S., Berzal-Herranz,A., Chowrira,B.M., Butcher,S.E., and Burke,J.M. (1993). Substrate selection rules for the hairpin ribozyme determined by in vitro selection, mutation, and analysis of mismatched substrates. Genes Dev. *7*, 130-138.

Kapturczak,M.H., Flotte,T., and Atkinson,M.A. (2001). Adeno-associated virus (AAV) as a vehicle for therapeutic gene delivery: improvements in vector design and viral production enhance potential to prolong graft survival in pancreatic islet cell transplantation for the reversal of type 1 diabetes. Curr. Mol. Med. *1*, 245-258.

Karnik,S.S., and Khorana,H.G. (1990). Assembly of functional rhodopsin requires a disulfide bond between cysteine residues 110 and 187. J. Biol. Chem. *265*, 17520-17524.

Karnik,S.S., Sakmar,T.P., Chen,H.B., and Khorana,H.G. (1988). Cysteine residues 110 and 187 are essential for the formation of correct structure in bovine rhodopsin. Proc. Natl. Acad. Sci. U. S. A *85*, 8459-8463.

Kaushal,S. and Khorana,H.G. (1994). Structure and function in rhodopsin. 7. Point mutations associated with autosomal dominant retinitis pigmentosa. Biochemistry *33*, 6121-6128.

Kaushal,S., Ridge,K.D., and Khorana,H.G. (1994). Structure and function in rhodopsin: the role of asparagine-linked glycosylation. Proc. Natl. Acad. Sci. U. S. A *91*, 4024-4028.

Keeler,C. (1966). Retinal degeneration in the mouse is rodless retina. J. Hered. *57*, 47-50.

Keller,C., Grimm,C., Wenzel,A., Hafezi,F., and Reme,C. (2001). Protective effect of halothane anesthesia on retinal light damage: inhibition of metabolic rhodopsin regeneration. Invest Ophthalmol. Vis. Sci. *42*, 476-480.

Kennan,A., Aherne,A., and Humphries,P. (2005). Light in retinitis pigmentosa. Trends Genet. *21*, 103-110.

Kennan,A., Aherne,A., Palfi,A., Humphries,M., McKee,A., Stitt,A., Simpson,D.A., Demtroder,K., Orntoft,T., Ayuso,C., Kenna,P.F., Farrar,G.J., and Humphries,P. (2002). Identification of an IMPDH1 mutation in autosomal dominant retinitis pigmentosa (RP10) revealed following comparative microarray analysis of transcripts derived from retinas of wild-type and Rho(-/-) mice. Hum. Mol. Genet. *11*, 547-557.

Kolb, H., Fernandez, E., and Nelson, R. Webvision: The Organization of the Retina and Visual System. Internet . 2005.

Ref Type: Electronic Citation

Kotin,R.M., Siniscalco,M., Samulski,R.J., Zhu,X.D., Hunter,L., Laughlin,C.A., McLaughlin,S., Muzyczka,N., Rocchi,M., and Berns,K.I. (1990). Site-specific integration by adeno-associated virus. Proc. Natl. Acad. Sci. U. S. A *87*, 2211-2215.

Lansel,N., Hafezi,F., Marti,A., Hegi,M., Reme,C., and Niemeyer,G. (1998). The mouse ERG before and after light damage is independent of p53. Doc. Ophthalmol. *96*, 311-320.

Lanum,J. (1978). The damaging effects of light on the retina. Empirical findings, theoretical and practical implications. Surv. Ophthalmol. *22*, 221-249.

Lau,D., and Flannery,J. (2003). Viral-mediated FGF-2 treatment of the constant light damage model of photoreceptor degeneration. Doc. Ophthalmol. *106*, 89-98.

Lau,D., McGee,L.H., Zhou,S., Rendahl,K.G., Manning,W.C., Escobedo,J.A., and Flannery,J.G. (2000). Retinal degeneration is slowed in transgenic rats by AAV-mediated delivery of FGF-2. Invest Ophthalmol. Vis. Sci. *41*, 3622-3633.

LaVail,M.M., Gorrin,G.M., Repaci,M.A., Thomas,L.A., and Ginsberg,H.M. (1987). Genetic regulation of light damage to photoreceptors. Invest Ophthalmol. Vis. Sci. *28*, 1043-1048.

LaVail,M.M., Yasumura,D., Matthes,M.T., Drenser,K.A., Flannery,J.G., Lewin,A.S., and Hauswirth,W.W. (2000). Ribozyme rescue of photoreceptor cells in P23H transgenic rats: long-term survival and late-stage therapy. Proc. Natl. Acad. Sci. U. S. A *97*, 11488-11493.

LaVail,M.M., Yasumura,D., Matthes,M.T., Lau-Villacorta,C., Unoki,K., Sung,C.H., and Steinberg,R.H. (1998). Protection of mouse photoreceptors by survival factors in retinal degenerations. Invest Ophthalmol. Vis. Sci. *39*, 592-602.

Lawwill,T., Crockett,R.S., Currier,G., and Rosenberg,R.B. (1980). Review of the macaque model of light damage with implications for the use of ophthalmic instrumentation. Vision Res. *20*, 1113-1115.

Lem,J., Flannery,J.G., Li,T., Applebury,M.L., Farber,D.B., and Simon,M.I. (1992). Retinal degeneration is rescued in transgenic rd mice by expression of the cGMP phosphodiesterase beta subunit. Proc. Natl. Acad. Sci. U. S. A *89*, 4422-4426.

Lem,J., Krasnoperova,N.V., Calvert,P.D., Kosaras,B., Cameron,D.A., Nicolo,M., Makino,C.L., and Sidman,R.L. (1999). Morphological, physiological, and biochemical changes in rhodopsin knockout mice. Proc. Natl. Acad. Sci. U. S. A *96*, 736-741.

Lewin,A.S., Drenser,K.A., Hauswirth,W.W., Nishikawa,S., Yasumura,D., Flannery,J.G., and LaVail,M.M. (1998). Ribozyme rescue of photoreceptor cells in a transgenic rat model of autosomal dominant retinitis pigmentosa. Nat. Med. *4*, 967-971.

Li,T., Sandberg,M.A., Pawlyk,B.S., Rosner,B., Hayes,K.C., Dryja,T.P., and Berson,E.L. (1998). Effect of vitamin A supplementation on rhodopsin mutants threonine-17 --> methionine and proline-347 --> serine in transgenic mice and in cell cultures. Proc. Natl. Acad. Sci. U. S. A *95*, 11933-11938.

Li,Z.Y., Jacobson,S.G., and Milam,A.H. (1994). Autosomal dominant retinitis pigmentosa caused by the threonine-17-methionine rhodopsin mutation: retinal histopathology and immunocytochemistry. Exp. Eye Res. *58*, 397-408.

Liang,F.Q., Dejneka,N.S., Cohen,D.R., Krasnoperova,N.V., Lem,J., Maguire,A.M., Dudus,L., Fisher,K.J., and Bennett,J. (2001). AAV-mediated delivery of ciliary neurotrophic factor prolongs photoreceptor survival in the rhodopsin knockout mouse. Mol. Ther. *3*, 241-248.

Liu,J., Timmers,A.M., Lewin,A.S., and Hauswirth,W.W. (2005). Ribozyme Knockdown of the {gamma}-Subunit of Rod cGMP Phosphodiesterase Alters the ERG and Retinal Morphology in Wild-Type Mice. Invest Ophthalmol. Vis. Sci. *46*, 3836-3844.

Liu,X., Wu,T.H., Stowe,S., Matsushita,A., Arikawa,K., Naash,M.I., and Williams,D.S. (1997). Defective phototransductive disk membrane morphogenesis in transgenic mice expressing opsin with a mutated N-terminal domain. J. Cell Sci. *110 (Pt 20)*, 2589-2597.

Loiler,S.A., Conlon,T.J., Song,S., Tang,Q., Warrington,K.H., Agarwal,A., Kapturczak,M., Li,C., Ricordi,C., Atkinson,M.A., Muzyczka,N., and Flotte,T.R. (2003). Targeting recombinant adeno-associated virus vectors to enhance gene transfer to pancreatic islets and liver. Gene Ther. *10*, 1551-1558.

Maita,H., Kitaura,H., Ariga,H., and Iguchi-Ariga,S.M. (2005). Association of PAP-1 and Prp3p, the products of causative genes of dominant retinitis pigmentosa, in the tri-snRNP complex. Exp. Cell Res. *302*, 61-68.

Maple,B.R., and Wu,S.M. (1996). Synaptic inputs mediating bipolar cell responses in the tiger salamander retina. Vision Res. *36*, 4015-4023.

Martinez-Gimeno,M., Gamundi,M.J., Hernan,I., Maseras,M., Milla,E., Ayuso,C., Garcia-Sandoval,B., Beneyto,M., Vilela,C., Baiget,M., Antinolo,G., and Carballo,M. (2003). Mutations in the pre-mRNA splicing-factor genes PRPF3, PRPF8, and PRPF31 in Spanish families with autosomal dominant retinitis pigmentosa. Invest Ophthalmol. Vis. Sci. *44*, 2171-2177.

McCabe,S.L., Pelosi,D.M., Tetreault,M., Miri,A., Nguitragool,W., Kovithvathanaphong,P., Mahajan,R., and Zimmerman,A.L. (2004). All-trans-retinal is a closed-state inhibitor of rod cyclic nucleotide-gated ion channels. J. Gen. Physiol *123*, 521-531.

McKechnie,N.M. and Ghafour,I.M. (1982). Potential retinal light damage from the use of therapeutic instruments. Trans. Ophthalmol. Soc. U. K. *102 (Pt 1)*, 140-146.

McKechnie,N.M., and Johnson,N.F. (1977). Light damage to the retina. Albrecht. Von. Graefes Arch. Klin. Exp. Ophthalmol. *203*, 283-292.

McLaughlin,S.K., Collis,P., Hermonat,P.L., and Muzyczka,N. (1988). Adeno-associated virus general transduction vectors: analysis of proviral structures. J. Virol. *62*, 1963-1973.

McNally,N., Kenna,P., Humphries,M.M., Hobson,A.H., Khan,N.W., Bush,R.A., Sieving,P.A., Humphries,P., and Farrar,G.J. (1999). Structural and functional rescue of murine rod photoreceptors by human rhodopsin transgene. Hum. Mol. Genet. *8*, 1309-1312.

McWilliam,P., Farrar,G.J., Kenna,P., Bradley,D.G., Humphries,M.M., Sharp,E.M., McConnell,D.J., Lawler,M., Sheils,D., Ryan,C., and . (1989). Autosomal dominant retinitis pigmentosa (ADRP): localization of an ADRP gene to the long arm of chromosome 3. Genomics *5*, 619-622.

Mendes,H.F., van der,S.J., Chapple,J.P., and Cheetham,M.E. (2005). Mechanisms of cell death in rhodopsin retinitis pigmentosa: implications for therapy. Trends Mol. Med. *11*, 177-185.

Meyers,S.M., and Bonner,R.F. (1982). Yellow filter to decrease the risk of light damage to the retina during vitrectomy. Am. J. Ophthalmol. *94*, 677.

Michels,M., Dawson,W.W., Feldman,R.B., and Jarolem,K. (1987). Infrared. An unseen and unnecessary hazard in ophthalmic devices. Ophthalmology *94*, 143-148.

Min,S.H., Molday,L.L., Seeliger,M.W., Dinculescu,A., Timmers,A.M., Janssen,A., Tonagel,F., Tanimoto,N., Weber,B.H., Molday,R.S., and Hauswirth,W.W. (2005). Prolonged recovery of retinal structure/function after gene therapy in an Rs1h-deficient mouse model of x-linked juvenile retinoschisis. Mol. Ther. *12*, 644-651.

Mittag,T.W., Bayer,A.U., and La VAIL,M.M. (1999). Light-induced retinal damage in mice carrying a mutated SOD I gene. Exp. Eye Res. *69*, 677-683.

Mohamad,N., Gutierrez,A., Nunez,M., Cocca,C., Martin,G., Cricco,G., Medina,V., Rivera,E., and Bergoc,R. (2005). Mitochondrial apoptotic pathways. Biocell *29*, 149-161.

Muzyczka,N., and Warrington,K.H., Jr. (2005). Custom adeno-associated virus capsids: the next generation of recombinant vectors with novel tropism. Hum. Gene Ther. *16*, 408-416.

Naash,M.I., Hollyfield,J.G., Al Ubaidi,M.R., and Baehr,W. (1993). Simulation of human autosomal dominant retinitis pigmentosa in transgenic mice expressing a mutated murine opsin gene. Proc. Natl. Acad. Sci. U. S. A *90*, 5499-5503.

Naash,M.L., Peachey,N.S., Li,Z.Y., Gryczan,C.C., Goto,Y., Blanks,J., Milam,A.H., and Ripps,H. (1996). Light-induced acceleration of photoreceptor degeneration in transgenic mice expressing mutant rhodopsin. Invest Ophthalmol. Vis. Sci. *37*, 775-782.

Nieuwlandt,D. (2000). In vitro selection of functional nucleic acid sequences. Curr. Issues Mol. Biol. *2*, 9-16.

Noell,W.K., Walker,V.S., Kang,B.S., and Berman,S. (1966). Retinal damage by light in rats. Invest Ophthalmol. *5*, 450-473.

Olsson,J.E., Gordon,J.W., Pawlyk,B.S., Roof,D., Hayes,A., Molday,R.S., Mukai,S., Cowley,G.S., Berson,E.L., and Dryja,T.P. (1992). Transgenic mice with a rhodopsin mutation (Pro23His): a mouse model of autosomal dominant retinitis pigmentosa. Neuron *9*, 815-830.

Opie,S.R., Warrington,K.H., Jr., Agbandje-McKenna,M., Zolotukhin,S., and Muzyczka,N. (2003). Identification of amino acid residues in the capsid proteins of adeno-associated virus type 2 that contribute to heparan sulfate proteoglycan binding. J. Virol. *77*, 6995-7006.

Pang,J.J., Chang,B., Kumar,A., Nusinowitz,S., Noorwez,S.M., Li,J., Rani,A., Foster,T.C., Chiodo,V.A., Doyle,T., Li,H., Malhotra,R., Tusner,J., Mcdowell,J.H., Min,S.H., Li,Q., Kaushal,S., and Hauswirth,W.W. (2005). Gene Therapy Restores Vision-Dependent Behavior as Well as Retinal Structure and Function in a Mouse Model of RPE65 Leber Congenital Amaurosis. Mol. Ther.

Papermaster,D.S., Schneider,B.G., DeFoe,D., and Besharse,J.C. (1986). Biosynthesis and vectorial transport of opsin on vesicles in retinal rod photoreceptors. J. Histochem. Cytochem. *34*, 5-16.

Peng,Y.W., Rhee,S.G., Yu,W.P., Ho,Y.K., Schoen,T., Chader,G.J., and Yau,K.W. (1997). Identification of components of a phosphoinositide signaling pathway in retinal rod outer segments. Proc. Natl. Acad. Sci. U. S. A *94*, 1995-2000.

Penn,J.S. (1985). Effects of continuous light on the retina of a fish, Notemigonus crysoleucas. J. Comp Neurol. *238*, 121-127.

Phylactou,L.A., Kilpatrick,M.W., and Wood,M.J. (1998). Ribozymes as therapeutic tools for genetic disease. Hum. Mol. Genet. *7*, 1649-1653.

Pierce,M.L., and Ruffner,D.E. (1998). Construction of a directed hammerhead ribozyme library: towards the identification of optimal target sites for antisense-mediated gene inhibition. Nucleic Acids Res. *26*, 5093-5101.

Piganeau,N., Thuillier,V., and Famulok,M. (2001). In vitro selection of allosteric ribozymes: theory and experimental validation. J. Mol. Biol. *312*, 1177-1190.

Portera-Cailliau,C., Sung,C.H., Nathans,J., and Adler,R. (1994). Apoptotic photoreceptor cell death in mouse models of retinitis pigmentosa. Proc. Natl. Acad. Sci. U. S. A *91*, 974-978.

Potter,M., Chesnut,K., Muzyczka,N., Flotte,T., and Zolotukhin,S. (2002). Streamlined large-scale production of recombinant adeno-associated virus (rAAV) vectors. Methods Enzymol. *346*, 413-430.

Rabinowitz,J.E., Rolling,F., Li,C., Conrath,H., Xiao,W., Xiao,X., and Samulski,R.J. (2002). Cross-packaging of a single adeno-associated virus (AAV) type 2 vector genome into multiple AAV serotypes enables transduction with broad specificity. J. Virol. *76*, 791-801.

Raisler,B.J., Berns,K.I., Grant,M.B., Beliaev,D., and Hauswirth,W.W. (2002). Adeno-associated virus type-2 expression of pigmented epithelium-derived factor or Kringles 1-3 of angiostatin reduce retinal neovascularization. Proc. Natl. Acad. Sci. U. S. A *99*, 8909-8914.

Rajan,R.S., Illing,M.E., Bence,N.F., and Kopito,R.R. (2001). Specificity in intracellular protein aggregation and inclusion body formation. Proc. Natl. Acad. Sci. U. S. A *98*, 13060-13065.

Ranchon,I., Chen,S., Alvarez,K., and Anderson,R.E. (2001). Systemic administration of phenyl-N-tert-butylnitrone protects the retina from light damage. Invest Ophthalmol. Vis. Sci. *42*, 1375-1379.

Ranchon,I., LaVail,M.M., Kotake,Y., and Anderson,R.E. (2003). Free radical trap phenyl-N-tert-butylnitrone protects against light damage but does not rescue P23H and S334ter rhodopsin transgenic rats from inherited retinal degeneration. J. Neurosci. *23*, 6050-6057.

Reme,C.E., Grimm,C., Hafezi,F., Marti,A., and Wenzel,A. (1998). Apoptotic cell death in retinal degenerations. Prog. Retin. Eye Res. *17*, 443-464.

Rivolta,C., Sharon,D., DeAngelis,M.M., and Dryja,T.P. (2002). Retinitis pigmentosa and allied diseases: numerous diseases, genes, and inheritance patterns. Hum. Mol. Genet. *11*, 1219-1227.

Roof,D.J., Adamian,M., and Hayes,A. (1994). Rhodopsin accumulation at abnormal sites in retinas of mice with a human P23H rhodopsin transgene. Invest Ophthalmol. Vis. Sci. *35*, 4049-4062.

Rosenfeld,P.J., and Dryja,T.P. (1995). Molecular Genetics of Retinitis Pigmentosa and Related Retinal Degenerations. In Molecular Genetics of Ocular Disease, Wiley-Liss Inc.).

Rupert,P.B., and Ferre-D'Amare,A.R. (2001). Crystal structure of a hairpin ribozyme-inhibitor complex with implications for catalysis. Nature *410*, 780-786.

Rutkowski,D.T., and Kaufman,R.J. (2004). A trip to the ER: coping with stress. Trends Cell Biol. *14*, 20-28.

Schnepp,B.C., Jensen,R.L., Chen,C.-L., Johnson,P.R., and Clark,K.R. (2005). Characterization of Adeno-Associated Virus Genomes Isolated from Human Tissues. J. Virol. *79*, 14793-14803.

Scott,W.G., Finch,J.T., and Klug,A. (1995). The crystal structure of an all-RNA hammerhead ribozyme: a proposed mechanism for RNA catalytic cleavage. Cell *81*, 991-1002.

Shimayama,T., Nishikawa,S., and Taira,K. (1995). Generality of the NUX rule: kinetic analysis of the results of systematic mutations in the trinucleotide at the cleavage site of hammerhead ribozymes. Biochemistry *34*, 3649-3654.

Sieving,P.A., Chaudhry,P., Kondo,M., Provenzano,M., Wu,D., Carlson,T.J., Bush,R.A., and Thompson,D.A. (2001). Inhibition of the visual cycle in vivo by 13-cis retinoic acid protects from light damage and provides a mechanism for night blindness in isotretinoin therapy. Proc. Natl. Acad. Sci. U. S. A *98*, 1835-1840.

Sigurdsson,S.T., and Eckstein,F. (1995). Structure-function relationships of hammerhead ribozymes: from understanding to applications. Trends Biotechnol. *13*, 286-289.

Smith,A.J., Schlichtenbrede,F.C., Tschernutter,M., Bainbridge,J.W., Thrasher,A.J., and Ali,R.R. (2003). AAV-Mediated gene transfer slows photoreceptor loss in the RCS rat model of retinitis pigmentosa. Mol. Ther. *8*, 188-195.

Sonoda,Y., and Streilein,J.W. (1992). Orthotopic corneal transplantation in mice--evidence that the immunogenetic rules of rejection do not apply. Transplantation *54*, 694-704.

Steinberg,R.H., Fisher,S.K., and Anderson,D.H. (1980). Disc morphogenesis in vertebrate photoreceptors. J. Comp Neurol. *190*, 501-508.

Stenkamp,R.E., Teller,D.C., and Palczewski,K. (2005). Rhodopsin: a structural primer for G-protein coupled receptors. Arch. Pharm. (Weinheim) *338*, 209-216.

Streilein,J.W., Wilbanks,G.A., and Cousins,S.W. (1992). Immunoregulatory mechanisms of the eye. J. Neuroimmunol. *39*, 185-200.

Stricker,H.M., Ding,X.Q., Quiambao,A., Fliesler,S.J., and Naash,M.I. (2005). The Cys214-->Ser mutation in peripherin/rds causes a loss-of-function phenotype in transgenic mice. Biochem. J. *388*, 605-613.

Sugden,B., De Troy,B., Roberts,R.J., and Sambrook,J. (1975). Agarose slab-gel electrophoresis equipment. Anal. Biochem. *68*, 36-46.

Sung,C.H., Davenport,C.M., and Nathans,J. (1993). Rhodopsin mutations responsible for autosomal dominant retinitis pigmentosa. Clustering of functional classes along the polypeptide chain. J. Biol. Chem. *268*, 26645-26649.

Sung,C.H., Makino,C., Baylor,D., and Nathans,J. (1994). A rhodopsin gene mutation responsible for autosomal dominant retinitis pigmentosa results in a protein that is defective in localization to the photoreceptor outer segment. J. Neurosci. *14*, 5818-5833.

Sung,C.H., Schneider,B.G., Agarwal,N., Papermaster,D.S., and Nathans,J. (1991). Functional heterogeneity of mutant rhodopsins responsible for autosomal dominant retinitis pigmentosa. Proc. Natl. Acad. Sci. U. S. A *88*, 8840-8844.

Surosky,R.T., Urabe,M., Godwin,S.G., McQuiston,S.A., Kurtzman,G.J., Ozawa,K., and Natsoulis,G. (1997). Adeno-associated virus Rep proteins target DNA sequences to a unique locus in the human genome. J. Virol. *71*, 7951-7959.

Tai,A.W., Chuang,J.Z., Bode,C., Wolfrum,U., and Sung,C.H. (1999). Rhodopsin's carboxy-terminal cytoplasmic tail acts as a membrane receptor for cytoplasmic dynein by binding to the dynein light chain Tctex-1. Cell *97*, 877-887.

Timmers,A.M., Zhang,H., Squitieri,A., and Gonzalez-Pola,C. (2001). Subretinal injections in rodent eyes: effects on electrophysiology and histology of rat retina. Mol. Vis. *7*, 131-137.

Tso,M.O., Zhang,C., Abler,A.S., Chang,C.J., Wong,F., Chang,G.Q., and Lam,T.T. (1994). Apoptosis leads to photoreceptor degeneration in inherited retinal dystrophy of RCS rats. Invest Ophthalmol. Vis. Sci. *35*, 2693-2699.

Vaux,D.L. (1993). Toward an understanding of the molecular mechanisms of physiological cell death. Proc. Natl. Acad. Sci. U. S. A *90*, 786-789.

Vermeulen,K., Van Bockstaele,D.R., and Berneman,Z.N. (2005). Apoptosis: mechanisms and relevance in cancer. Ann. Hematol. *84*, 627-639.

Wang,M., Lam,T.T., Tso,M.O., and Naash,M.I. (1997). Expression of a mutant opsin gene increases the susceptibility of the retina to light damage. Vis. Neurosci. *14*, 55-62.

Warrington,K.H., Jr., Gorbatyuk,O.S., Harrison,J.K., Opie,S.R., Zolotukhin,S., and Muzyczka,N. (2004). Adeno-associated virus type 2 VP2 capsid protein is nonessential and can tolerate large peptide insertions at its N terminus. J. Virol. *78*, 6595-6609.

Weitzman,M.D., Kyostio,S.R., Kotin,R.M., and Owens,R.A. (1994). Adeno-associated virus (AAV) Rep proteins mediate complex formation between AAV DNA and its integration site in human DNA. Proc. Natl. Acad. Sci. U. S. A *91*, 5808-5812.

Wenzel,A., Grimm,C., Samardzija,M., and Reme,C.E. (2005). Molecular mechanisms of light-induced photoreceptor apoptosis and neuroprotection for retinal degeneration. Prog. Retin. Eye Res. *24*, 275-306.

Wenzel,A., Grimm,C., Seeliger,M.W., Jaissle,G., Hafezi,F., Kretschmer,R., Zrenner,E., and Reme,C.E. (2001a). Prevention of photoreceptor apoptosis by activation of the glucocorticoid receptor. Invest Ophthalmol. Vis. Sci. *42*, 1653-1659.

Wenzel,A., Iseli,H.P., Fleischmann,A., Hafezi,F., Grimm,C., Wagner,E.F., and Reme,C.E. (2002). Fra-1 substitutes for c-Fos in AP-1-mediated signal transduction in retinal apoptosis. J. Neurochem. *80*, 1089-1094.

Wenzel,A., Reme,C.E., Williams,T.P., Hafezi,F., and Grimm,C. (2001b). The Rpe65 Leu450Met variation increases retinal resistance against light-induced degeneration by slowing rhodopsin regeneration. J. Neurosci. *21*, 53-58.

Werner,M., and Uhlenbeck,O.C. (1995). The effect of base mismatches in the substrate recognition helices of hammerhead ribozymes on binding and catalysis. Nucleic Acids Res. *23*, 2092-2096.

Wilson,J.H., and Wensel,T.G. (2003). The nature of dominant mutations of rhodopsin and implications for gene therapy. Mol. Neurobiol. *28*, 149-158.

Woodruff,M.L., Lem,J., and Fain,G.L. (2004). Early receptor current of wild-type and transducin knockout mice: photosensitivity and light-induced Ca2+ release. J. Physiol *557*, 821-828.

Wu,T.H., Ting,T.D., Okajima,T.I., Pepperberg,D.R., Ho,Y.K., Ripps,H., and Naash,M.I. (1998). Opsin localization and rhodopsin photochemistry in a transgenic mouse model of retinitis pigmentosa. Neuroscience *87*, 709-717.

Wu,W.C., Lai,C.C., Chen,S.L., Sun,M.H., Xiao,X., Chen,T.L., Tsai,R.J., Kuo,S.W., and Tsao,Y.P. (2004). GDNF gene therapy attenuates retinal ischemic injuries in rats. Mol. Vis. *10*, 93-102.

Yang,G.S., Schmidt,M., Yan,Z., Lindbloom,J.D., Harding,T.C., Donahue,B.A., Engelhardt,J.F., Kotin,R., and Davidson,B.L. (2002). Virus-mediated transduction of murine retina with adeno-associated virus: effects of viral capsid and genome size. J. Virol. *76*, 7651-7660.

Young,R.W., and Bok,D. (1969). Participation of the retinal pigment epithelium in the rod outer segment renewal process. J. Cell Biol. *42*, 392-403.

Zhou,X., and Muzyczka,N. (1998). In vitro packaging of adeno-associated virus DNA. J. Virol. *72*, 3241-3247.

Zhu,L., Jang,G.F., Jastrzebska,B., Filipek,S., Pearce-Kelling,S.E., Aguirre,G.D., Stenkamp,R.E., Acland,G.M., and Palczewski,K. (2004). A naturally occurring mutation of the opsin gene (T4R) in dogs affects glycosylation and stability of the G protein-coupled receptor. J. Biol. Chem. *279*, 53828-53839.

BIOGRAPHICAL SKETCH

Alan White was born in Atlanta, Georgia, in 1974, the son of Dennis and Joan White. Soon after, the family moved to Raleigh, North Carolina, where Alan's sister Elizabeth was born in 1978. The family returned to the Atlanta area in 1981, where his parents live to this day.

Alan graduated with honors from Parkview High School in 1992, where he lettered in football, wrestling, and track, and was the male recipient of the school's Scholar Athlete Award. He was also a member of the Beta Club, and was elected to the student council during his junior and senior years.

Following high school, Alan attended the University of Georgia from 1992 to 1996, participating in the university's honors program and majoring in genetics. His studies were supported by a scholarship from the Gwinnett County Bulldog Club, a Georgia State Hope Scholarship, and a National Merit Scholarship. His summers were spent as a lifeguard for Gwinnett County Parks and Recreation. He graduated in June of 1996 with a Bachelor of Science in genetics.

In the Fall of 1997, he entered into his graduate studies at the University of Florida as a student in the Interdisciplinary Program in Biomedical Sciences, and has pursued his dissertation research in the laboratory of Dr. Alfred Lewin. Following completion of his Ph.D., he plans to continue his studies in the field of vision research with a postdoctoral fellowship in the lab of Dr. Shalesh Kaushal.